

AD-A066 217

PROTOTYPE DEVELOPMENT ASSOCIATES INC SANTA ANA CALIF
FLAME NOSETIP RECOVERY VEHICLE FLIGHT TEST SERIES.(U)

F/G 16/3

UNCLASSIFIED

JUN 78 D H SMITH

PDA-TR-1027-00-01

DNA-4654F

DNA001-74-C-0295

NL

1 OF 1
AD
A066 217



END
DATE
FILMED
'5--79
DDC

12 LEVEL III
NW

AD-E 300 453

DNA 4654F

ADA066217

FLAME NOSETIP RECOVERY VEHICLE FLIGHT TEST SERIES

Prototype Development Associates, Inc.
1740 Garry Avenue
Santa Ana, California 92705

June 1978

Final Report for Period July 1975—March 1977

CONTRACT No. DNA 001-74-C-0295

APPROVED FOR PUBLIC RELEASE;
DISTRIBUTION UNLIMITED.

THIS WORK SPONSORED BY THE DEFENSE NUCLEAR AGENCY
UNDER RDT&E RMSS CODE B342076462 L37HAXYX90518 H2590D.

Prepared for
Director
DEFENSE NUCLEAR AGENCY
Washington, D. C. 20305

DDC
RECEIVED
MAR 22 1979
B

79 01 24 039

DDC FILE COPY

Destroy this report when it is no longer
needed. Do not return to sender.

PLEASE NOTIFY THE DEFENSE NUCLEAR AGENCY,
ATTN: TISI, WASHINGTON, D.C. 20305, IF
YOUR ADDRESS IS INCORRECT, IF YOU WISH TO
BE DELETED FROM THE DISTRIBUTION LIST, OR
IF THE ADDRESSEE IS NO LONGER EMPLOYED BY
YOUR ORGANIZATION.



(18) DNA, SBIE

UNCLASSIFIED

SECURITY CLASSIFICATION OF THIS PAGE (When Data Entered)

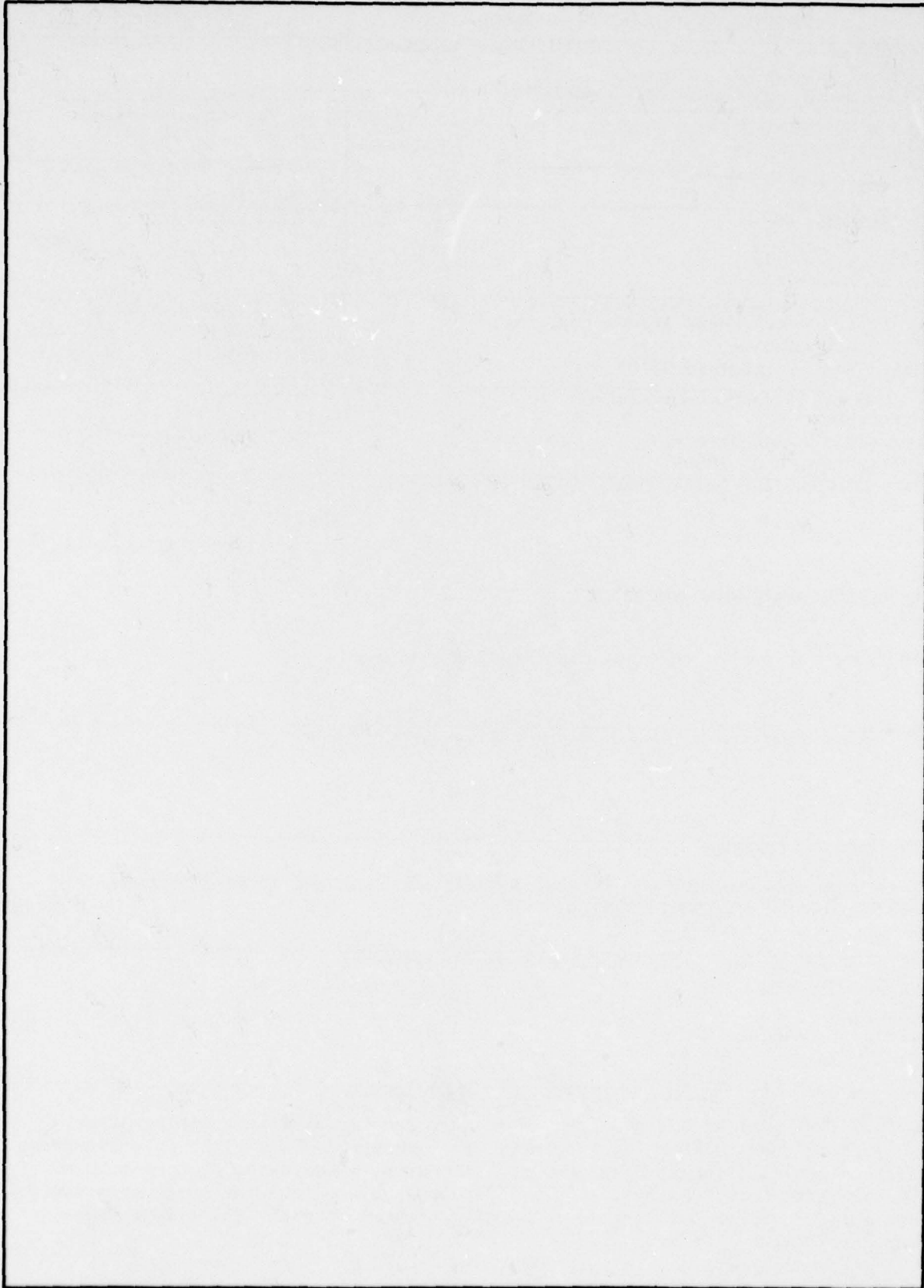
REPORT DOCUMENTATION PAGE		READ INSTRUCTIONS BEFORE COMPLETING FORM
1. REPORT NUMBER DNA 4654F	2. GOVT ACCESSION NO. AD-E300 453	3. RECIPIENT'S CATALOG NUMBER
4. TITLE (and Subtitle) FLAME NOSETIP RECOVERY VEHICLE FLIGHT TEST SERIES	5. TYPE OF REPORT & PERIOD COVERED Final Report, For Period July 1975 - March 1977	6. PERFORMING ORG. REPORT NUMBER PDA-TR-1027-00-01
7. AUTHOR(s) David H. Smith	8. CONTRACT OR GRANT NUMBER(s) DNA 001-74-C-0295 new	9. PROGRAM ELEMENT, PROJECT, TASK AREA & WORK UNIT NUMBERS NWET Subtask L37HAXYX905-18
11. CONTROLLING OFFICE NAME AND ADDRESS Director Defense Nuclear Agency Washington, D.C. 20305	12. REPORT DATE June 1978	13. NUMBER OF PAGES 90
14. MONITORING AGENCY NAME & ADDRESS (if different from Controlling Office)	15. SECURITY CLASS (of this report) UNCLASSIFIED	15a. DECLASSIFICATION/DOWNGRADING SCHEDULE
16. DISTRIBUTION STATEMENT (of this Report) Approved for public release; distribution unlimited.		
17. DISTRIBUTION STATEMENT (of the abstract entered in Block 20, if different from Report)		
18. SUPPLEMENTARY NOTES This work sponsored by the Defense Nuclear Agency under RDT&E RMSS Code B342076462 L37HAXYX90518 H2590D.		
19. KEY WORDS (Continue on reverse side if necessary and identify by block number) Nosetip Testing Recovery System Aircraft Launched Rocket		
20. ABSTRACT (Continue on reverse side if necessary and identify by block number) The FLAME payload was designed to recover reentry vehicle nosetips after subjecting them to ICBM-level reentry environments. The payload is a two-stage solid propellant rocket fired towards the earth, after being dropped from an F4 aircraft at 60,000 feet. The payload employs a unique two-stage hypersonic decelerator system for nosetip recovery. A total of eight (8) flight tests were performed.		

390 714

79 01 24 039 log

UNCLASSIFIED

SECURITY CLASSIFICATION OF THIS PAGE(When Data Entered)



UNCLASSIFIED

SECURITY CLASSIFICATION OF THIS PAGE(When Data Entered)

Conversion factors for U.S. customary
to metric (SI) units of measurement.

To Convert From	To	Multiply By
angstrom	meters (m)	1.000 000 X E -10
atmosphere (normal)	kilo pascal (kPa)	1.013 25 X E +2
bar	kilo pascal (kPa)	1.000 000 X E +2
barn	meter ² (m ²)	1.000 000 X E -28
British thermal unit (thermochemical)	joule (J)	1.054 350 X E +3
calorie (thermochemical)	joule (J)	4.184 000
cal (thermochemical)/cm ²	mega joule/m ² (MJ/m ²)	4.184 000 X E -2
curie	giga becquerel (GBq)*	3.700 000 X E +1
degree (angle)	radian (rad)	1.745 329 X E -2
degree Fahrenheit	degree kelvin (K)	$t_K = (t_F + 459.67)/1.8$
electron volt	joule (J)	1.602 19 X E -19
erg	joule (J)	1.000 000 X E -7
erg/second	watt (W)	1.000 000 X E -7
foot	meter (m)	3.048 000 X E -1
foot-pound-force	joule (J)	1.355 818
gallon (U.S. liquid)	meter ³ (m ³)	3.785 412 X E -3
inch	meter (m)	2.540 000 X E -2
jerk	joule (J)	1.000 000 X E +9
joule/kilogram (J/kg) (radiation dose absorbed)	Gray (Gy)**	1.000 000
kilotons	terajoules	4.183
kip (1000 lbf)	newton (N)	4.448 222 X E +3
kip/inch ² (ksi)	kilo pascal (kPa)	6.894 757 X E +3
ktap	newton-second/m ² (N-s/m ²)	1.000 000 X E +2
micron	meter (m)	1.000 000 X E -6
mil	meter (m)	2.540 000 X E -5
mile (international)	meter (m)	1.609 344 X E +3
ounce	kilogram (kg)	2.834 952 X E -2
pound-force (lbf avoirdupois)	newton (N)	4.448 222
pound-force inch	newton-meter (N·m)	1.129 848 X E -1
pound-force/inch	newton/meter (N/m)	1.751 268 X E +2
pound-force/foot ²	kilo pascal (kPa)	4.788 026 X E -2
pound-force/inch ² (psi)	kilo pascal (kPa)	6.894 757
pound-mass (lbm avoirdupois)	kilogram (kg)	4.535 924 X E -1
pound-mass-foot ² (moment of inertia)	kilogram-meter ² (kg·m ²)	4.214 011 X E -2
pound-mass/foot ³	kilogram/meter ³ (kg/m ³)	1.601 846 X E +1
rad (radiation dose absorbed)	Gray (Gy)**	1.000 000 X E -2
roentgen	coulomb/kilogram (C/kg)	2.579 760 X E -4
shake	second (s)	1.000 000 X E -8
slug	kilogram (kg)	1.459 390 X E +1
torr (mm Hg, 0° C)	kilo pascal (kPa)	1.333 22 X E -1

*The becquerel (Bq) is the SI unit of radioactivity; 1 Bq = 1 event/s.

**The Gray (Gy) is the SI unit of absorbed radiation.

A more complete listing of conversions may be found in "Metric Practice Guide E 380-74," American Society for Testing and Materials.

TABLE OF CONTENTS

	<u>Page</u>
1.0 INTRODUCTION	5
2.0 SYSTEM CONCEPT	9
2.1 The FLAME Concept	9
2.2 Mass-Jettison Drogue Recovery Concept	9
2.3 Recovery Vehicle Characteristics	18
2.4 Recovery Vehicle Electronics	18
3.0 GROUND TESTS	22
3.1 Mortar Tests	22
3.2 Air Drop Tests	22
3.3 Holloman Sled Tests	23
3.4 Fairing Deployment Test	25
3.5 Sandia Sled Tests	25
4.0 FLIGHT TESTS	31
4.1 Flight F-001	31
4.2 Flight F-002	35
4.3 Flight F-003	46
4.4 Flight F-004	47
4.5 Flight F-005	51
4.6 Flight F-006	56
4.7 Flight F-007	68
4.8 Flight F-008	76
5.0 CONCLUSIONS	82

ACCESSION for	
NTIS	White Section <input checked="" type="checkbox"/>
DDC	Buff Section <input type="checkbox"/>
UNANNOUNCED	<input type="checkbox"/>
JUSTIFICATION _____	
BY _____	
DISTRIBUTION/AVAILABILITY CODES	
Dist. AVAIL. and/or SPECIAL	
A	

LIST OF FIGURES

		<u>Page</u>
1-1	Mass Jettison Drogue (MJD) recovery concept.	6
2-1	FLAME mission profile.	10
2-2	FLAME vehicle Pedro/Recruit.	11
2-3	F4-J with FLAME.	12
2-4	flame recovery vehicle.	14
2-5	FLAME recovery vehicle cut-away.	15
2-6	FLAME terminal recovery system (Flights F-001 through F-006).	16
2-7	FLAME conical ribbon parachute detail (Flights F-007 and F-008).	17
3-1	Holloman chute test installation.	24
3-2	Holloman chute test velocity profiles.	26
3-3	Comparison of separation system ground test results.	27
3-4	Recovered Sandia chute test vehicle.	29
3-5	Sandia chute test velocity profile.	30
4-1	FLAME F-001 velocity history.	37
4-2	FLAME F-001 altitude history.	38
4-3	FLAME F-002 telemetry.	40
4-4	FLAME vehicle velocity as a function of altitude.	41
4-5	FLAME F-002 velocity history.	43
4-6	FLAME F-002 acceleration history.	44
4-7	FLAME F-002 altitude history.	45
4-8	FLAME F-003 velocity history.	49
4-9	FLAME F-003 altitude history.	50
4-10	FLAME F-004 velocity history.	53
4-11	FLAME F-004 acceleration history.	54
4-12	FLAME F-004 altitude history.	55
4-13	Damaged boom and drogue heatshield.	57
4-14	Recovered tungsten nosetip from FLAME F-005.	58
4-15	FLAME F-005 calculated altitude versus range comparison.	60
4-16	FLAME F-005 calculated velocity history comparison.	61
4-17	FLAME F-005 calculated stagnation pressure history comparison.	62
4-18	FLAME F-005 velocity history.	65
4-19	FLAME F-005 acceleration history.	66
4-20	FLAME F-005 altitude history.	67
4-21	FLAME F-006 velocity history.	69
4-22	FLAME F-006 acceleration history.	70
4-23	FLAME F-006 altitude history.	71
4-24	FLAME F-007 velocity history.	73
4-25	FLAME F-007 acceleration history.	74
4-26	FLAME F-007 altitude history.	75
4-27	Recovered gasjet nosetip from FLAME F-008.	77
4-28	FLAME F-008 velocity history.	79
4-29	FLAME F-008 acceleration history.	80
4-30	FLAME F-008 altitude history.	81
5-1	FLAME drag data comparison.	83

LIST OF TABLES

	<u>Page</u>	
2-1	FLAME F-002 weight summary.	19
2-2	Mortar throw weight summary.	20
2-3	FLAME instrumentation.	21
4-1	FLAME recovery vehicle performance summary.	32
4-2	FLAME booster performance summary.	33
4-3	FLAME F-001 data source summary.	34
4-4	FLAME F-001 flight data summary.	36
4-5	FLAME F-001 vehicle performance evaluation.	36
4-6	FLAME F-002 data source summary.	39
4-7	FLAME F-002 flight data summary.	39
4-8	FLAME F-002 vehicle performance evaluation.	42
4-9	FLAME F-003 data source summary.	47
4-10	FLAME F-003 flight data summary.	48
4-11	FLAME F-003 vehicle performance evaluation.	48
4-12	FLAME F-004 data source summary.	52
4-13	FLAME F-004 vehicle performance evaluation.	52
4-14	FLAME F-005 data source summary.	59
4-15	FLAME F-005 flight data summary.	63
4-16	FLAME F-005 vehicle performance evaluation.	64
4-17	FLAME F-007 data source summary.	68
4-18	FLAME F-007 flight data summary.	72
4-19	FLAME F-007 vehicle performance evaluation.	72
4-20	FLAME F-008 data source summary.	76
4-21	FLAME F-008 flight data summary.	78
4-22	FLAME F-008 vehicle performance evaluation.	78

High performance reentry vehicles may experience drag and dynamic behavior anomalies which may degrade accuracy and survivability. Many of these problems would be directly associated with nosetip performance. Ground tests cannot simulate the flight environment completely, and flight test nosetips cannot be instrumented with the quantity and quality of instrumentation needed to understand the cause and effect relationships between materials response, erosive environment, and vehicle survivability. Nosetip recovery is judged to be the best means of obtaining the required data.

To fulfill the need for a low-cost nosetip recovery system, Prototype Development Associates (PDA) began exploratory studies of the "mass-jettison drogue" (MJD) concept in 1972, first with in-house funds and later under contract to the Defense Nuclear Agency (DNA). The MJD concept is especially suitable for nosetip recession and shape-change investigations since recovery can be initiated at very low altitudes (typically about 10 Kft). Low altitude recovery initiation obviously is essential for hydrometeor erosion experiments; however, it is also important for clear air recession studies since "shape-stable" turbulent nosetip ablation on high performance vehicles usually is not achieved until comparatively low altitudes are reached.

The operation of the MJD system is shown in Figure 1-1. Two side panels containing approximately half of the mass of the vehicle are removed pyrotechnically. The drag of the remainder of the vehicle is approximately tripled by the exposure of the steep-angle drogue to the flow, resulting in rapid deceleration to an airspeed at which the parachute stowed in the drogue can be deployed.

The simplicity of the MJD concept resulted in a high confidence design with a minimum of performance uncertainties. There were two basic approaches available to resolve these remaining uncertainties:

- (1) An orderly development program beginning with extensive wind tunnel and other ground tests of the basic phenomena essential to the concept followed, first, by component development tests and, finally, by a full system flight test; or,
- (2) a full-scale system flight test using a low-cost launch vehicle preceded by only a minimum of component development tests.

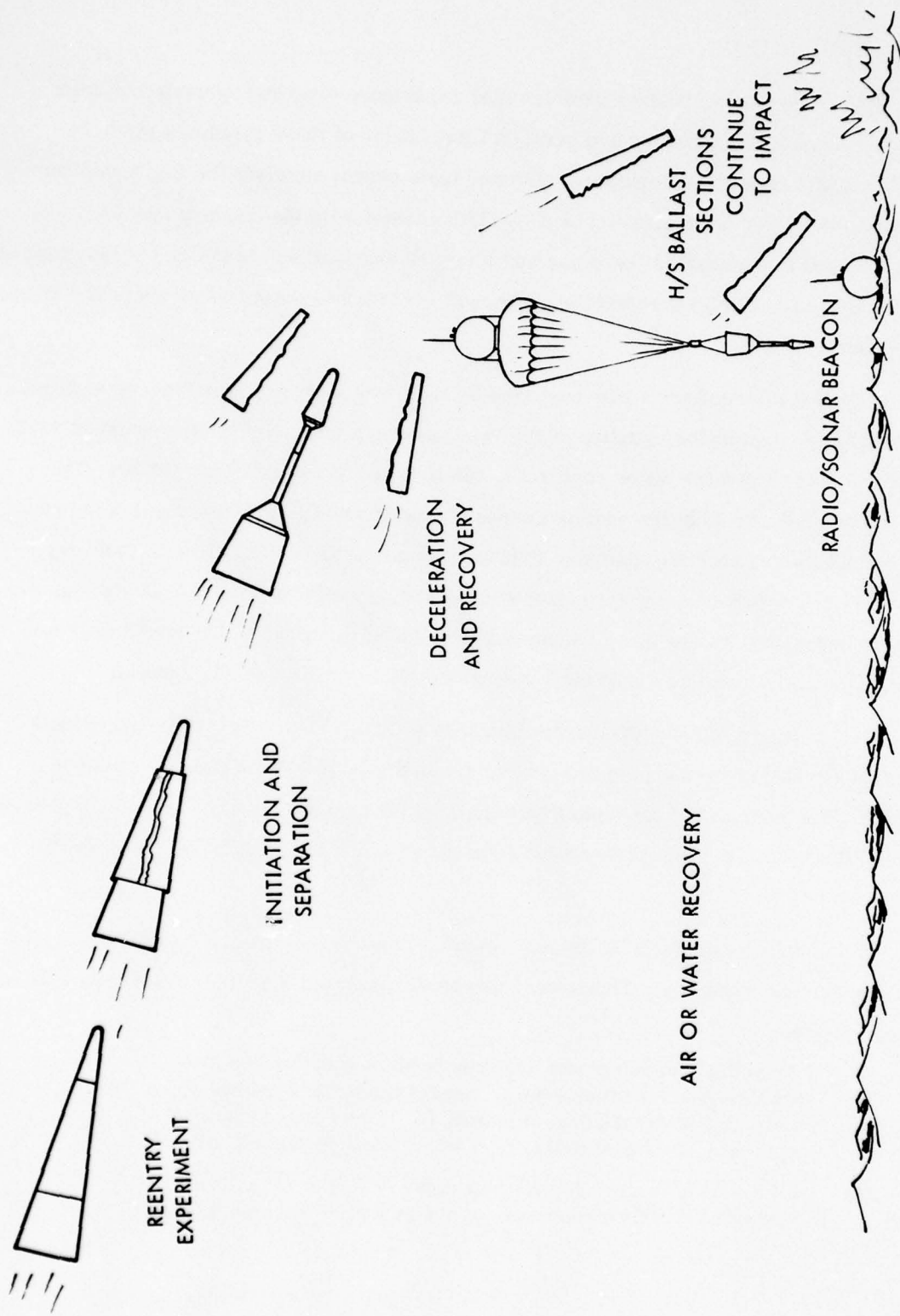


Figure 1-1. Mass Jettison Drogue (MJD) recovery concept.

The second approach was selected since it was believed to offer the better opportunity for a rapid and low-cost evaluation of the overall concept performance.

The first flight test program of the MJD concept to be funded was the HEART Recovery Vehicle (HRV) Test Program. This program included two sounding rocket tests of prototype units, both conducted at White Sands Missile Range in June of 1974. One of the two flights was a no-test because of a booster failure. The other demonstrated the basic feasibility of the MJD concept, but insufficient data were obtained to make a detailed performance evaluation (Reference 1).

The reentry vehicle tested under the HRV program originally was envisioned as a prototype recovery system for future utilization under the DNA/Hydrometeor Erosion and Recession Test (HEART) program. However, it was later decided by DNA to incorporate the MJD vehicle as an integral part of a newly conceived system: the Fighter Launched Advanced Material Experiment (FLAME) system.

The FLAME program was intended to provide a complete low-cost nosetip material evaluation flight test capability, including nosetip recovery. PDA was responsible for the development and flight test of the recovery system. The present report presents a description of the recovery vehicle together with the results of the flight test program.

The FLAME vehicle consists of an MJD recovery vehicle payload boosted by a two-stage Pedro/Recruit rocket. The FLAME vehicle is carried on the centerline position of an F4-J aircraft, and is released from the aircraft during a maximum-power high altitude pull-up maneuver. After the vehicle coasts through apogee and achieves the predetermined entry-angle, the rocket motor is ignited by ground command and accelerates the vehicle up to a planned velocity of 13,200 ft/sec. At second stage burn-out, the payload separates from the empty motor case, and coasts down to an altitude of 15,000 ft, where recovery is initiated.

Eight FLAME vehicles were flown including tests of six different nosetip concepts. Initially, six FLAME flights were scheduled. The first flight used a refurbished HRV vehicle, while the following five flights used a new series of vehicles. These new vehicles incorporated detail engineering changes to the HRV design, and a new terminal recovery system designed for water recovery. These six vehicles were flown during the period from 4 February 1975 to 4 June 1975. Flights one and three were conducted at Wallops Island, Virginia, and the other four flights were conducted at Tonopah Test Range, Nevada.

Following the sixth flight, two more flights were scheduled. Since these were also planned to be fired at Tonopah, it was decided to develop a terminal recovery system optimized for land recovery. This was accomplished, and the final two flights were flown on 22 January 1976 and 26 January 1976.

The program accomplishments are summarized below:

- Successfully demonstrated a low altitude recovery system capability.
- Developed a reliable fairing deployment system.
- Developed a low package-volume terminal recovery system for water recovery.
- Demonstrated recovery system compatibility with varying nosetip designs.
- Provided instrumentation capability after recovery initiation for evaluation of recovery effects on the experiment.

This report describes the FLAME vehicle operation, and ground and flight testing. Design details of the MJD recovery vehicle and of the rocket booster system are given in References 1 and 2.

Reference 1: "HEART Recovery Vehicle (HRV) Test Program Final Report,"
DNA 3842F, 10 November 1975.

Reference 2: "FLAME Test Vehicle 1976 Flight Test Series Final Report,"
DNA 4222F, February 1977.

2.0 SYSTEM CONCEPT

The FLAME system includes a Navy F4-J aircraft, a two stage solid propellant air launched booster, and the recovery vehicle payload. System integration was performed in-house by DNA, with Aerojet Liquid Rocket Company (ALRC) supplying the booster and PDA supplying the recovery vehicle. The nosetip test specimens for the various flights were supplied by General Electric (G. E.), PDA, Martin-Marietta, and Aerotherm Accurex Corporation. The recovery vehicle telemetry systems were provided by G. E. With the exception of the terminal recovery system (parachute and flotation), and minor engineering changes, the recovery vehicle is identical to the HRV vehicles described in Reference 1.

2.1 The FLAME Concept

The FLAME mission profile is illustrated in Figure 2-1. The major components of the system include:

- (1) An F4-J aircraft dedicated to the program by the Naval Air Test Center at Patuxent River, Md.
- (2) A two stage Pedro/Recruit booster. The booster was assembled by ALRC and designed for external mount and launch from the F4-J.
- (3) The recovery vehicle provided by PDA.

The geometry of the FLAME booster/recovery vehicle assembly is shown in Figure 2-2. A photograph of the complete system installed on the aircraft is presented in Figure 2-3.

With the planned mission profile, the aircraft drops the assembled vehicle during a pull-up maneuver. The nominal launch Mach number is 1.3 with a velocity vector 30° above the local horizontal. The FLAME vehicle is then allowed to coast through apogee. First stage (Pedro) ignition, controlled by ground command or backup timer, occurs approximately 27 seconds after launch when the predicted vehicle velocity is 1000 fps and the flight path angle is 13° below the horizontal. Second stage (Recruit) ignition occurs at Pedro burnout. The booster accelerates the recovery vehicle up to a maximum velocity of 13,200 fps at a nominal altitude of 37 kft at which point the flight path angle is -18.5° . The recovery vehicle then separates from the expended recruit casing and follows a ballistic trajectory until recovery initiation.

2.2 The Mass-Jettison Drogue Recovery Concept

The nosetip recovery concept is a combination of mass jettison and wake drogue decelerator and is referred to as the MJD recovery concept. This recovery system provides an

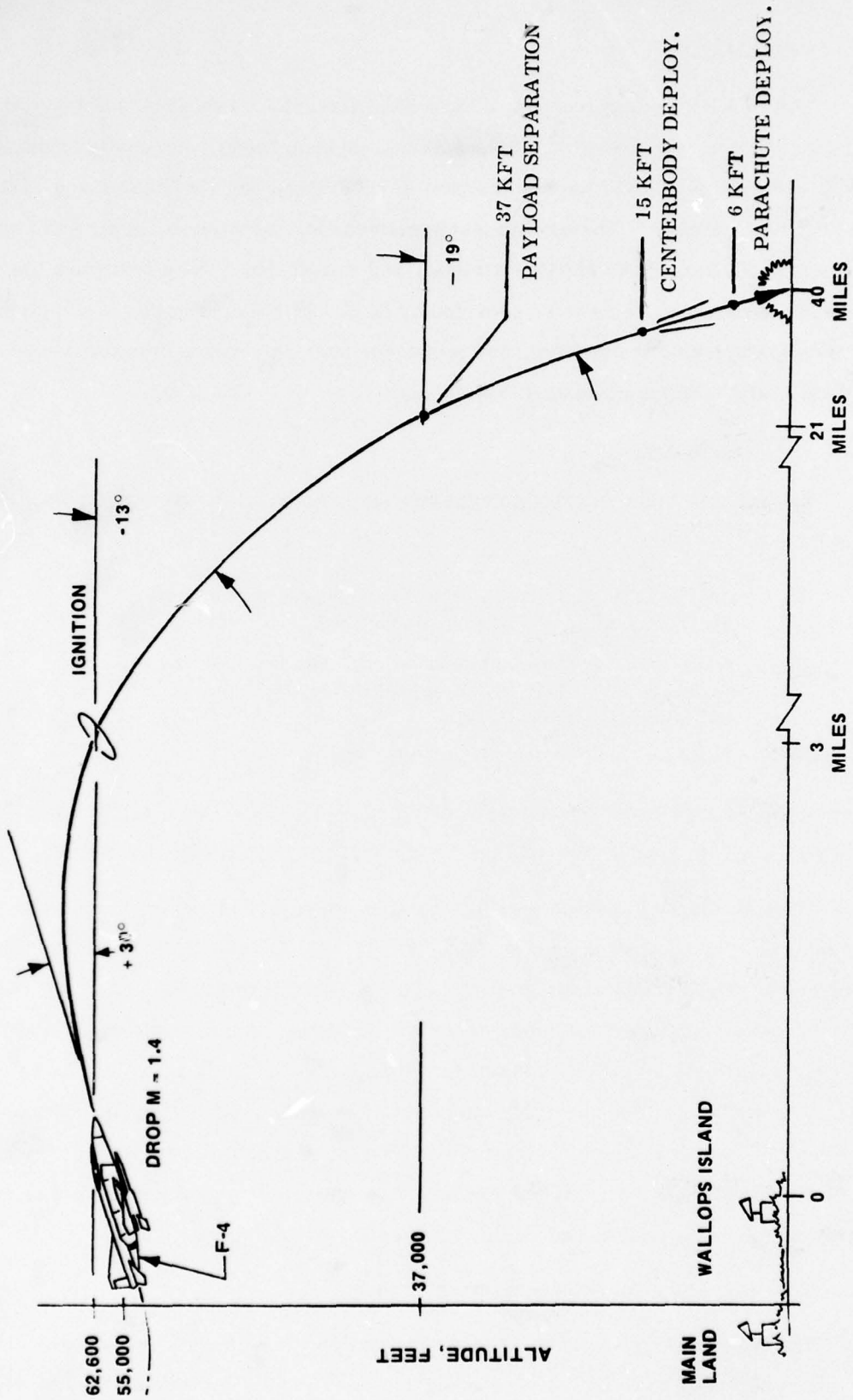


Figure 2-1. FLAME mission profile.

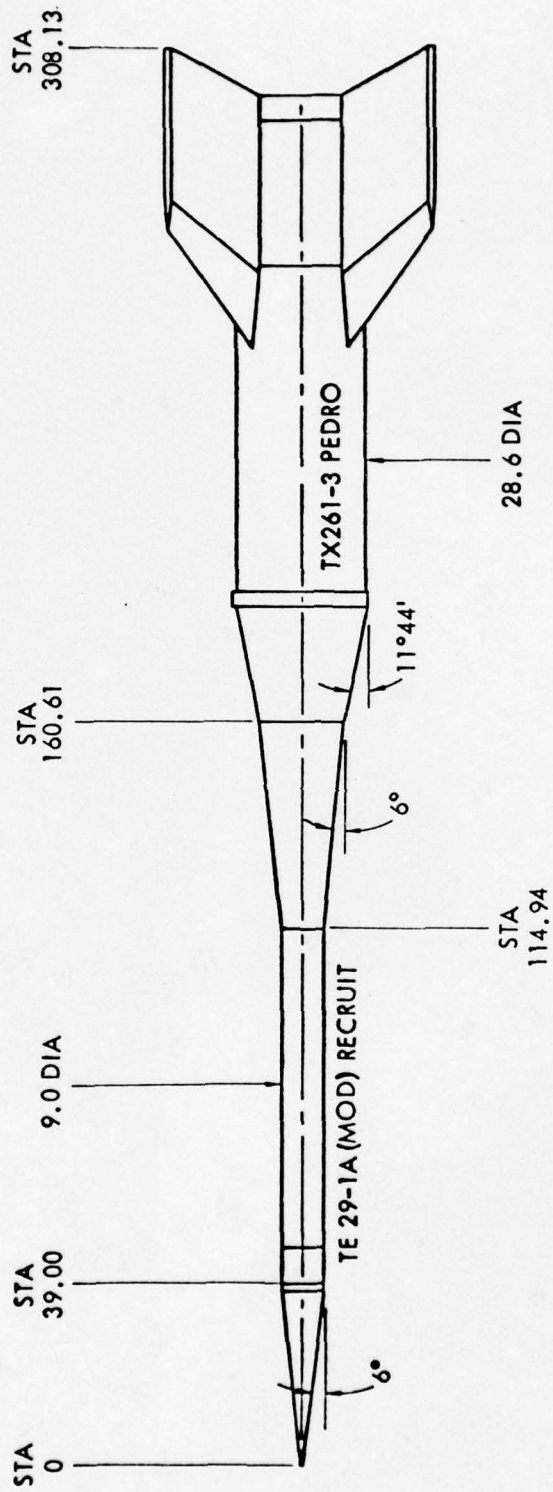


Figure 2-2. FLAME vehicle Pedro/Recruit

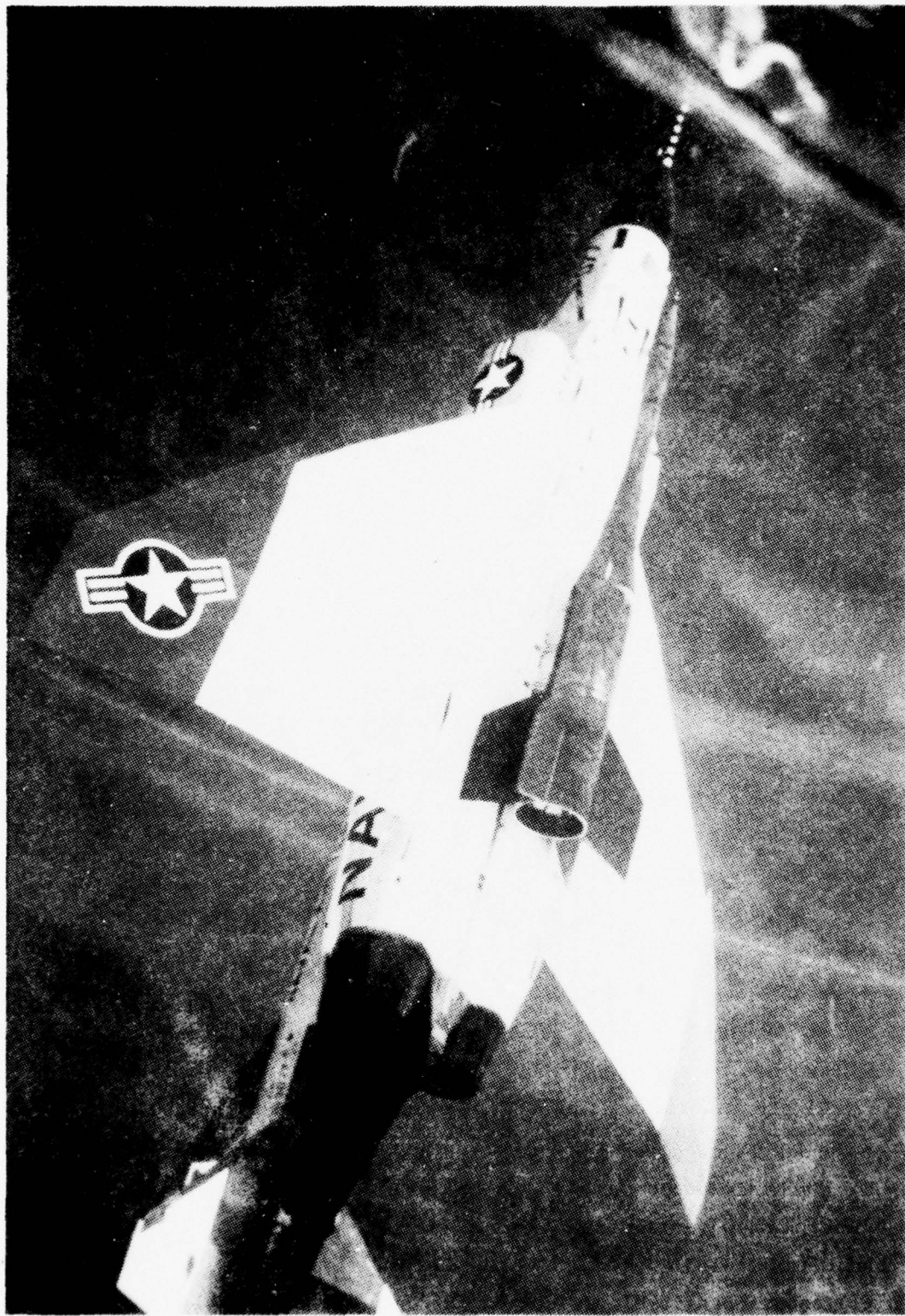


Figure 2--3. F4-J with FLAME.

extremely high deceleration effectiveness by combining large mass removal with a high drag device. The recovered payload consists of the nosetip, electronics/instrumentation package, parachute, aft portion of the vehicle heatshield and, in case of water recovery, a flotation bag, location beacon and sonar pinger.

Some of the characteristics of the FLAME recovery vehicle (R/V) configuration are illustrated in Figure 2-4. Approximately one-half of the initial vehicle weight is contained in the two centerbody ballast/heatshield sections which are jettisoned at the recovery initiation altitude by means of pyrotechnic devices along the joints separating the two frustum segments. Upon removal of these centerbody sections, the enclosed aft section of the vehicle (containing the parachute and electronics package) becomes a lightweight, high-efficiency drogue connected to the nosetip section by a rigid structural member or boom. The combined weight loss and drag increase results in a decrease in ballistic coefficient by a factor of over six. The pyrotechnic train that initiates recovery performs two functions:

- Linear flexible shaped charges (LFSC) inside the fairing segments cut the fairing substructure and heatshield.
- Piston thrusters in each fairing ballast section push the sections away from the vehicle.

The pyrotechnic elements are shown in black on the vehicle cut-away in Figure 2-5. The vehicle decelerates rapidly and separates from the ballast segments, which are blown away from the vehicle by the pyrotechnic charges. After approximately 20 seconds, the vehicle approaches a terminal velocity of about 650 fps. The terminal recovery system is then mortar deployed. Two terminal recovery systems were used. The terminal recovery system used on flights F-001 through F-006 is shown in Figure 2-6. This system is completely packed in a fabric deployment bag and consists of a parachute, flotation bag, UHF beacon, and sonar pinger. For missions over land, the beacon and pinger were replaced by dummy items of the same sizes and weights.

The terminal recovery system used for the final two FLAME flights was redesigned to take advantage of the fact that these flights were planned from inception to be recovered on land. The flotation bag, beacon, and pinger were removed, and the volume that they had occupied was used by enlarging the parachute. The parachute designed for these flights was an 8.4 ft diameter conical ribbon chute as shown in Figure 2-7.

The entire terminal recovery system is mortar-deployed by a pyrotechnic charge that drives a sabot initially packed at the bottom of the parachute canister. The sabot, the contents

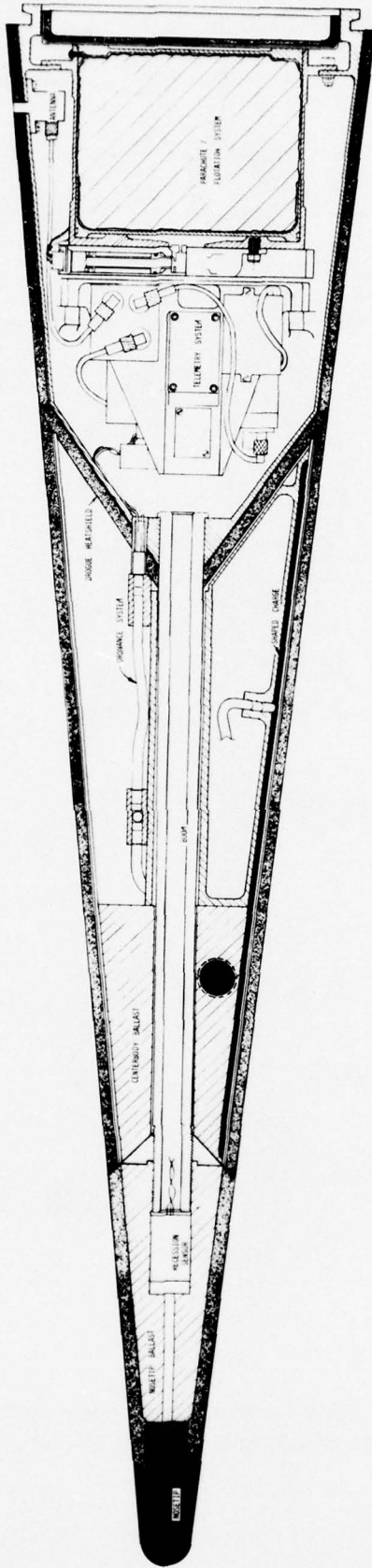


Figure 2-5. FLAME recovery vehicle cut-away.

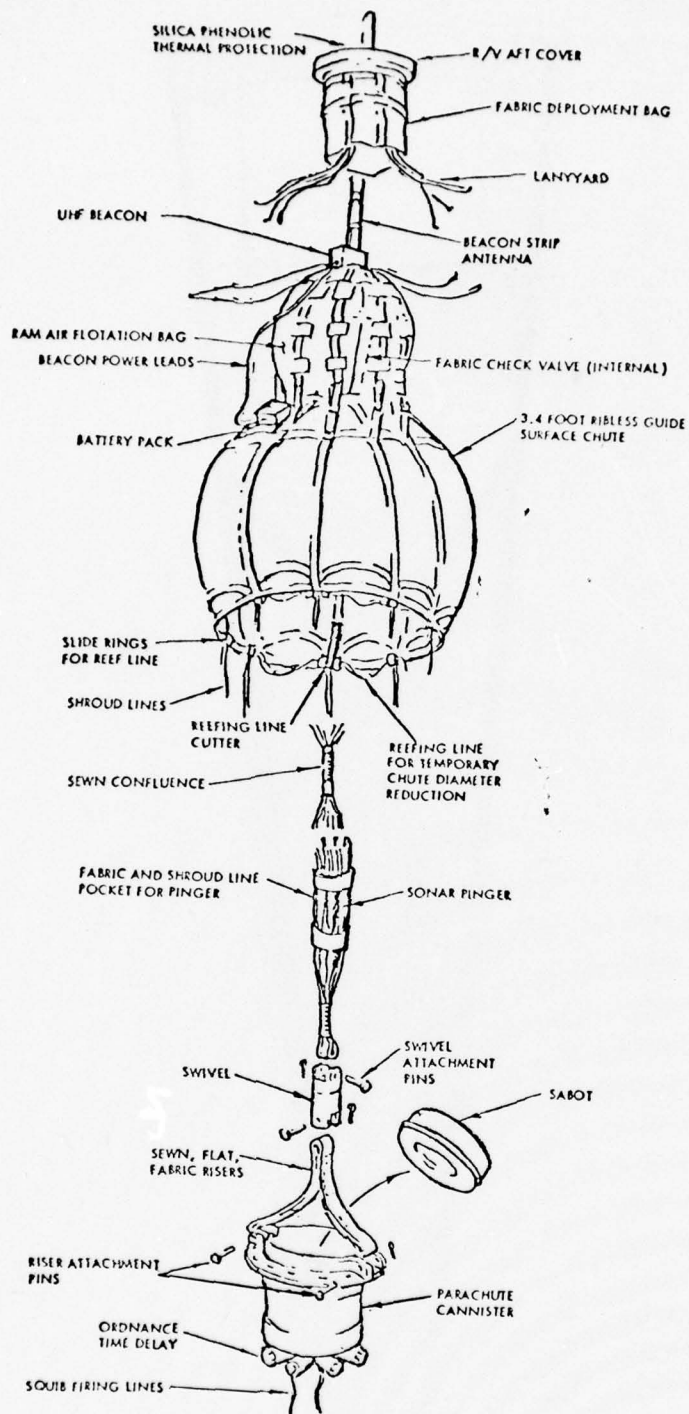


Figure 2-6. FLAME terminal recovery system.
(Flights F-001 through F-006)

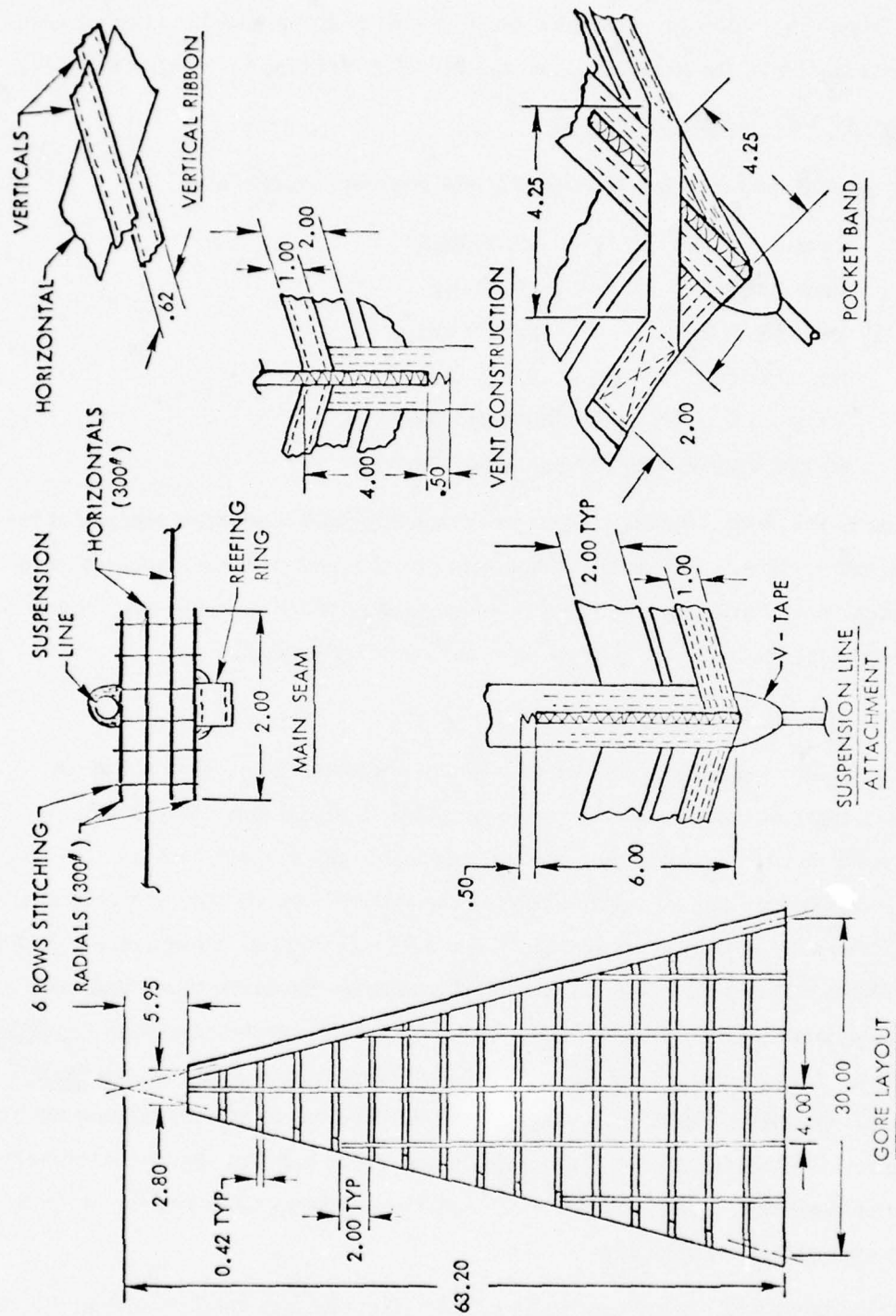


Figure 2-7. FLAME conical ribbon parachute detail.
(Flights F-007 and F-008)

of the parachute canister, and the vehicle aft cover are all accelerated up to a velocity of approximately 60 ft/sec. When the parachute suspension lines become taut, the weight of the aft cover draws the deployment bag off of the parachute, and the parachute inflates in the airstream.

2.3 Recovery Vehicle Characteristics

The nominal characteristics of the FLAME recovery vehicle are:

- Length: 39.00 inch
- Cone Angle: 6.00 deg
- Base Diameter: 9.212 inch
- Nose Radius: 0.625 inch
- Weight before fairing deployment: 72-81 lb
- Weight after fairing deployment: 39-45 lb

The range in weights is due to the varying weights of the nosetips and associated equipment installed on the different vehicles. The actual weights are given in each vehicle's subsection in Section 4.0. A typical weight and center-of-gravity breakdown is listed in Table 2-1. Table 2-2 summarizes the weights of the mortar-deployed terminal recovery system.

2.4 Recovery Vehicle Electronics

The recovery vehicle electronics system, provided by G. E., consists of an FM-FM transmitter, thermal battery, 3 axis accelerometers, a signal conditioning unit, nosetip recession measurement electronics package, and two antennas. Seven vehicles were also equipped with a PDA supplied radar transponder and antennas. The system was powered by the aircraft power supply until release. At release a signal initiated a 28 volt thermal battery that provided power during free flight. This signal also started the capacitance-discharge timer that later fired the fairing deployment pyrotechnics and initiated the 22 second pyrotechnic delay timer for the parachute mortar. All vehicles except flight F-005 had radar transponders to enhance the R/V radar signature. On Flight F-005, the transponder was removed to provide volume for a nosetip recession sensor. All vehicles except F-001, F-006 and F-008 had five channel telemetry units. F-001 had an eight channel unit, and F-006 and F-008 had the telemetry units removed to provide volume for nosetip experiment components.

All flights with telemetry had three-axis accelerometers, and in addition, flights F-002, F-003, F-004, and F-007 had both low and high-range axial accelerometers. Flights F-001, F-002, and F-005 had nosetip recession sensors, while flights F-004 and F-007 had magnetometers to measure R/V roll rate. Flight F-005 had an acoustic boundary layer transition

Table 2-1. FLAME F-002 weight summary.

	<u>Weight</u>	<u>CG*</u>
Delay Timers	0.40	40.21
Nosetip Assembly	12.95	12.90
Conical Nut	0.96	15.64
Drogue Structure	12.94	34.73
Parachute and Canister	6.53	40.39
Aft Cover	0.79	43.54
Instrument Package	4.75	35.65
S-Band Antennas (2)	0.46	41.41
Balance Weights	0.13	35.29
	0.07	42.51
Miscellaneous Hardware & Cabling	<u>0.10</u>	<u>41.5</u>
Total After Centerbody Separation	40.08	28.58
Centerbody Assembly	35.53	20.98
Balance Weights	<u>0.03</u>	<u>32.6</u>
Vehicle Total	75.64	25.01

Static Margin Summary

Before Deployment	$X_{CG} = 25.01$
	$X_{CP} = 30.21$
	$SM = 13.5\%$
After Deployment	$X_{CG} = 28.58$
	$X_{CP} = 33.0$
	$SM = 11.5\%$

* Aft of Theoretical Apex

Table 2-2. Mortar throw weight summary.

<u>Item</u>	<u>Weight</u>
1. Parachute/Bag Assembly	1.50
2. Pinger	0.56
3. Beacon	0.17
4. Battery	0.50
5. Swivel Assembly	0.35 (Est)
6. Sabot	0.40
7. Parachute Cover	0.30 (Est)
8. Base Cover	0.67 (Est)
	<hr/>
	0.45 lb

Sabot Area $\approx 24.85 \text{ in}^2$

Sabot Stroke $\approx 4.5 \text{ in}$

experiment, and flight F-004 had a thermister that measured the temperature of the conical aluminum shell of the R/V drogue. Table 2-3 summarizes the instrumentation on the eight vehicles.

Table 2-3. FLAME instrumentation.

Channel	1	2	3	4	5	6	7	8
1	$\pm 500 A_X$	+0 $-80 A_X$	+0 $-80 A_X$	+0 $-80 A_X$	+175 $-80 A_X$	--	$\pm 200 A_X$	--
2	$\pm 200 A_Y$	+175 $-825 A_X$	+175 $-825 A_X$	+175 $-825 A_X$	$\pm 100 A_Y$	--	+200 $-400 A_X$	--
3	$\pm 200 A_Z$	$\pm 100 A_Y$	$\pm 100 A_Y$	$\pm 100 A_Y$	$\pm 100 A_Z$	--	$\pm 100 A_Y$	--
4	Nosetip Recession	$\pm 100 A_Z$	$\pm 100 A_Z$	$\pm 100 A_Z$	Acoustic Transition Sensor	--	$\pm 100 A_Z$	--
5	Boom Strain Gage	Nosetip Recession	Roll Magne- tometer	Drogue Shell Temp	Nosetip Recession	--	Roll Magne- tometer	--
6	Boom Strain Gage	--	--	--	--	--	--	--
7	Boom Strain Gage	--	--	--	--	--	--	--
8	Separation Signal	--	--	--	--	--	--	--

3.0 GROUND TESTS

Five ground tests series were conducted to verify the terminal recovery system:

- Mortar Tests.
- Air Drop Tests.
- Holloman Rocket Sled Tests.
- Fairing Deployment Test.
- Sandia Rocket Sled Tests.

The mortar and air drop tests were performed prior to the flight test program. The Holloman sled series was conducted in support of a parachute redesign effort initiated when a shroud failure was observed on the second flight (Section 4.0). The fairing deployment test was conducted after an apparent pyrotechnic failure on the third flight. The second rocket sled test series was conducted to qualify a new parachute design used for Flights F-007 and F-008.

3.1 Mortar Tests

Several mortar deployment tests were conducted at Irvin Industries, Inc., Gardena, California, to verify packing procedures, ejection velocity, and component integrity. A 1,000 frames-per-second camera provided pack exit velocities and deployment sequences.

Pack exit velocity was determined from the photographic data to be approximately 60 feet persecond. The pack exited the canister cleanly, and the deployment bag was pulled off of the chute by the momentum of the aft cover, as planned.

3.2 Air Drop Tests

Three aircraft drop tests were conducted over water at the Salton Sea National Parachute Test Range. A mock-up of the FLAME vehicle was used, duplicating the actual configuration and mass properties after fairing deployment.

The first test conducted on 22 August 1974 incorporated a static line deployment at an altitude of 500 feet. The chute functioned properly, but dynamic pressure was insufficient to provide full inflation of the ram air bag, resulting in submersion of the vehicle shortly after water impact. The test vehicle was recovered with the aid of the sonar pinger by the Navy Seal Team.

The remaining two tests included mortar deployment using 24 second flight time delays. The nominal test conditions were:

- Aircraft drop altitude - 8,500 ft
- Altitude at mortar deployment - 2,000 ft
- Velocity at mortar deployment - 450 fps
- Dynamic pressure at mortar deployment - 170 psf

The 3 September 1974 test resulted in breakaway of the chute at line stretch. Film data and the recovered hardware indicated the cause to be a sequential failure of the eight shroud lines attributed to the inability of the confluence to evenly distribute the shroud loads.

A system with a redesigned confluence was successfully tested on 11 September 1974. The vehicle was left in the water for 20 minutes to verify the integrity of the flotation system.

3.3 Holloman Sled Tests

The FLAME F-002 parachute system broke away from the R/V at chute deployment because the recovery vehicle's hypersonic drag was somewhat lower than predicted. The resulting dynamic pressure at chute deployment was 320 psf, while the design ultimate deployment condition was 180 psf. The recovered vehicle and parachute permitted identification of the failure modes resulting in the following design changes:

- Strengthen parachute rise lines,
- Strengthen sonar pinger attachment in its harness,
- Improve bond strength of flotation bag seams,
- Strengthen flotation bag flapper valve,
- Reduce opening loads by reefing the chute.

Verification of the above changes was accomplished by two rocket sled tests at Holloman AFB, New Mexico. Figure 3-1 shows the installation of the vehicle mock-up on the rocket sled.

The first test was conducted on March 12. In this test, the reefing line failed on deployment and the chute tore off the R/V, essentially duplicating the Tonopah failure. Post-test inspection revealed that the reefing line cutters had not been installed securely and had worked loose on deployment. This allowed the reefing line load to be applied directly on the sharp cutter edge resulting in premature failure of the line. In addition, it was found that the shroud line confluence had not been properly fabricated resulting in a sequential tensile failure of all shroud

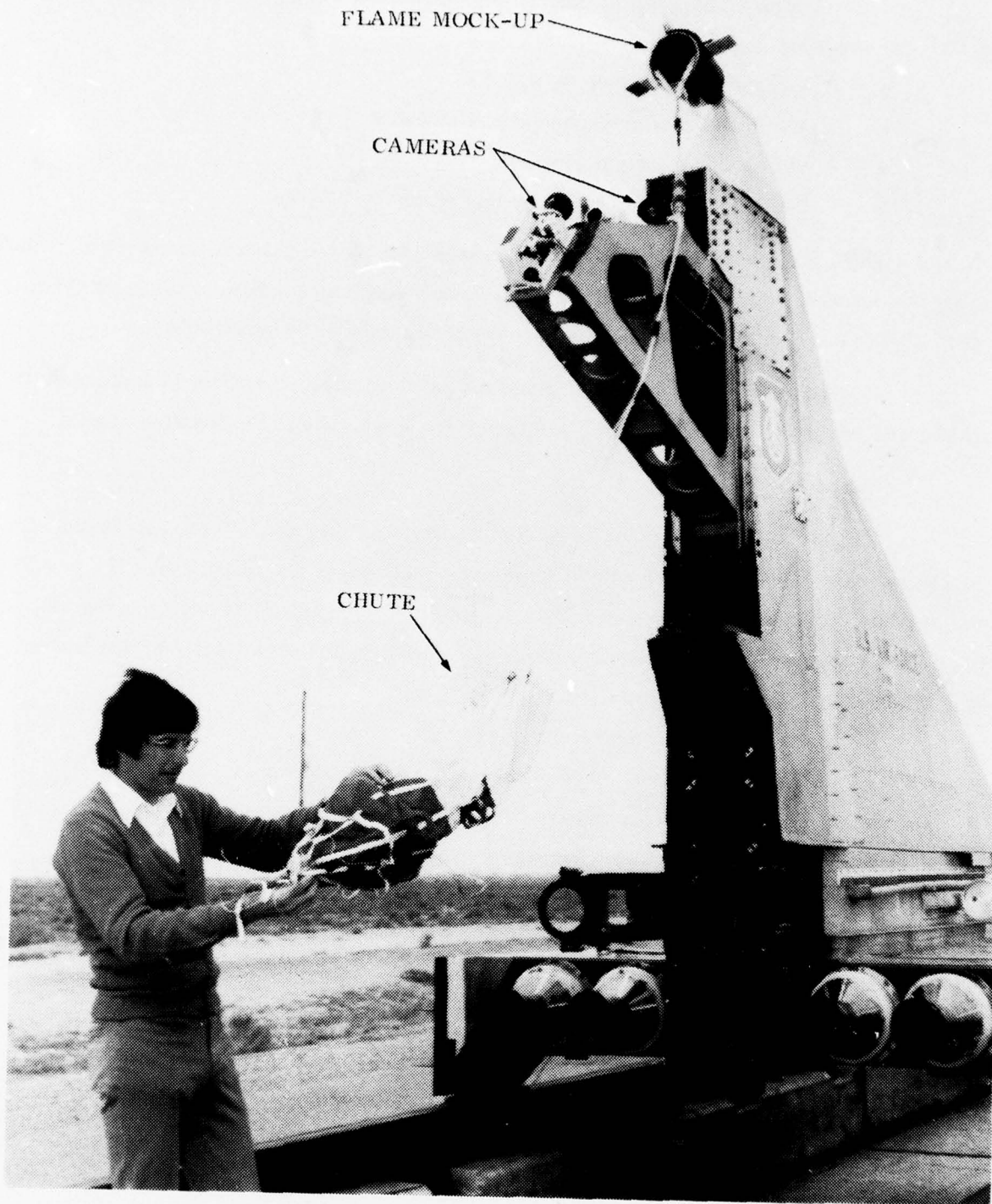


Figure 3-1. Holloman chute test installation.

4
lines. Excellent high speed motion picture coverage allowed these and several additional minor problems to be identified, and remedial action was taken at Irvin Industries on March 13.

A second sled test of the twice-modified system was conducted on March 14 and the system performed satisfactorily in all respects. The reef system worked, keeping the chute loads down during deceleration from 400 psf to 100-150 psf, at which time the reefing line was automatically cut and the chute bloomed to full diameter without parachute damage. Rebound damage to/from the beacon and battery pack was eliminated by the two-step parachute opening. The flotation bag inflated and the sonar pinger stayed in its harness. Post-test movies showed that (1) the deployment sequence was orderly with the new snubbing line modifications, (2) the mortar-sabot cleared cleanly, (3) flotation bag inflation/rebound was improved by reefing the chute, and (4) the swivel permitted orderly deployment while the R/V was spinning at 4-5 rps.

Two final minor modifications were suggested by the second test and these were to stitch the ground plane wires of the beacon to the flotation bag ribbon-harness and to increase the length of the doubler along the flotation bag check valve. These modifications, as well as the modifications discussed earlier, were incorporated into vehicles flown on Flights 003 through 006.

Figure 3-2 compares the sled velocity histories for the two runs.

3.4 Fairing Deployment Test

It is believed that on the third flight, the pyrotechnic system failed to cut the fairing away cleanly (Section 4.0). To correct this problem, the pyrotechnic system was redesigned and was tested at the Space Ordnance Systems, Inc. facility at Saugus, California. The HRV ground test model, equipped with the modified pyrotechnics and a FLAME fairing heatshield, was hung vertically by a flexible cable. The pyrotechnic system was then fired, and fairing deployment was recorded using two 1,000 frame-per-second motion picture cameras. Fairing section position histories were computed by a frame-by-frame analysis of the film data, and the resultant separation velocity and rotation rate (average for the two sections) are shown in Figure 3-3. Inspection of the severed structure and heatshield showed clean cutting action over the full length of both charges.

3.5 Sandia Sled Tests

The redesigned terminal recovery chute system used on Flights 007 and 008 was qualified on a rocket sled at the Sandia Laboratories' 5,000 ft track at Albuquerque, New Mexico. The technique used for these tests was significantly different from that used at Holloman. Rather than permanently mounting the vehicle to the sled, the vehicle was accelerated until motor burn-out,

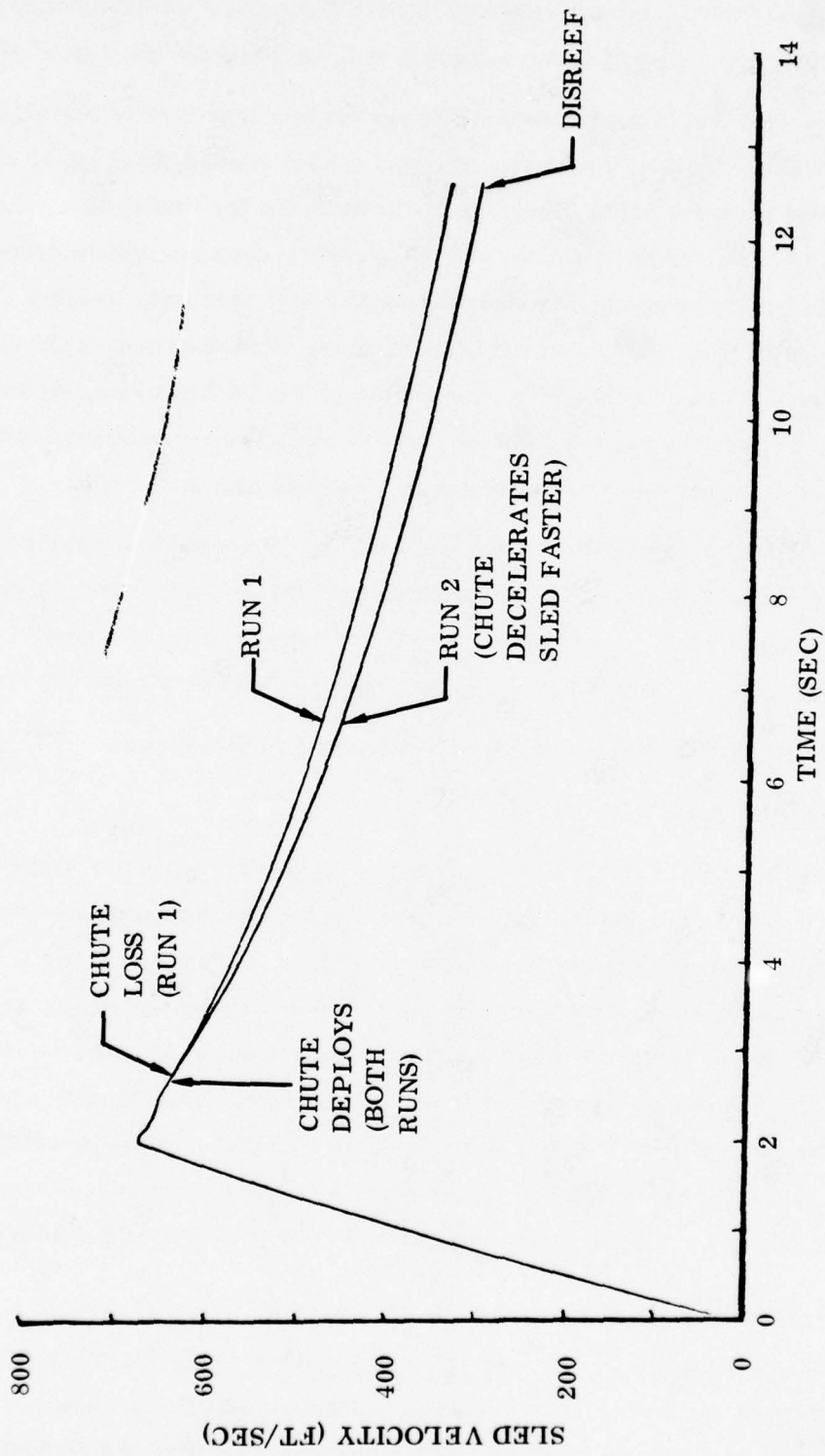
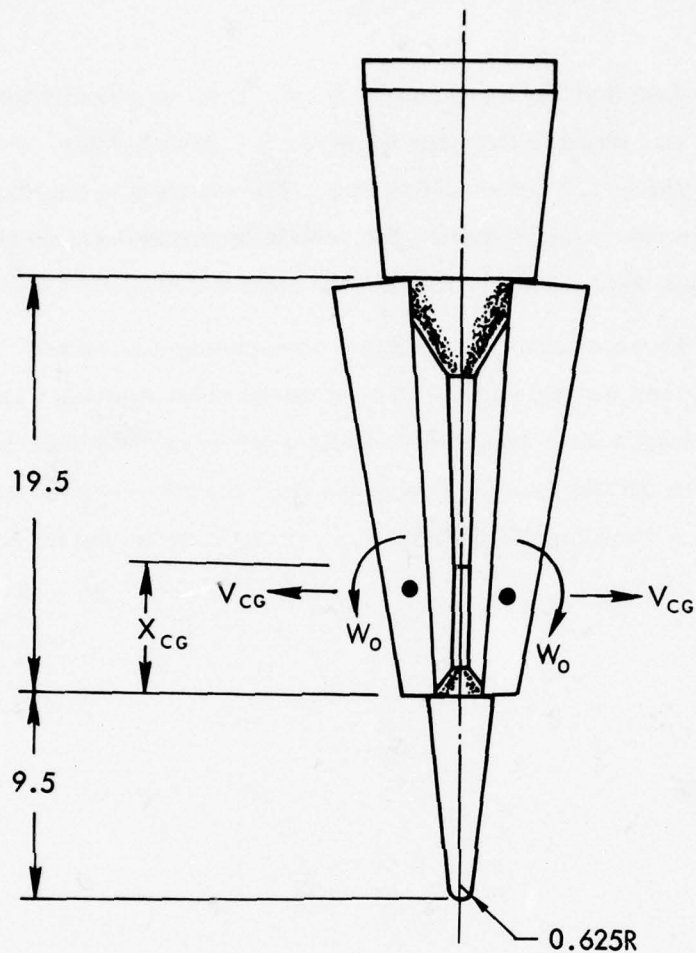


Figure 3-2. Holloman chute test velocity profiles.



	ORIGINAL SYSTEM	MODIFIED SYSTEM
LATERAL VELOCITY, V_{CG} (FPS)	49 FPS	53 FPS
ROTATION RATE, W_0 (RAD/SEC)	42 RAD/SEC	72 RAD/SEC
SECTION WEIGHT	16.5 LB	15.6 LB
ROTATIONAL INERTIA	354 LB/IN ²	330 LB/IN ² (EST)
CENTER OF GRAVITY (X_{CG})	6.6 IN.	5.7 IN.

Figure 3-3. Comparison of separation system ground test results.

then ejected upward into free flight by a pneumatic piston. Ejection velocity was approximately 110 ft/sec. The mortar was timed to fire approximately 2.1 seconds later, and the chute reefing line cutter fired approximately 1.5 seconds after that. The vehicle was approximately 120 ft above the track during parachute deployment. The vehicle impacted the ground at nearly terminal parachute descent velocity, approximately 7.5 seconds after it was ejected from the sled.

Four tests were conducted and all were completely successful. The chute performed properly on all four tests and the test vehicle was recovered undamaged each time, as shown in Figure 3-4. Tests 1 through 3 were essentially identical and ejected the vehicle when the sled was traveling between 830 and 840 ft/sec. Test 4 was conducted at lower velocity with vehicle ejection when the sled was traveling 655 ft/sec. The velocity profiles for the tests are shown in Figure 3-5.



Figure 3-4. Recovered Sandia chute test vehicle.

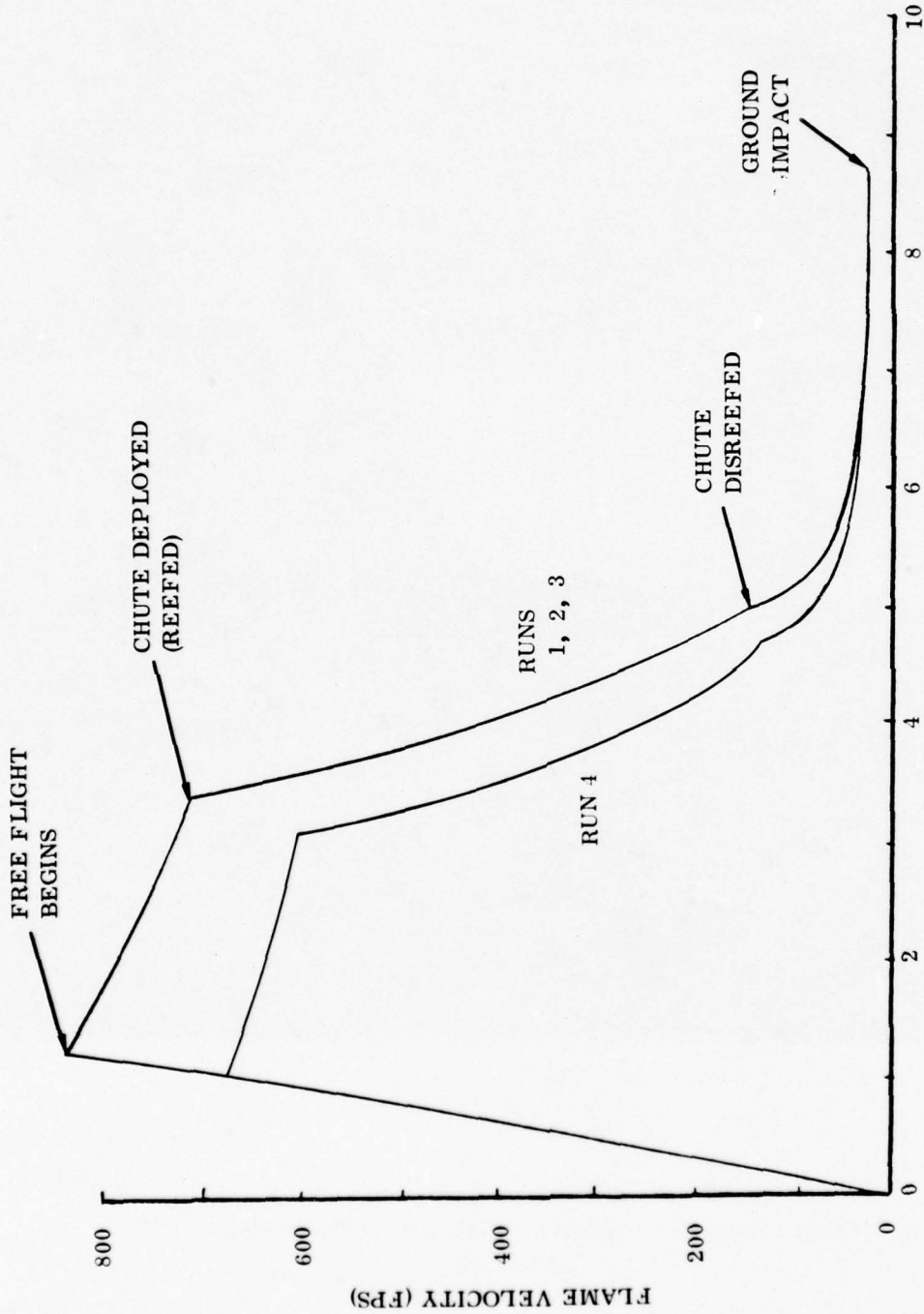


Figure 3-5. Sandia chute test velocity profile.

4.0 FLIGHT TESTS

Eight FLAME vehicles were flown with two vehicles launched from Wallops Island, Virginia, and the remainder flown at the Tonopah Test Range (TTR), operated by Sandia Laboratories at Tonopah, Nevada. Wallops Island has the advantage of being at sea level (the altitude of TTR is approximately 5000 ft) and provides more opportunity to perform hydrometeor erosion experiments. However, it was decided after the third flight that the difficulties associated with water recovery were an unacceptable drawback.

The performance of the recovery vehicles is summarized in Table 4-1 and the performance of the booster system is summarized in Table 4-2.

4.1 Flight F-001

The first FLAME flight was conducted at Wallops Island, Virginia, on 4 February 1975. The recovery vehicle characteristics were:

- Modified HRV ground test vehicle.
- CP109 nosetip with recession sensor.
- 5-watt radar transponder.
- 8 channel S-band FM/FM telemetry package.
- Weight and Static Margin | 71.97 lb and 12.5 percent before deployment
38.79 lb and 10.7 percent after deployment.

The nosetip and the recession sensor were provided by General Electric.

The aircraft launch and rocket boost phases of the flight were as planned; however, only limited data was obtained from the recovery phase. Telemetry from the vehicle ceased shortly after fairing deployment, and both radar and optical tracking were lost before parachute deployment. Recovery was hampered by bad weather and the vehicle was not found. Table 4-3 summarizes the information obtained from the various sources of flight data.

Telemetry immediately following fairing deployment showed high lateral decelerations. The radar tracked the vehicle for approximately one-half second after fairing deployment, and appeared to show a cloud of debris. Initially, it was feared that the vehicle had broken up; however, data from later flights and an evaluation of the telemetry unit indicated that the deployment was probably normal, and that the telemetry signal loss was due to battery shorting under

Table 4-1. FLAME recovery vehicle performance summary.

PROGRAM	TEST GOAL	TEST I.D.	DATE RANGE	NOSETIP	PERFORMANCE		
					SIDE PANEL DEPLOYMENT	RECOVERY	COMMENTS
HIRV	TEST RECOVERY CONCEPT	HRV-1	17 Jun 74 WSMR	ATJS	Yes (TM)	Yes	
		HRV-2	18 Jun 74 WSMR	ATJS	No test		Third Stage Booster Failure
	F-001	4 Feb 75 Wallops	CP109	Yes (TM/No Optics)	No	L.O.S. After Side Panel Deployment Probable Chute Failure	
	F-002	27 Feb 75 TTR	CP109	Yes (TM/Optics)	Yes (Chute Failure)	Redesign Chute and Overload on Rocket Sled	
	F-003	28 May 75 Wallops	SEG W	No (TM/No Optics)	No (Ordnance Failure)	Modify Ordnance System and Ground Test	
	F-004	18 Apr 75 TTR	223CC	No Test		Pedro Nozzle Failure	
	F-005	3 Jun 75 TTR	SOLID W	Yes (TM/Optics)	Yes	Late Payload Separation Modify Separation System Assy Procedure	
	F-006	4 Jun 75 TTR	Gas Jet TA-10W	No Test		Pedro Nozzle Failure	
FLAME	NOSETIP PERFORMANCE DATA	F-007	22 Jan 76 TTR	LTA	Yes (TM/Optics)	No (Ignition Angle 5.6 deg Low)	Deceleration Lower than Previous Tests Nominal Ignition Angle Would Allow Recovery
		F-008	26 Jan 76 TTR	Gas Jet TA-10W	Yes (Optics/No TM)	No	Probable Nostrip Gas Generator Failure After Side Panel Deployment

Table 4-2. FLAME booster performance summary.

Test ID	Date/Range	AIRCRAFT DROP			FIRST STAGE				SECOND STAGE			
		Altitude (ft)	Mach No.	γ (deg)	Ignition Alt (ft)	Ignition γ (deg)	Burnout Vel (ft/sec)	Burnout Roll Rate (cps)	Burnout Alt (ft)	Burnout Vel (ft/sec)	Burnout γ (deg)	
1	2/4/75 Wallops	56,000	1.36	31.1	62,750 (est)	-9.5	7828	1.3	45,000	13,206	-15.5	
2	2/27/75 TTR	55,100	1.3	30	59,914	-12.9	7836	2.2	39,103	13,157	-18.6	
3	3/28/75 Wallops	56,000	1.38	31	61,000 (est)	-11.7	7850 (est)	2.2	39,000 (est)	13,000 (est)	-18.6 (est)	
4	4/18/75 TTR	56,100	1.25	32	61,400	-10.0	7500	2.0	--	--	--	
5	6/3/75 TTR	54,600	1.2	30	59,960	-8.0	7800	N/A	N/A	13,200 (est)	N/A	
6	6/4/75 TTR	55,200	1.3	29	61,050	-8.0	7700	N/A	--	--	--	
7	1/22/76 TTR	54,500 (est)	1.1	30.5	59,350	-16.3 (est)	7750	1.46	34,000	12,500	-21.8	
8	1/26/76 TTR	55,000	1.3	31 (est)	60,000	-13.7	7850	1.43	36,000	12,750	-20.0	

Table 4-3. FLAME F-001 data source summary.

Booster Telemetry	- Data to recruit ignition (nominal)
Payload Telemetry	- L.O.S. 0.12 sec after recovery initiation
Tracking Radar	- Transponder track until approximately recovery initiation
Optics	- Trap aircraft lost track during Pedro burn (went into clouds)
Recovery Radar	- Object(s) reported breaking up at flight termination. Tracked one large piece to impact
Recovery Aircraft	- No sign of payload in estimated impact area - Possible 3-4 sec VHF beacon signal
Recovery Helicopter	- Not sent out (bad weather)
Recovery Ship	- No sonar beacon signal located (one attempt - - - no search)

the high acceleration forces. In retrospect, it seems probable that the fact that the vehicle was not recovered was due to a parachute failure such as occurred on the following flight.

Table 4-4 summarizes the critical mission parameters and Table 4-5 summarizes the conclusions reached concerning the flight. Figures 4-1 and 4-2 show the vehicle trajectory data obtained by radar.

4.2 Flight F-002

The second FLAME vehicle was flown at the Tonopah Test Range on 27 February 1975. The recovery vehicle characteristics were:

- CP109 nosetip with recession sensor.
- 5-watt radar transponder.
- 5-channel S-band FM/FM telemetry package.
- Weight and Static Margin | 75.64 lb and 13.5 percent before deployment
40.08 lb and 11.5 percent before deployment

The carbon phenolic nosetip and recession sensor were again provided by General Electric and were identical to the units flown on the previous flight.

The mission appeared to be nominal until parachute deployment. The parachute broke away from the R/V when it inflated, and the R/V impacted at high subsonic velocity. The R/V, although heavily damaged by the impact, was recovered and the parachute system was also recovered some distance away. Table 4-6 summarizes the various sources of flight data. The telemetered accelerometer data agreed well with the small amount of telemetry data obtained from Flight F-001. Figure 4-3 shows the telemetry data during the critical phases of Flight F-002. Examination of the trajectory data showed that the deceleration of the vehicle after fairing deployment was lower than anticipated, as shown in Figure 4-4. Since the parachute is deployed by a timer, this resulted in parachute deployment at 320 psf, nearly double the design dynamic pressure of 180 psf. The parachute system was redesigned to be able to withstand deployment at this higher dynamic pressure, and rocket sled tests (discussed in Section 3.3) were conducted to verify its effectiveness.

Table 4-7 summarizes the critical mission parameters and Table 4-8 summarizes the conclusions reached concerning the flight. Figures 4-5 through 4-7 show the vehicle trajectory data obtained by radar.

Table 4-4. FLAME F-001 flight data summary.

	TIME (SEC)	ALTITUDE (FEET)	GAMMA (DEG)	VELOCITY (FT/SEC)	MACH NUMBER	DYNAMIC PRESSURE LB/SQ. FT
AIRCRAFT DROP	0.0	55,600	---	1,440	1.32	-----
PEDRO IGNITION	26.3	63,900	---	1,040	-----	-----
RECRUIT IGNITION	37.2	50,400	---	8,400	-----	-----
MAX VELOCITY	39.2	44,800	---	13,200	13.6	42,150
PAYLOAD SEPARATION	39.9	44,100	-16	13,190	13.6	42,100
MAX Q	----	-----	---	-----	-----	-----
FAIRING DEPLOYMENT	42.65	34,800	---	11,900	12.3	53,500

Table 4-5. FLAME F-001 vehicle performance evaluation.

FACTOR	INITIAL CONCERN	BASED ON ADDITIONAL FLIGHT TESTS
RADAR OBSERVED DEBRIS	PIECES OF VEHICLE	FROM SUBSEQUENT TESTS FAIRING DEPLOYMENT USUALLY APPEARS TO BE VEHICLE BREAKUP
LOSS OF TLM AND TRANSPONDER SIGNALS	LOST AT BREAKUP	BATTERY SHORTED DUE TO DEPLOYMENT LOADS
HIGH LATERAL ACCELERATIONS	RESULTED IN BOOM OR OTHER STRUCTURAL FAILURE	MAGNITUDE AND DAMPING SAME AS SUBSEQUENT FLIGHTS
LOW AXIAL DECELERATION	ORDNANCE MALFUNCTION CAUSED PARTIAL DEPLOYMENT	130G DECELERATION SAME AS SUBSEQUENT FLIGHTS
NO UHF BEACON SIGNAL	BEACON DESTROYED	MAGNETIC REED SWITCH LANYARD FAILED ON SUB- SEQUENT FLIGHT
NO OBSERVED FLOTATION	-----	F-002 FLIGHT TEST CHUTE FAILED DUE TO HYPERSONIC DRAG PREDICTION BEING TOO HIGH
NO SONAR BEACON	-----	INCOMPLETE SEARCH, CURRENTS WOULD CARRY AWAY SEPARATED CHUTE

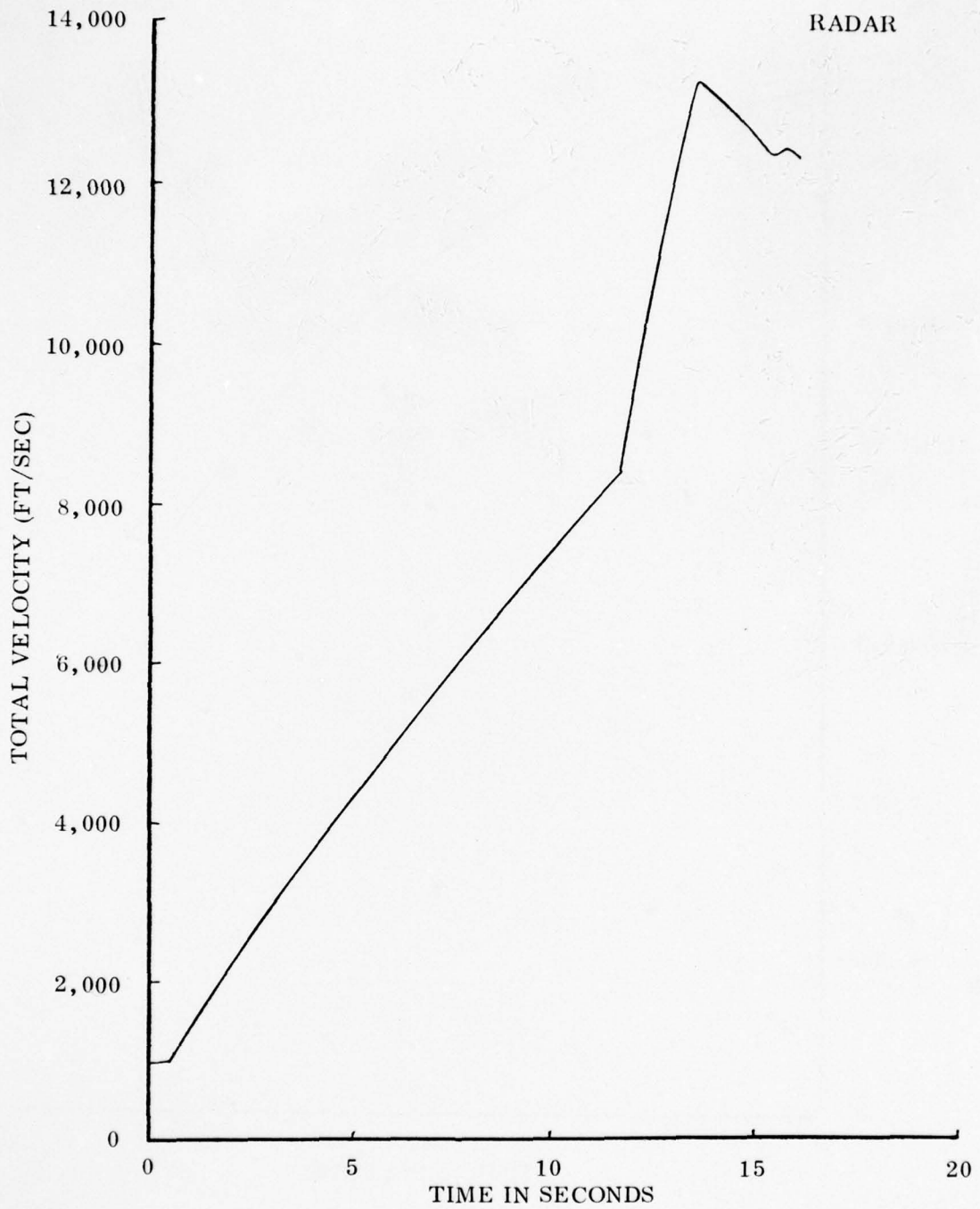


Figure 4-1. FLAME F-001 velocity history.

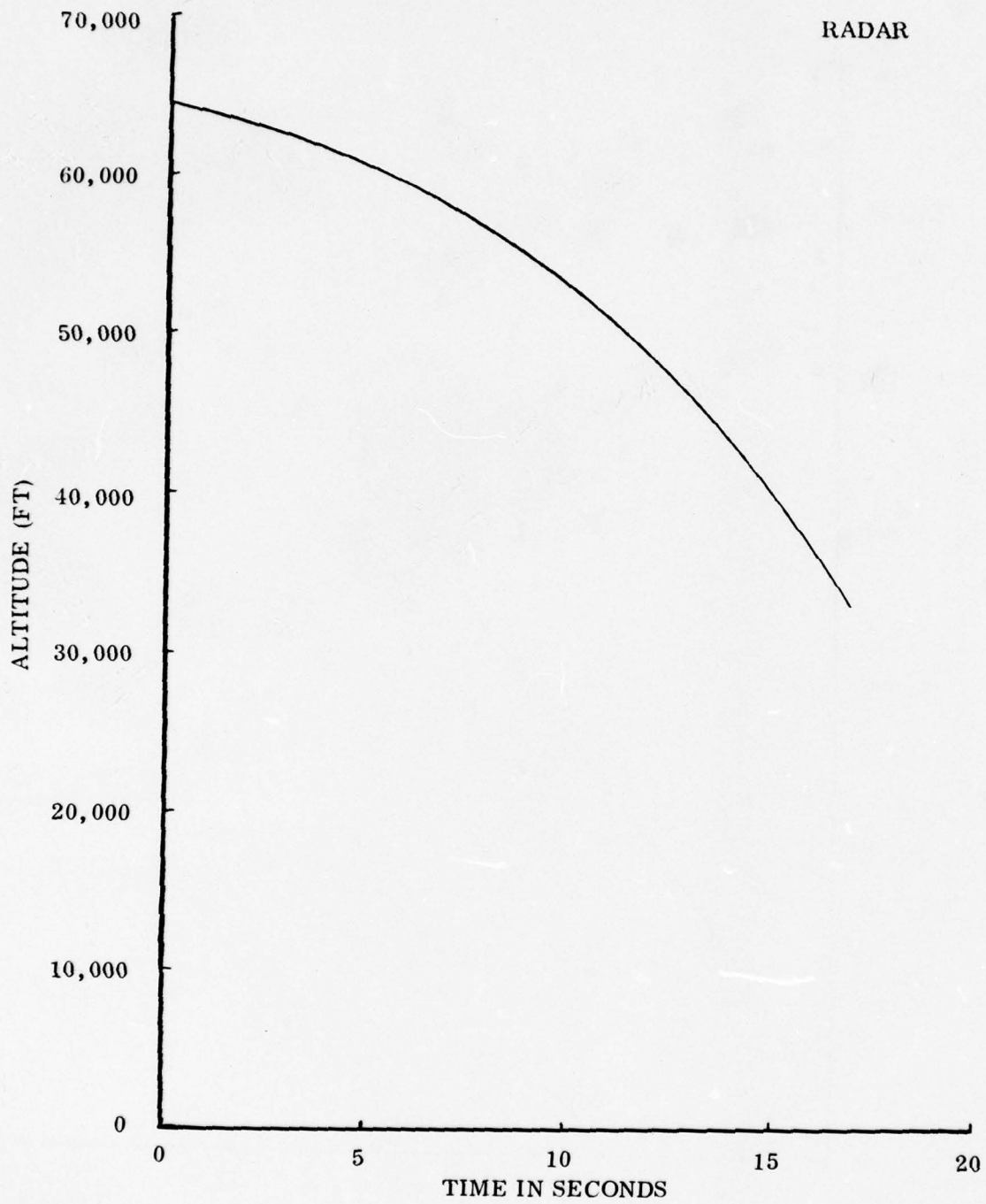


Figure 4-2. FLAME F-001 altitude history.

Table 4-6. FLAME F-002 data source summary.

PAYLOAD TELEMETRY	TRACKING RADAR	OPTICS
Good data to impact	Track to impact	Track down to 22,000 ft altitude
0-80G axial accelerometer	Good position data	
Permanently offset after deployment		Data used for decelerator performance

Table 4-7. FLAME F-002 flight data summary.

	TIME (SEC)	ALTITUDE (FEET)	GAMMA (DEG)	VELOCITY (FT/SEC)	MACH NUMBER	DYNAMIC PRESSURE LB/SQ. FT
AIRCRAFT DROP	0.00	54,790	30.2	1,290	1.3	250
PEDRO IGNITION	26.70	60,000	-13.0	1,300	1.2	193
RECRUIT IGNITION	37.51	45,090	-18.5	8,320	8.6	16,220
MAX VELOCITY	39.30	39,100	-18.5	13,160	13.8	55,730
PAYLOAD SEPARATION	39.37	37,820	-18.4	12,560	13.1	53,420
MAX Q	42.05	28,230	-19.2	11,260	11.6	60,590
FAIRING DEPLOYMENT	43.32	23,800	-19.6	10,230	9.9	57,820

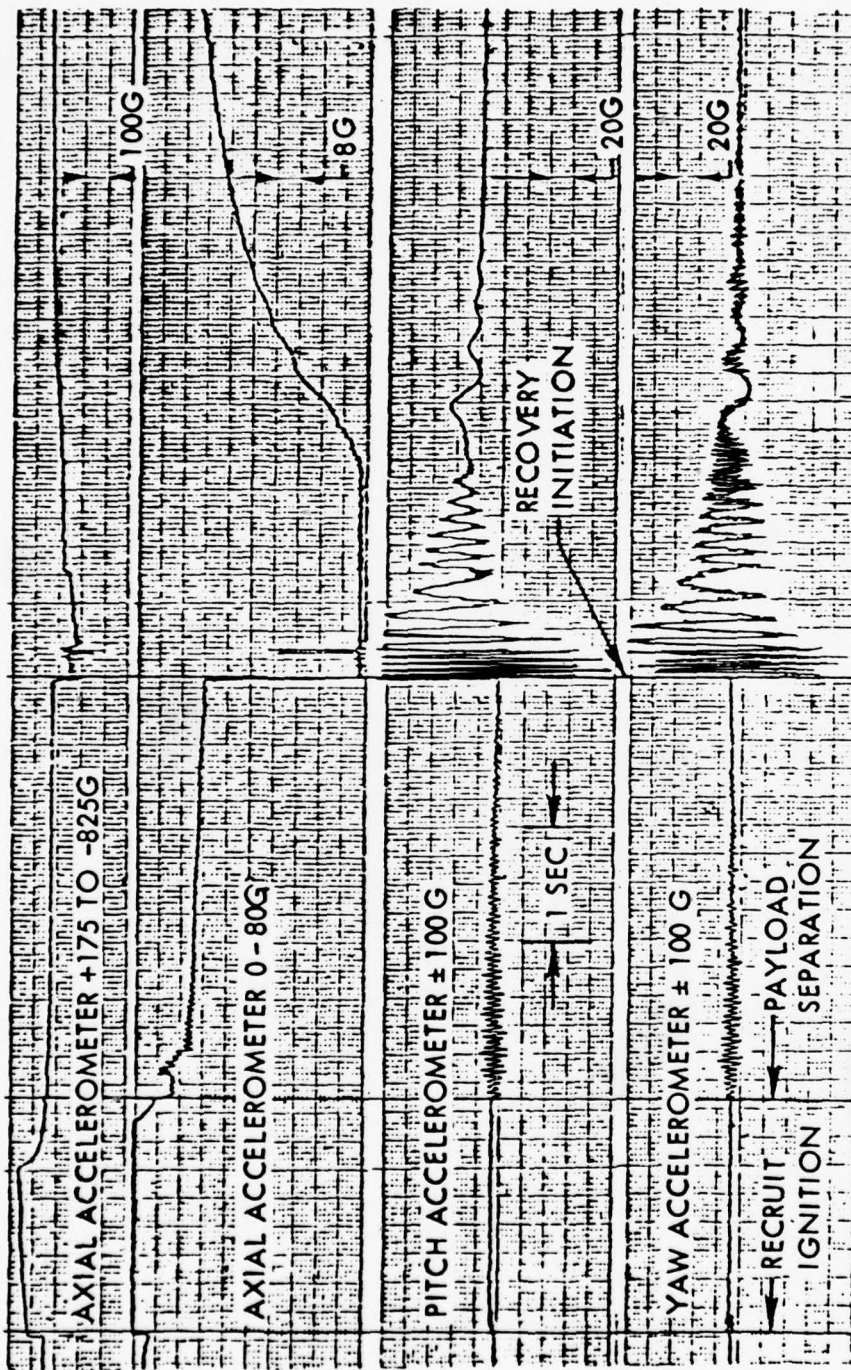


Figure 4-3. FLAME F-002 telemetry.

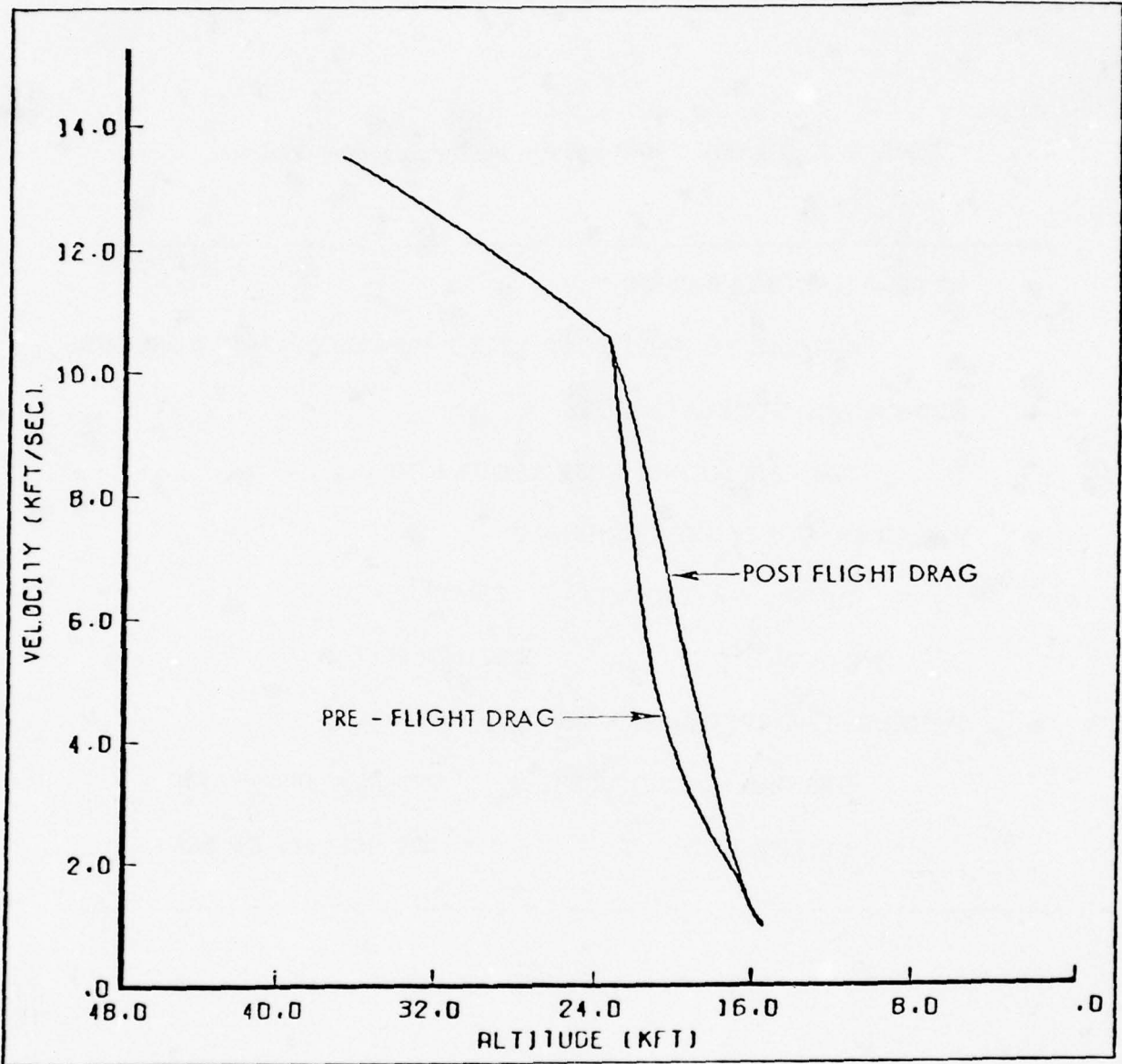


Figure 4-4. FLAME vehicle velocity as a function of altitude.

Table 4-8. FLAME F-002 vehicle performance evaluation.

- LATERAL ACCELERATION

SIMILAR TO F-001 TEST ABOUT 100G DAMPED IN 2 SECONDS

- HYPERSONIC DECELERATION

SIMILAR TO F001 TEST ABOUT 130G

- BALLISTIC COEFFICIENT CHANGE

INITIAL PREDICTION $2700/170 = 16$

ACTUAL $2700/370 = 7.3$

- PARACHUTE DEPLOYMENT

DESIGN AND DROP TEST 180 PSF 400 FT/SEC

FLIGHT TEST 320 PSF 620 FT/SEC

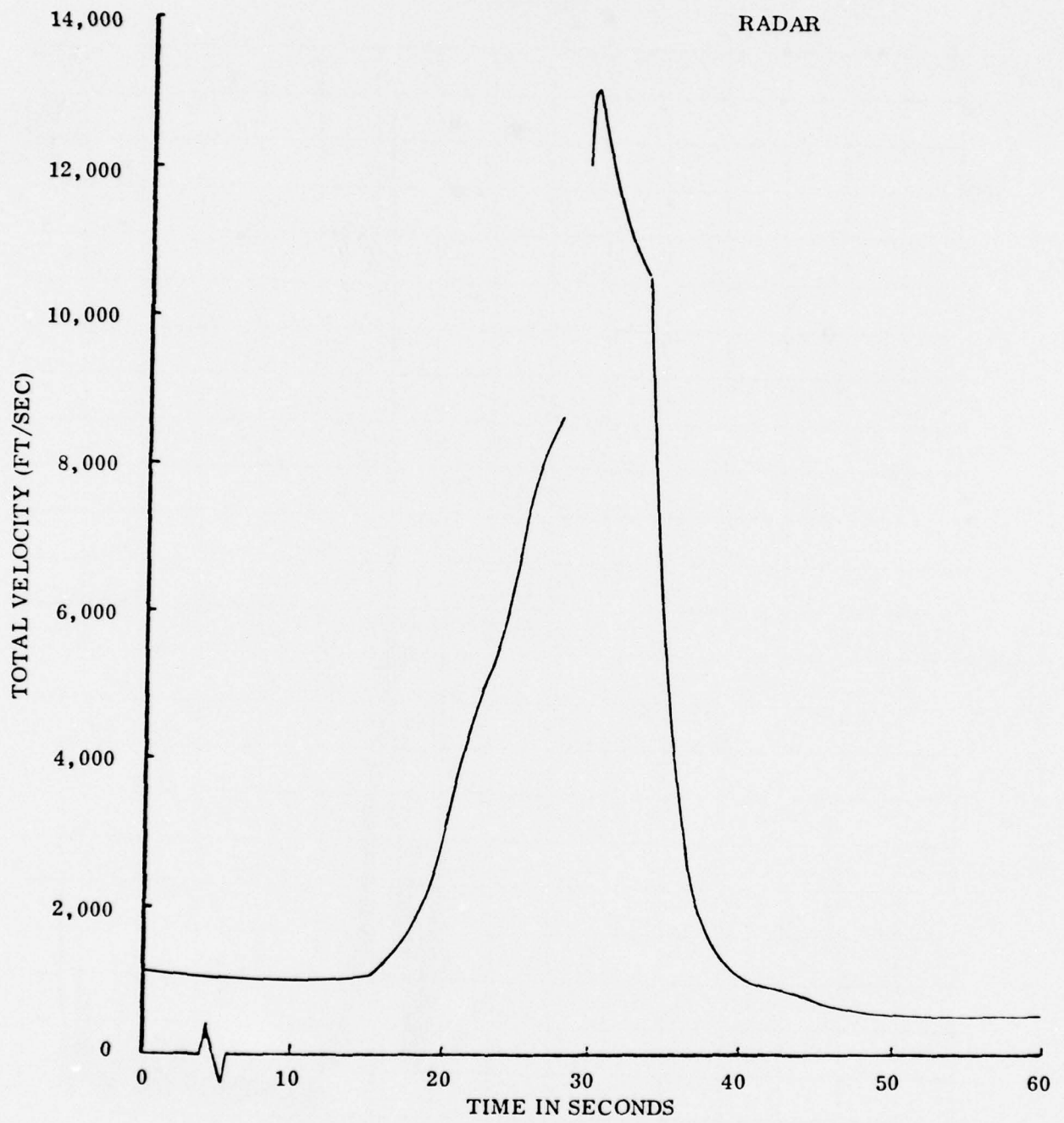


Figure 4-5. FLAME F-002 velocity history.

G VS TIME

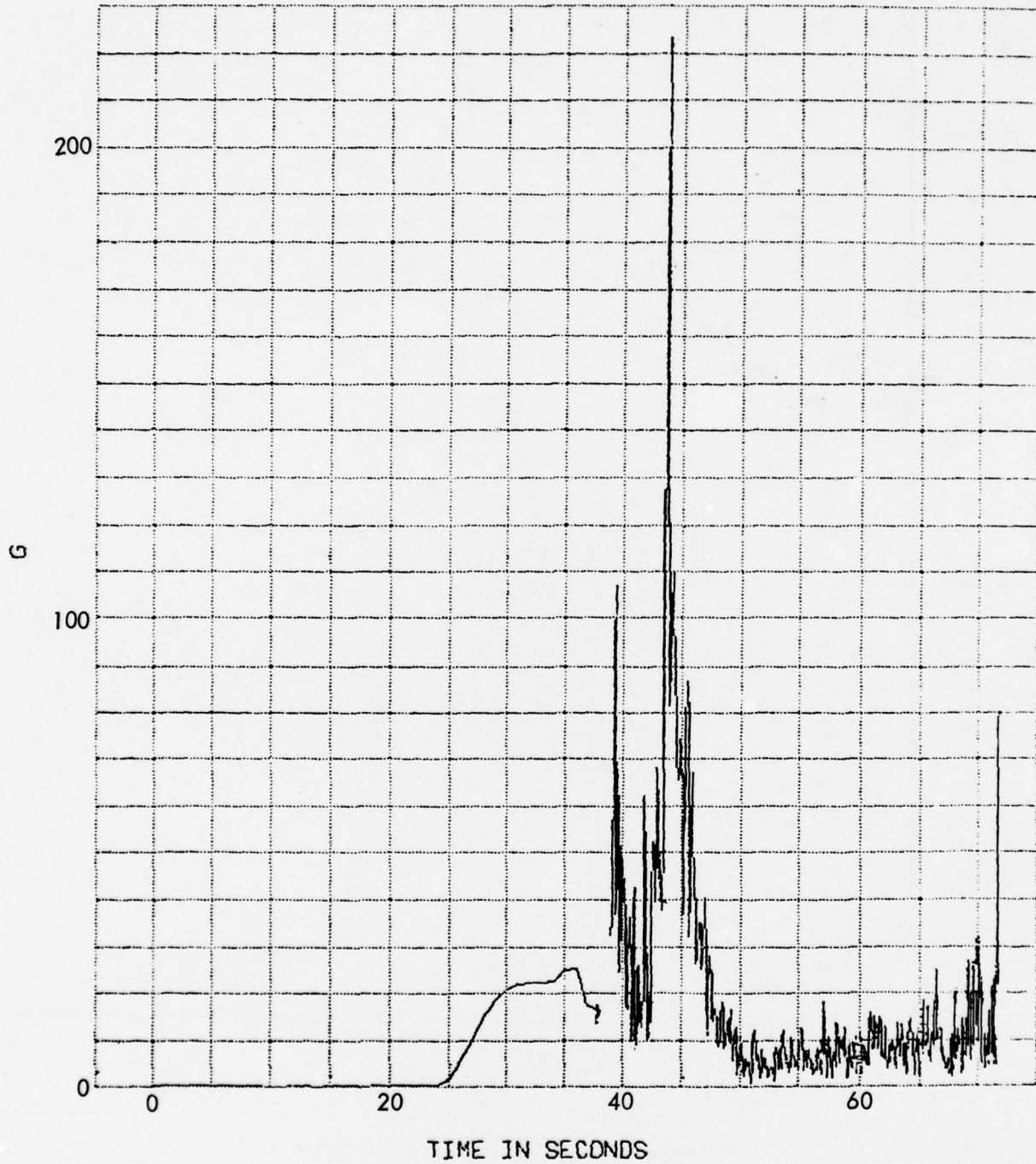


Figure 4-6. FLAME F-002 acceleration history.

ALTITUDE VS TIME

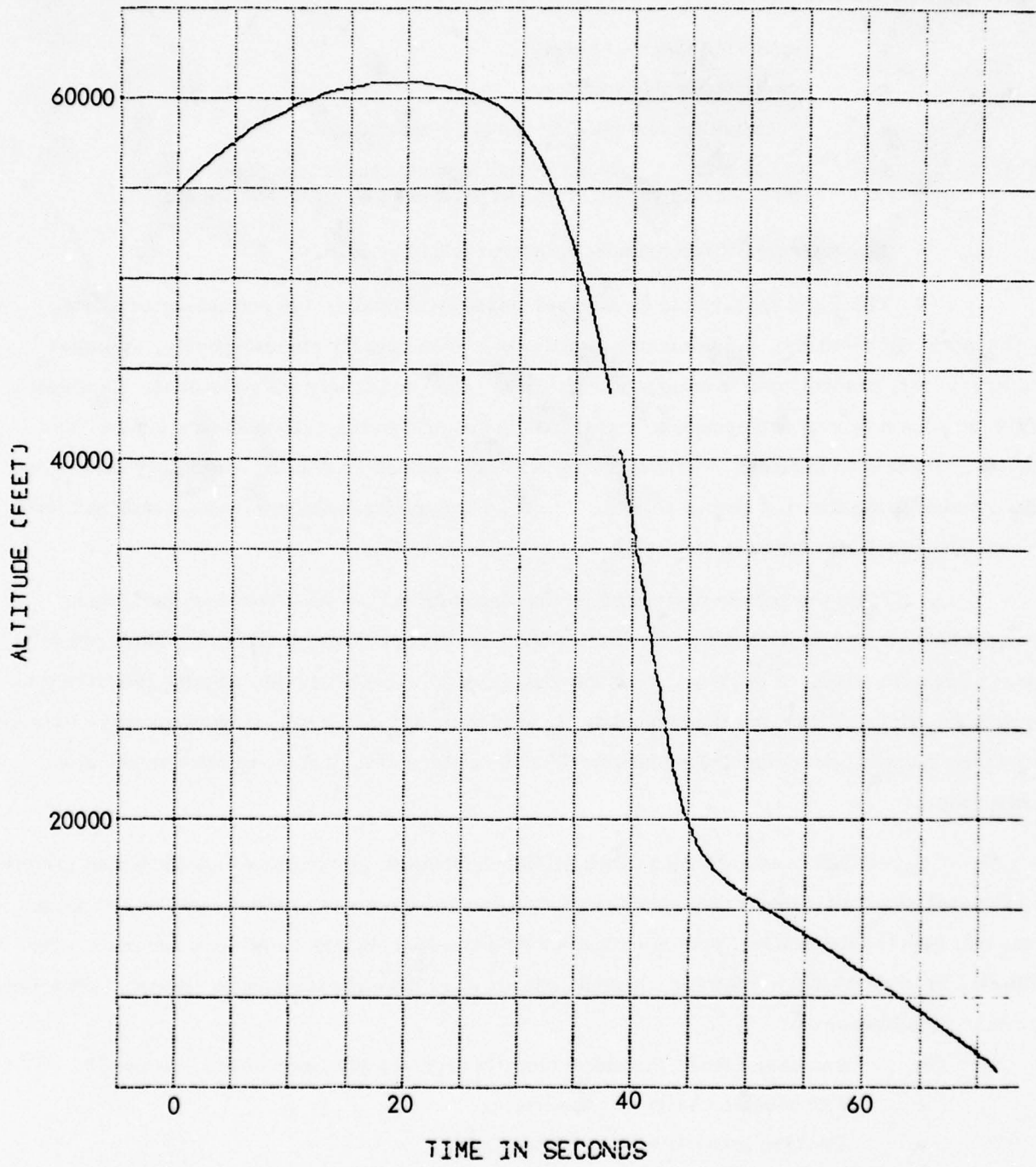


Figure 4-7. FLAME F-002 altitude history.

Flight F-003

The third flight was conducted at Wallops Island on 28 March 1975. The recovery vehicle characteristics were:

- Segmented tungsten nosetip.
- 5-watt radar transponder.
- 5-channel S-band FM/FM telemetry package.
- Weight and Static Margin | 76.65 lb and 14.4 percent before deployment
41.29 lb and 13.2 percent after deployment.

The segmented tungsten nosetip was provided by PDA.

The flight appeared to be nominal until approximately 1.6 seconds after fairing deployment. At that time, the telemetry signal was lost and nearly simultaneously, the radar track was lost, probably due to transponder failure. The vehicle was not recovered. Evaluation of the data from fairing deployment to signal loss indicated that the axial deceleration was substantially lower than expected, and that the vehicle experienced increasing oscillatory lateral and drag forces during that 1.6 second period. Table 4-9 summarizes the information obtained from the various flight data sources.

Since the vehicle drag after fairing deployment was less than that due to mass change alone, it was concluded that the fairing sections did not separate from the vehicle after the pyrotechnics fired. It is thought that only one side was completely cut, causing the fairing to spread and slip back over the drogue. Extremely high local heating caused by shock wave impingement then burned through the drogue heatshield and substructure, destroying the telemetry and transponder.

A detailed re-examination of the fairing deployment system was then conducted resulting in the conclusion that either 1) one or more of the pyrotechnic devices did not function, or 2) the bolts that held the two fairing segments together during assembly had never been removed. The following procedural and pyrotechnic system changes were developed to ensure against a recurrence of either possible cause:

- Increase Linear Flexible Shaped Charge (LFSC) from 10 to 15 Grains/ft.
- Add booster charges to manifolds.
- Positive inspection of LFSC standoff.
- X-ray centerbody with installed ordnance.
- Provide detailed written assembly procedures.

Table 4-9. FLAME F-003 data source summary.

PAYLOAD TELEMETRY	—	GOOD DATA THRU DEPLOYMENT L.O.S 1.62 SECONDS AFTER DEPLOYMENT
TRACKING RADAR	—	GOOD DATA THRU DEPLOYMENT LOST TRACK 1.66 SECONDS AFTER DEPLOYMENT
OPTICS	—	NOT ATTEMPTED

A ground test (described in Section 3.4) of the redesigned system was then conducted, and the system was found to function properly.

Table 4-10 summarizes the critical mission parameters, and Table 4-11 summarizes the conclusions reached concerning the flight. Figures 4-8 and 4-9 show the vehicle trajectory data obtained by radar.

4.4 Flight F-004

Due principally to the problems encountered on recovery, it was decided to fly the remainder of the FLAME flights at the Tonopah Test Range. Flight F-004 was flown there on 18 April 1975. The recovery vehicle characteristics were:

Table 4-10. FLAME F-003 flight data summary.

	TIME (SEC)	ALTITUDE (FEET)	GAMMA (DEG)	VELOCITY (FT/SEC)	MACH NUMBER	DYNAMIC PRESSURE LB/SQ. FT
AIRCRAFT DROP	0.0	56,400	---	1,340	1.3	-----
PEDRO IGNITION	27.52	62,900	---	1,100	----	-----
RECRUIT IGNITION	39.19	48,000	---	8,200	----	-----
MAX VELOCITY	41.29	41,100	---	12,800	13.2	47,300
PAYLOAD SEPARATION	41.29	41,100	---	12,800	13.2	47,300
MAX Q	-----	-----	---	-----	----	-----
FAIRING DEPLOYMENT	47.02	20,700	---	9,300	8.9	54,000

Table 4-11. FLAME F-003 vehicle performance evaluation.

- LATERAL ACCELERATION
 - LOWER AMPLITUDE AND FREQUENCY THAN PREVIOUS TESTS
 - AMPLITUDE AND FREQUENCY INCREASE AFTER DEPLOYMENT
- HYPERSONIC DECELERATION
 - INITIAL DECELERATION LOWER THAN MASS JETTISON ALONE
 - AXIAL DECELERATIONS BECOME OSCILLATORY ABOUT THE INITIAL NOMINAL LEVEL AND INCREASE IN MAGNITUDE TO $\pm 80G$
- OVERALL CONCLUSIONS
 - STRUCTURAL TIE(S) EXISTED BETWEEN CENTERBODY SECTIONS AT COMPLETION OF ORDNANCE SYSTEM FUNCTION
- POSSIBLE CAUSES
 - INCOMPLETE ORDNANCE FUNCTION (ONE SHAPED CHARGE DID NOT COMPLETELY CUT FAIRING)
 - BALLAST BOLTS NOT REMOVED

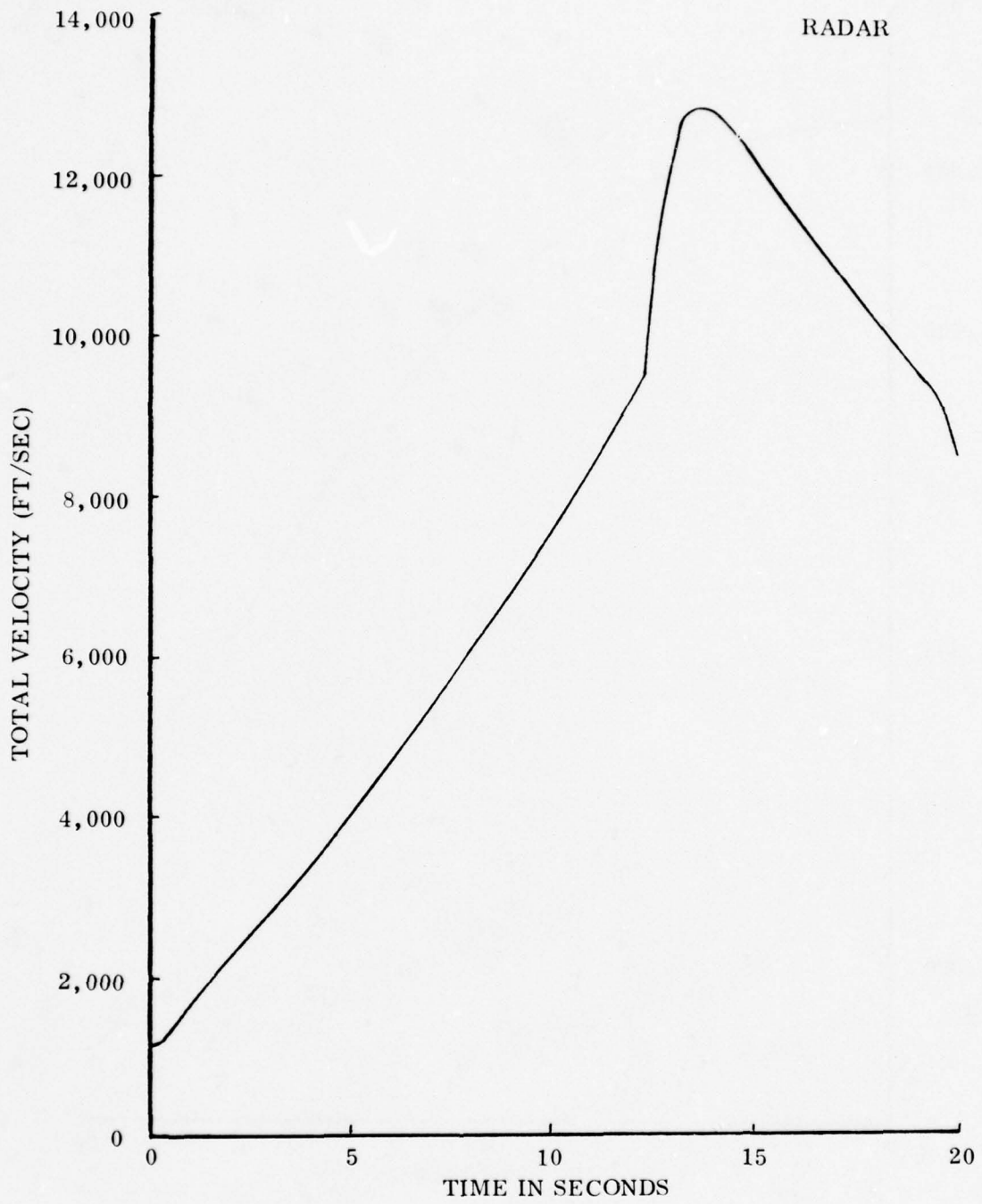


Figure 4-8. FLAME F-003 velocity history.

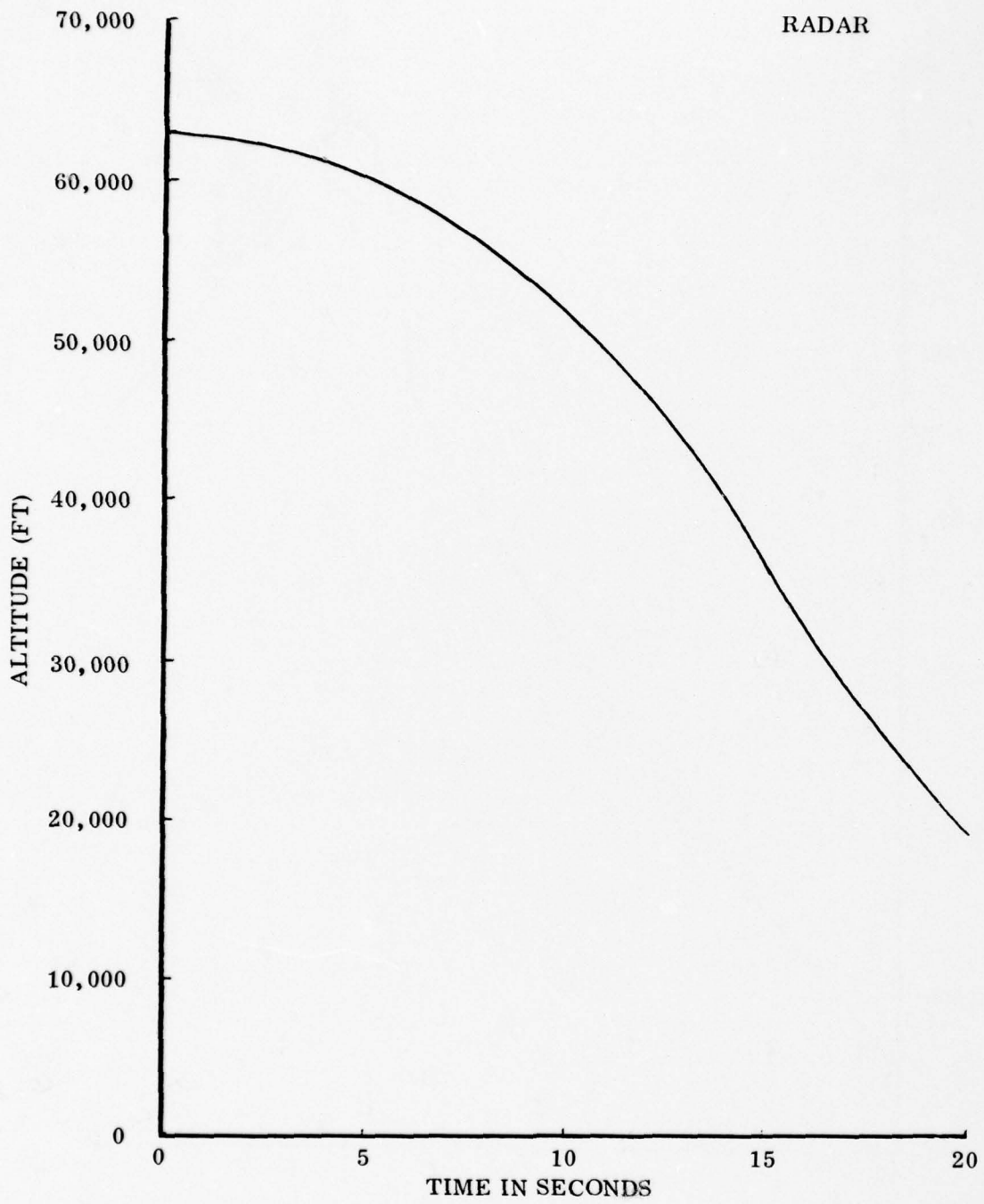


Figure 4-9. FLAME F-003 altitude history.

- 223 CC nosetip.
- 5-watt radar transponder.
- 5-channel S-band FM/FM telemetry package.
- Weight and Static Margin | 77.09 lb and 14.1 percent before deployment
41.48 lb and 13.0 percent after deployment.

The 223 carbon-carbon nosetip was provided by General Electric. This flight was negated by a failure of the first stage (Pedro) rocket motor nozzle, causing the vehicle to break up in flight. The payload was stable to impact despite a rearward center-of-gravity shift caused by a portion of the second stage that remained attached to the recovery vehicle base.

Table 4-12 summarizes the flight data obtained and Table 4-13 summarizes the conclusions reached concerning the flight. The flight trajectory is given in Figures 4-10 through 4-12.

4.5 Flight F-005

Flight F-005 was flown at the Tonopah Test Range on 3 June 1975. The recovery vehicle characteristics were:

- Solid tungsten nosetip.
- Ultrasonic recession sensor.
- No radar transponder.
- 5-channel S-band FM/FM telemetry package.
- Acoustic boundary layer transition sensor.
- Weight and Static Margin | 76.93 lb and 15.0 percent before deployment
41.37 lb and 14.0 percent after deployment.

The tungsten nosetip was provided by PDA, and the radar transponder was removed to provide volume for a nosetip recession sensor.

The mission was nearly nominal except for the fact that the entry angle was less steep than desired. Pedro ignition was planned at a shallower than nominal entry angle; however, due to a pilot error in releasing the vehicle from the aircraft, ignition occurred at an entry angle even shallower than planned. Consequently, the trajectory was substantially milder than desired. Due to the deletion of the transponder, the radar could not track the R/V, and unfortunately the optical tracking system lost track at fairing deployment. The vehicle was recovered undamaged, and the nosetip provided valuable information on the ablation of tungsten nosetips. The acoustic

Table 4-12. FLAME F-004 data source summary.

●	PAYLOAD TELEMETRY	-	GOOD DATA TO IMPACT
●	TRACKING RADAR	-	TRACK TO IMPACT
●	OPTICS	-	TRACK THROUGH PEDRO NOZZLE MALFUNCTION

Table 4-13. FLAME F-004 vehicle performance evaluation.

-
- NO TEST
 - PEDRO NOZZLE FAILURE NEAR END OF BURN RESULTED IN BREAK OFF OF 2ND STAGE AND PAYLOAD FROM 2ND STAGE
 - FAILURE OCCURRED AT BOLT PATTERN AFT OF PAYLOAD SEPARATION PLANE
 - PAYLOAD FLEW STABLE TO IMPACT WITH ADDITIONAL 7 LBS OF ELECTRONICS AND SEPARATION MECHANISM ATTACHED TO THE BASE
-

TOTAL VELOCITY VS TIME

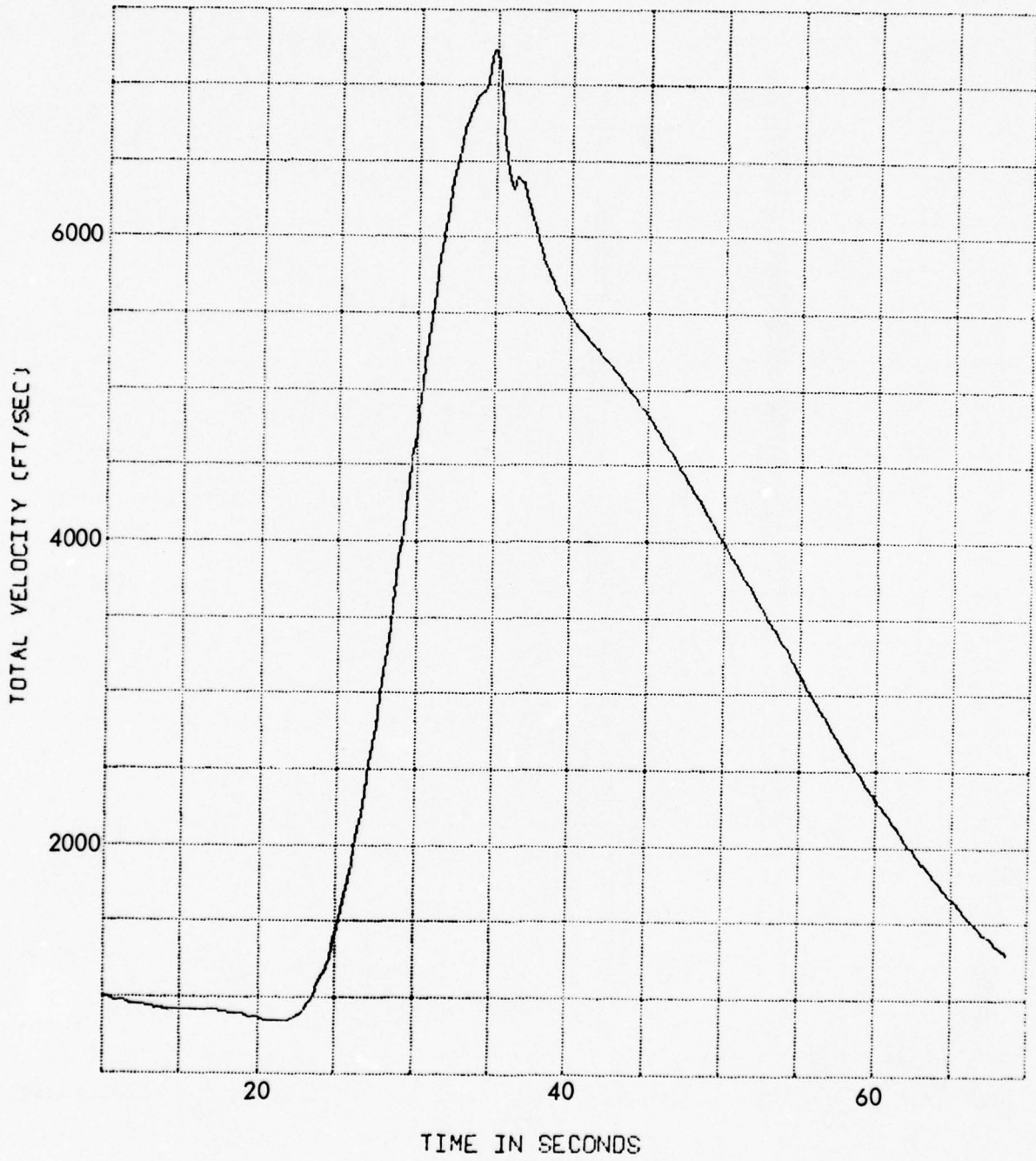


Figure 4-10. FLAME F-004 velocity history.

G VS TIME

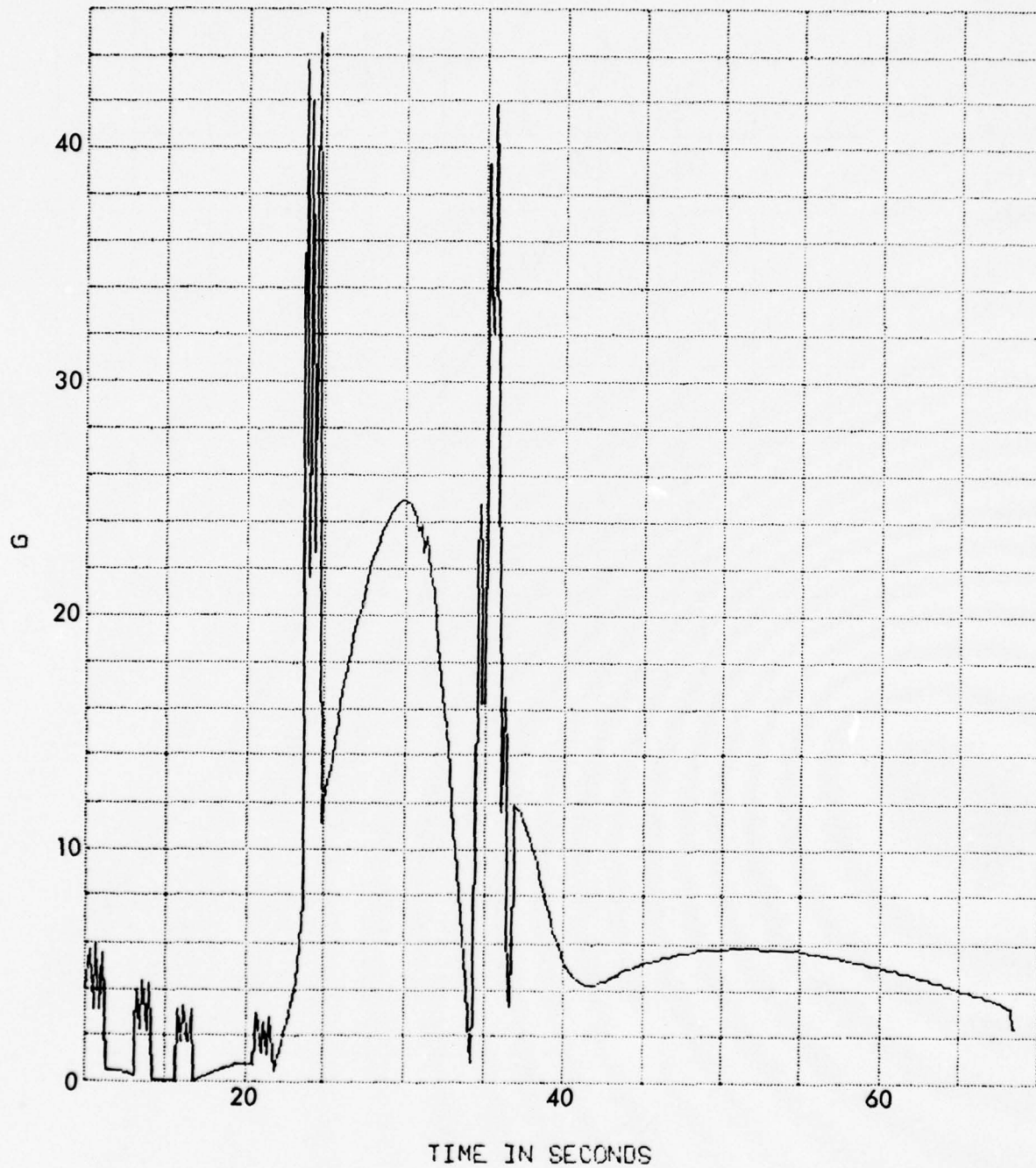


Figure 4-11. FLAME F-004 acceleration history.

ALTITUDE VS TIME

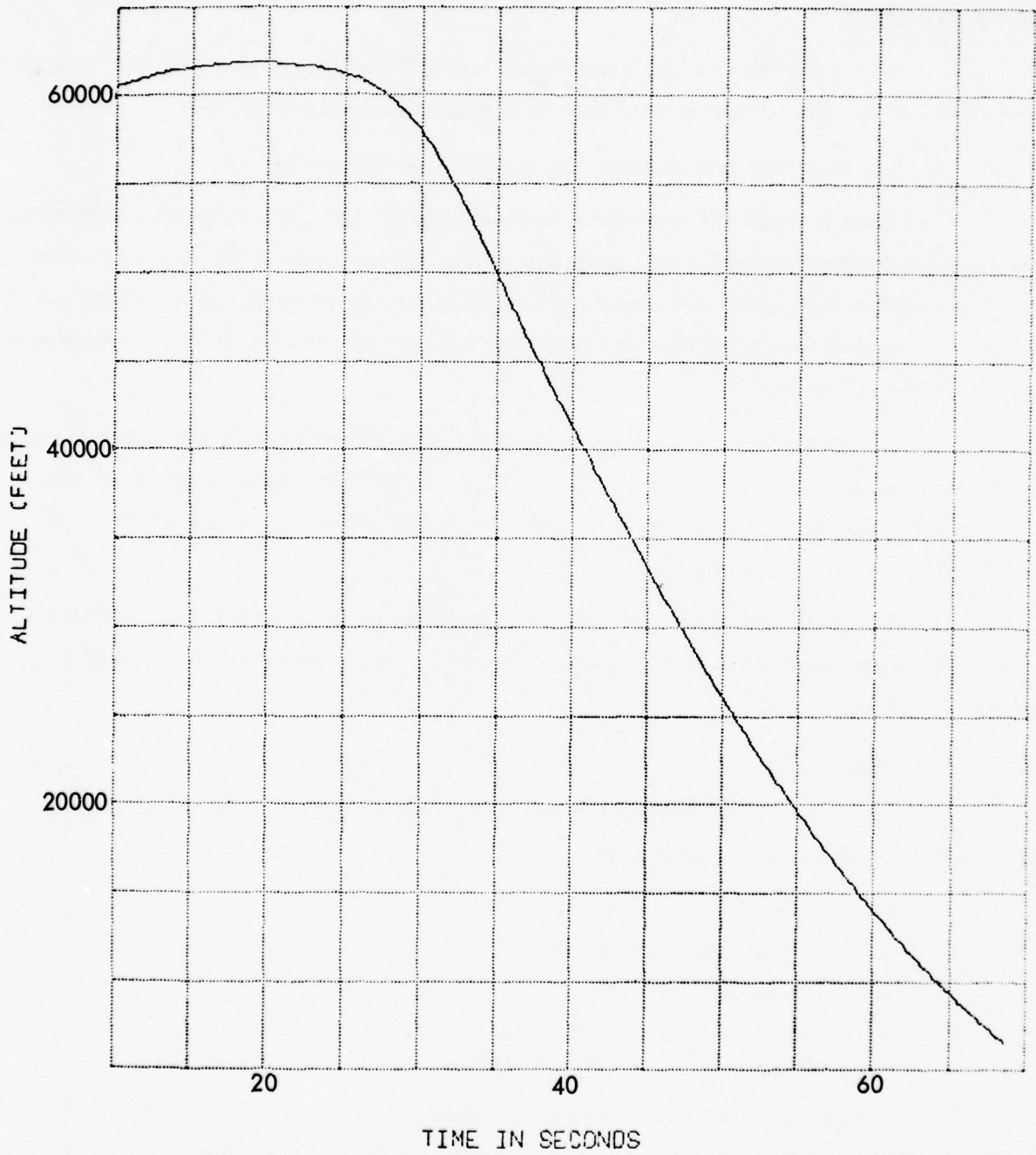


Figure 4-12. FLAME F-004 altitude history.

transition sensor indicated boundary layer transition approximately 0.5 second before Pedro burn-out. Due to the low nosetip recession produced by the mild trajectory, the nosetip recession sensor data signal-to-noise ratio was too low to allow any conclusions to be reached concerning sensor performance.

The recovered R/V was found to have a bent boom and a damaged drogue heatshield as shown in Figure 4-13. The recovered nosetip is shown in Figure 4-14.

The flight test data obtained is summarized in Table 4-14.

Since no trajectory data was obtained during recovery, the probable trajectory has been reconstructed from vehicle aerodynamic data obtained from previous flights and from the trajectory conditions at fairing deployment obtained from the optical tracker data. Figures 4-15 through 4-17 compare the trajectories and stagnation pressure histories calculated for the nominal, planned, and actual trajectories.

Evaluation of the data indicates that the boom and heatshield damage were caused by asymmetric separation from the second (Recruit) stage rocket motor casing. Except for this problem and the fact that the axial accelerometer failed shortly after fairing deployment, the recovery vehicle performed properly.

The critical mission parameters are summarized in Table 4-15 and conclusions regarding the flight are listed in Table 4-16. The optical trajectory data obtained is shown in Figures 4-18 through 4-20.

4.6 Flight F-006

The sixth FLAME vehicle was flown on 4 June 1975 at the Tonopah Test Range. The recovery vehicle characteristics were:

- Ta-10W gas jet nosetip.
- 5-watt payload transponder.
- No payload telemetry.
- Weight and Static Margin | 81.46 lb and 12.9 percent before deployment
45.27 lb and 12.6 percent after deployment.

The gas jet nosetip was supplied by Martin-Marietta. The nosetip consisted of a Ta-10W tip with an axial centerline passage connected to a 2,500 psi gas generator in the drogue. The passage through the boom was lined with a ceramic insulator to protect the boom tube from the high temperature gases. The gas generator was ignited by a timer 5.5 seconds after Pedro



Figure 4-13. Damaged boom and drogue heatshield.



Figure 4-14. Recovered tungsten nosetip from FLAME F-005.

Table 4-14. FLAME F-005 data source summary.

- PAYLOAD TELEMETRY
 - GOOD RECEPTION TO IMPACT
 - +175 TO -825G ACCELEROMETER LOST .3 SECONDS AFTER DEPLOYMENT
 - 0-80 G ACCELEROMETER WAS REPLACED BY ACOUSTIC TRANSITION SENSOR
 - TRACKING RADAR
 - LOST TRACK AT PEDRO BURN OUT
 - RADAR TRANSPONDER WAS LOCATED IN PEDRO
 - OPTICS
 - LOST TRACK AT FAIRING DEPLOYMENT
-

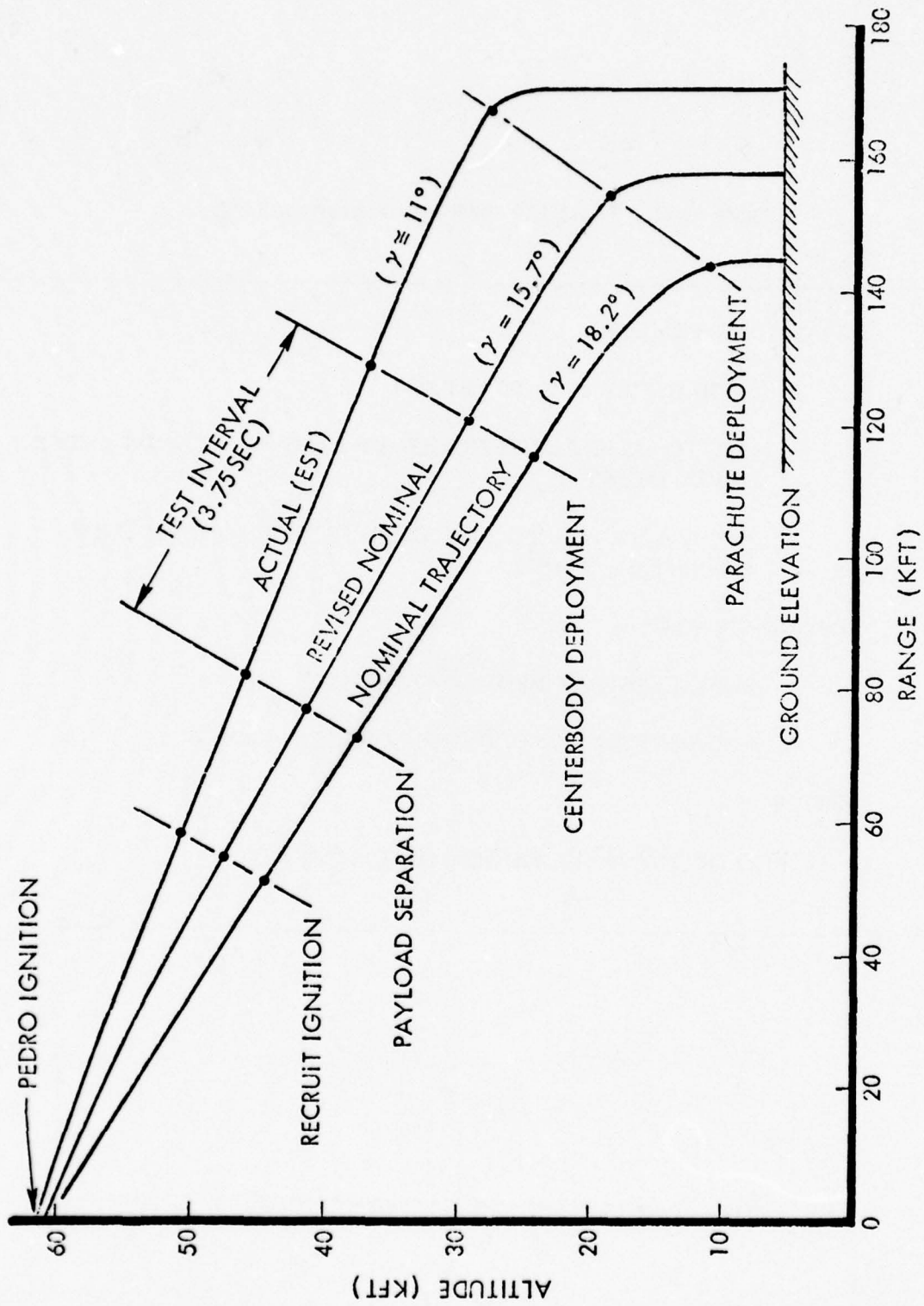


Figure 4-15. FLAME F-005 calculated altitude versus range comparison.

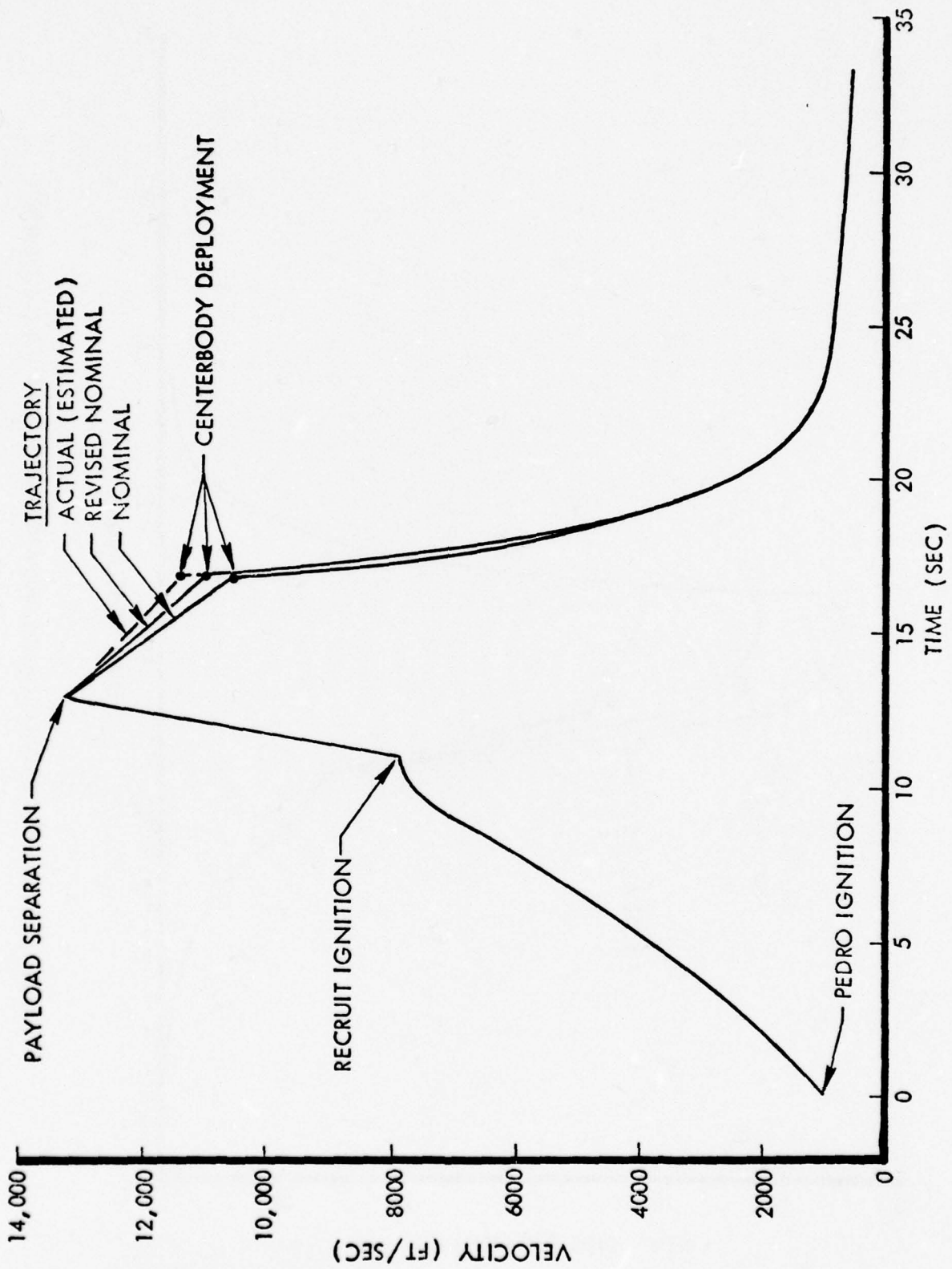


Figure 4-16. FLAME F-005 calculated velocity history comparison.

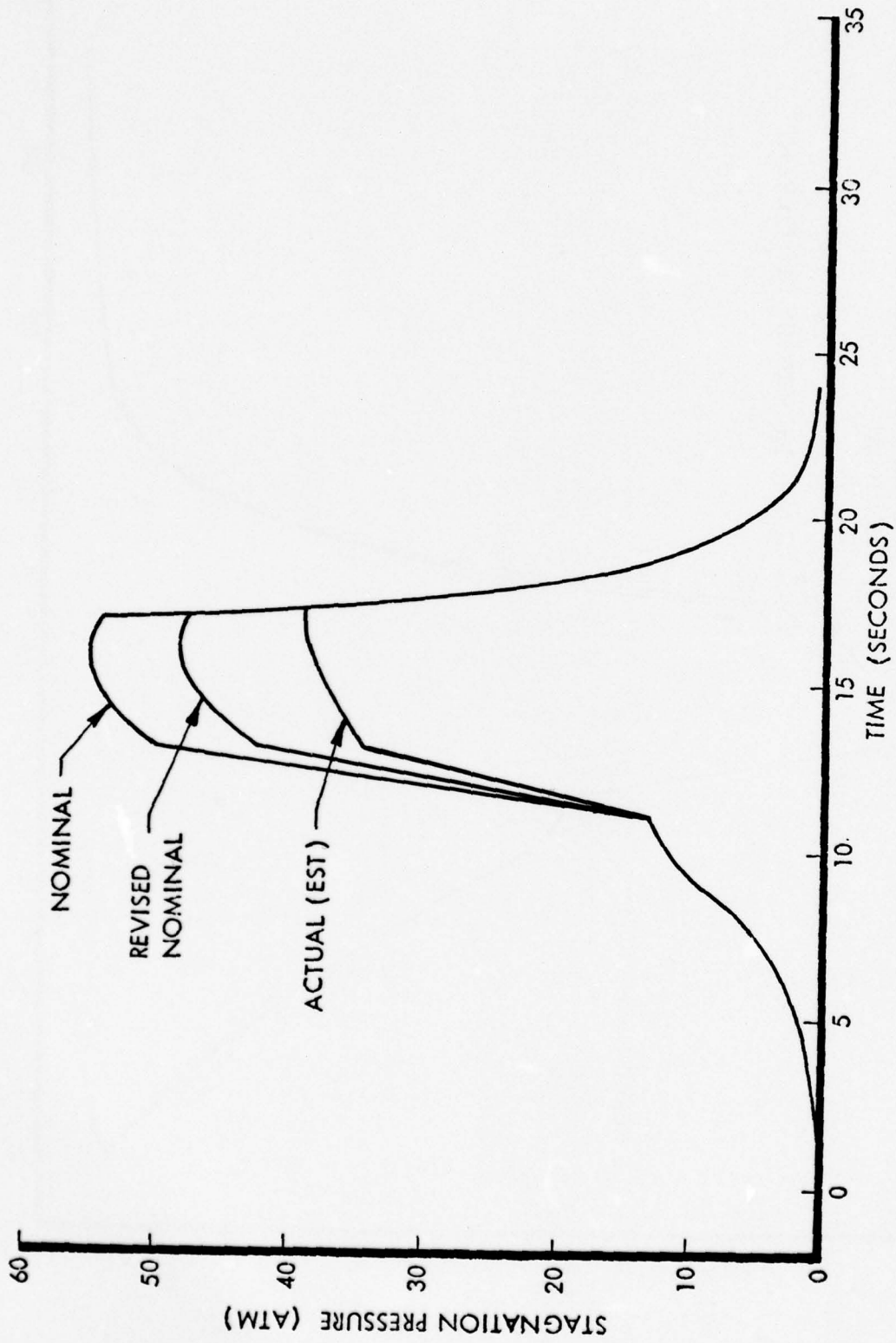


Figure 4-17. FLAME F-005 calculated stagnation pressure history comparison.

Table 4-15. FLAME F-005 flight data summary.
(Based on trajectory reconstruction)

	TIME (sec)	ALTITUDE (feet)	GAMMA (deg)	VELOCITY (ft/sec)	MACH NUMBER	DYNAMIC PRESSURE (lb/sq ft)
Aircraft Drop*	0.00	54,699	30.10	1,239	1.280	223
Pedro Ignition	20.30 ⁽¹⁾	60,164	- 4.53	957	.990	102
Recruit Ignition	30.70 ⁽¹⁾	52,562	-11.25	7,343	7.590	8,681
Maximum Velocity	33.35 ⁽¹⁾	47,364	-11.54	13,013	13.530	35,926
Payload Separation	34.20 ⁽²⁾	48,105	-11.59	13,073	13.500	34,050
	32.78 ⁽¹⁾	48,811	-11.31	12,615	13.160	34,179
Maximum Q	37.95 ⁽²⁾	38,474	-11.92	11,366	11.740	40,813 44,900 ⁽¹⁾
Fairing Deployment	36.56 ⁽¹⁾	38,474	-11.92	11,366	11.740	40,813
Chute Deployment	56.20 ⁽²⁾	26,127	-33.78	745	.737	284.7
Chute Disreef	60.20 ⁽²⁾	24,811	-44.78	401.9	.395	86.68
Impact	257.64 ⁽²⁾	5,600	-90.00	83.4	----	----

* From radar release conditions.

(1) From optics.

(2) From "Thrust" program.

Table 4-16. FLAME F-005 vehicle performance evaluation.

- LATERAL ACCELERATION
 - INITIALLY LOWER MAGNITUDE THAN PREVIOUS TESTS
 - AFTER .3 SECOND ABRUPT INCREASE IN MAGNITUDE AND FREQUENCY
 - 4 SECONDS TO DAMP VERSUS 2 SECONDS FOR F-002

 - HYPERSONIC DECELERATION
 - 240G DECELERATION FOR .3 SECONDS WHEN ACCELEROMETER STOPS FUNCTIONING

 - PARACHUTE DEPLOYMENT
 - PARACHUTE AND REEFING SYSTEM PERFORMED PROPERLY
 - PARACHUTE DESCENT RATE NEAR PREDICTED 85 FPS
 - FLOTATION BAG INFLATED WHEN RECOVERED
 - LANYARD FOR UHF TRANSMITTER BATTERY REED SWITCH FAILED

 - NOSETIP
 - SMOOTH SYMMETRIC ABLATION
 - NO APPARENT CRACKS

 - CONCLUSIONS
 - T/M AND OPTICS DATA INDICATE CONCLUSIVELY THAT THE PAYLOAD WAS MECHANICALLY ATTACHED TO THE RECRUIT UNTIL .3 SECONDS AFTER RECOVERY INITIATION
 - AN EVENT INDICATED BY BOTH LATERAL ACCELEROMETERS, THE AXIAL ACCELEROMETER, AND OPTICS OCCURRED AT THE SCHEDULED TIME FOR PAYLOAD SEPARATION
 - BOTH OPTICS AND T/M INDICATE THE PAYLOAD SEPARATED AT A SIGNIFICANT ANGLE OF ATTACK
 - THE BENT BOOM AND DROGUE HEATSHIELD DAMAGE WERE PROBABLY CAUSED BY THE ABOVE MISALIGNMENT AT SEPARATION
-

TOTAL VELOCITY VS TIME

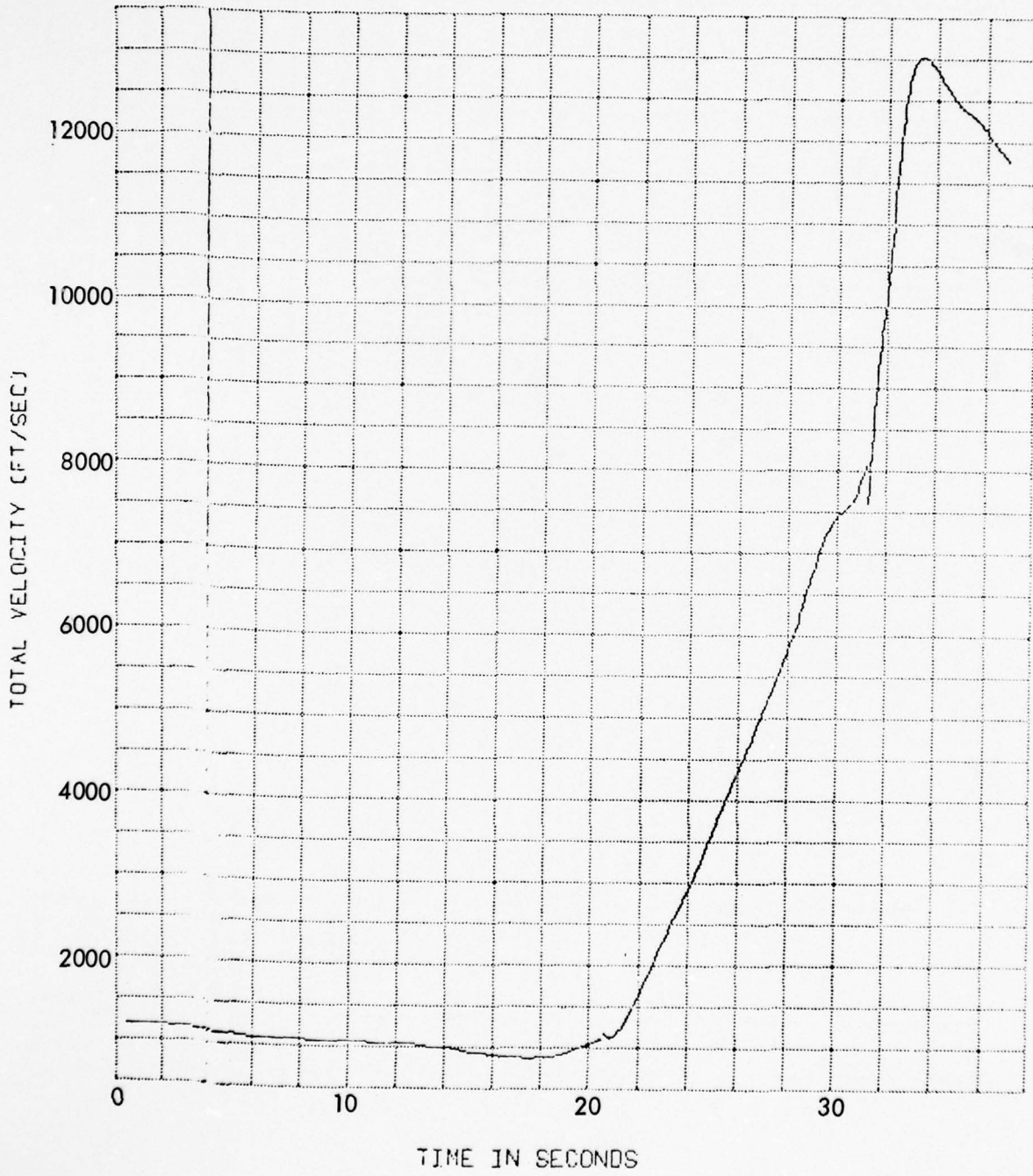


Figure 4-18. FLAME F-005 velocity history.

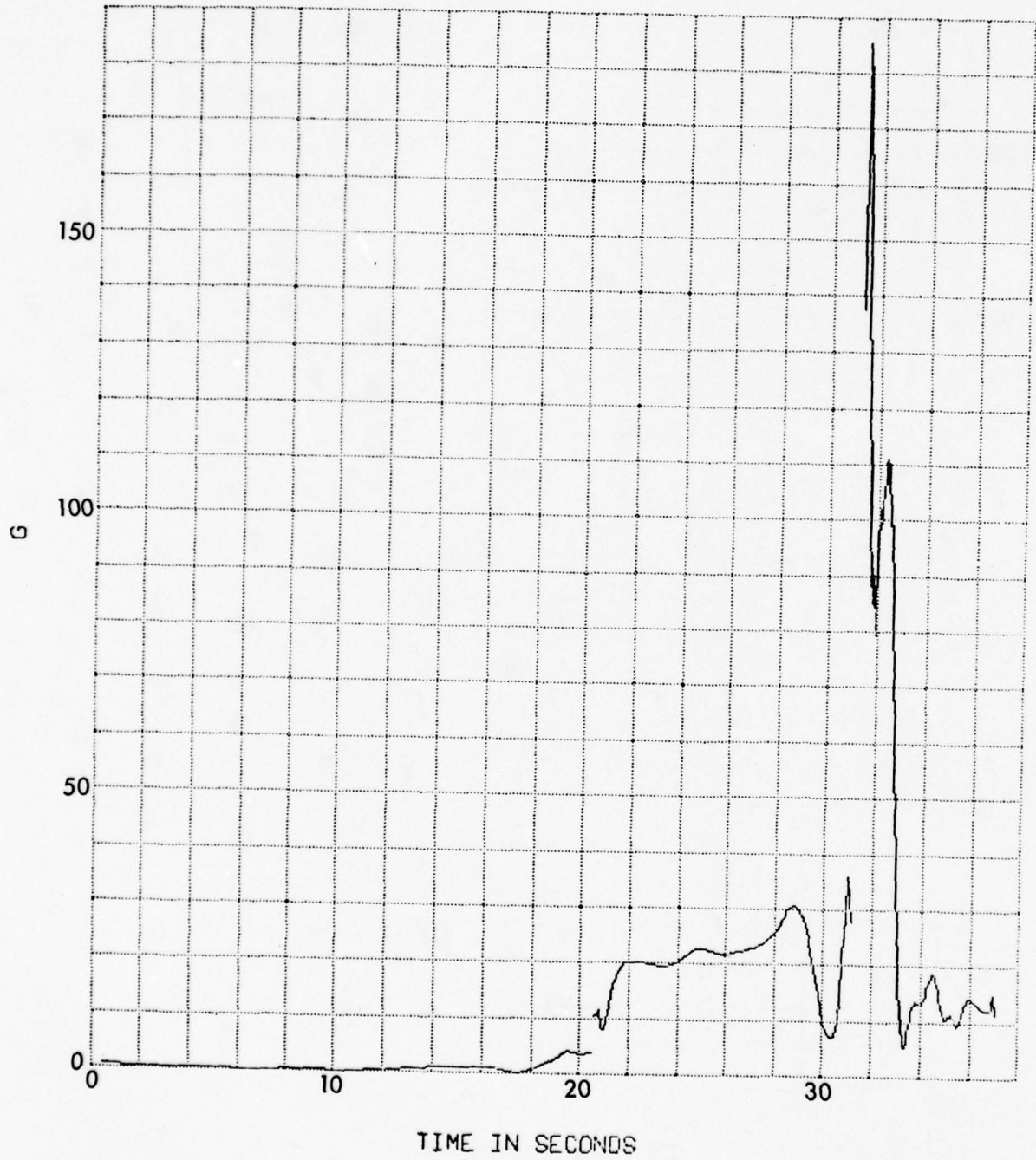


Figure 4-19. FLAME F-005 acceleration history.

ALTITUDE VS TIME

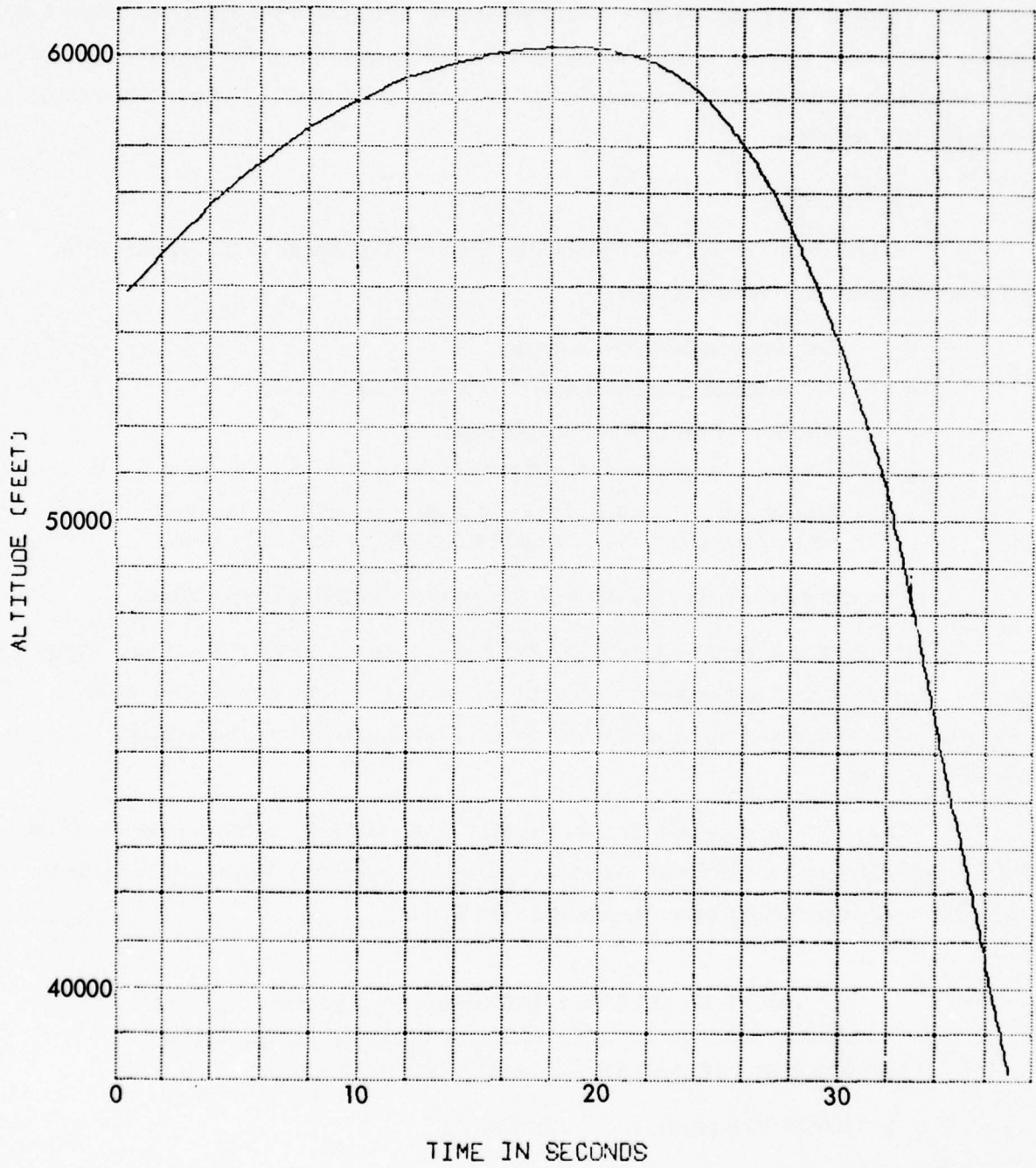


Figure 4-20. FLAME F-005 altitude history.

ignition, and the propellant grain was designed to burn for 15 seconds. The volume of the gas generator was such that all electronics except the radar transponder had to be removed from the drogue.

The flight was negated by a failure apparently identical to the failure on Flight F-004. Just before Pedro burn-out, the nozzle failed, resulting in the breakup of the vehicle. The R/V was tracked by radar until impact; however, no optical data was obtained. Figures 4-21 through 4-23 show the R/V trajectory.

4.7 Flight F-007

FLAME Flight F-007 was flown at the Tonopah Test Range on 22 January 1976.

The recovery vehicle characteristics were:

- Low trim angle (LTA) nosetip.
- 8.4 ft ribbon parachute with no water recovery aids.
- 5-watt payload radar transponder.
- 5-channel S-band FM/FM telemetry package.
- Weight and Static Margin | 80.06 lb and 15.5 percent before deployment
44.53 lb and 16.1 percent after deployment.

The passive low trim angle nosetip was supplied by Aerotherm/Acurex.

The flight was nominal except that the Pedro motor fired when the vehicle was at too steep of an entry angle. Consequently, although all recovery functions were performed properly, the vehicle impacted the ground at transonic speed before the timer commanded parachute deployment.

Table 4-17 summarizes the data obtained from the flight, Table 4-18 presents the critical mission parameters, and Table 4-19 lists conclusions reached. Figures 4-24 through 4-26 show the optical trajectory data obtained from the flight.

Table 4-17. FLAME F-007 data source summary.

● PAYLOAD TELEMETRY	- GOOD DATA TO IMPACT
● TRACKING RADAR	- NO DATA .
● OPTICS	- TRACK TO 9,100 FT ALTITUDE

TOTAL VELOCITY VS TIME

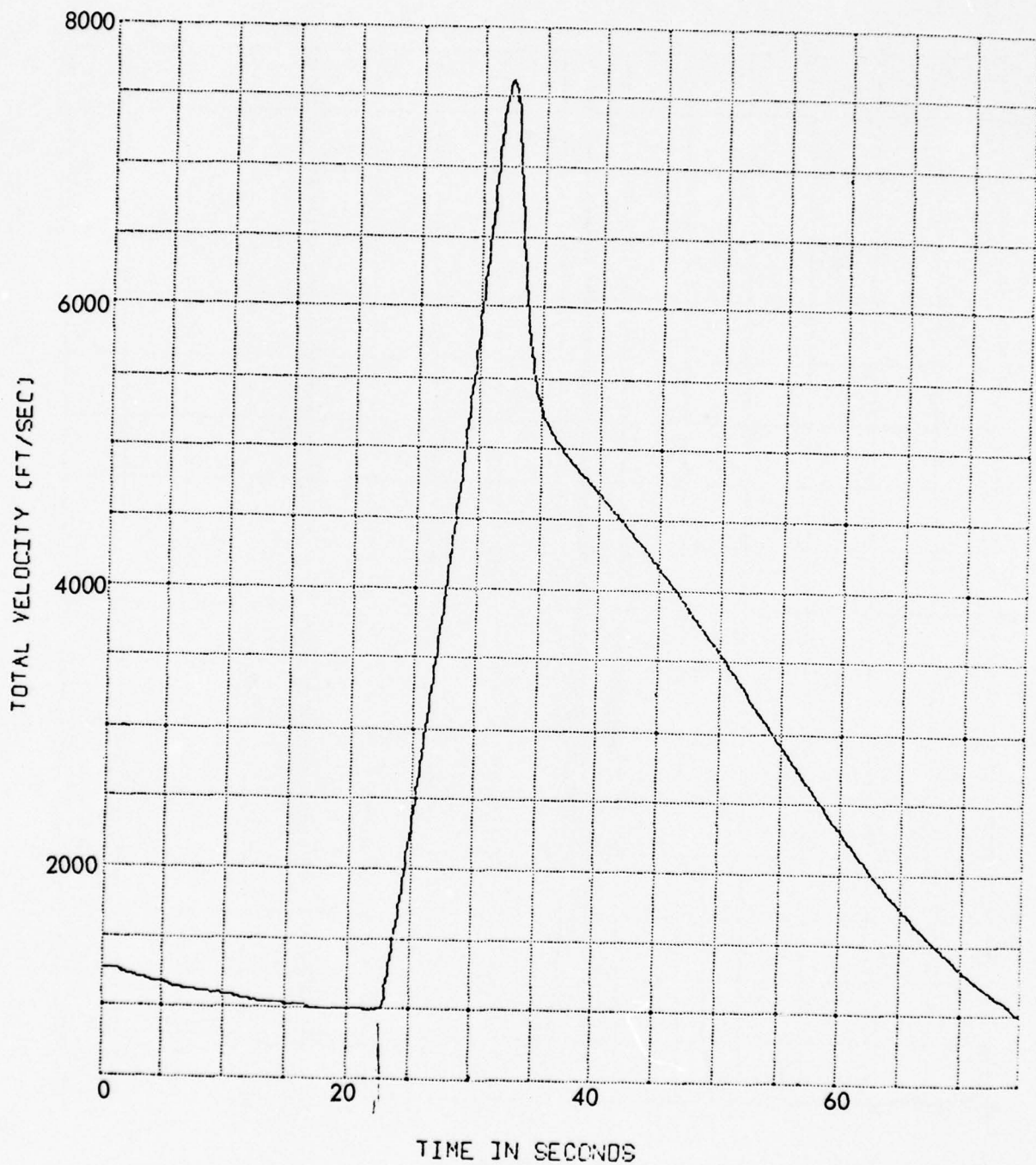


Figure 4-21. FLAME F-006 velocity history.

G VS TIME

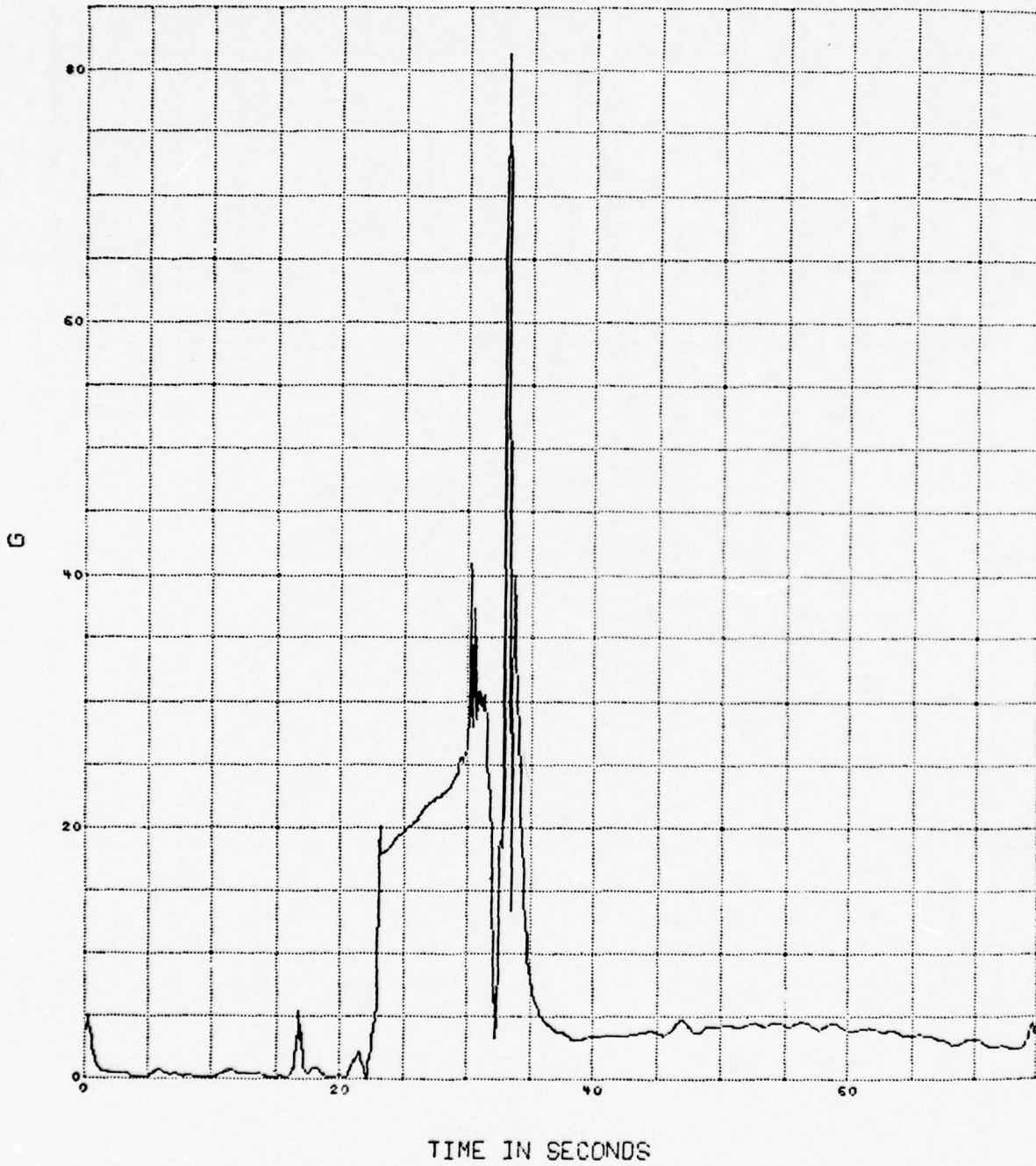


Figure 4-22. FLAME F-006 acceleration history.

ALTITUDE VS TIME

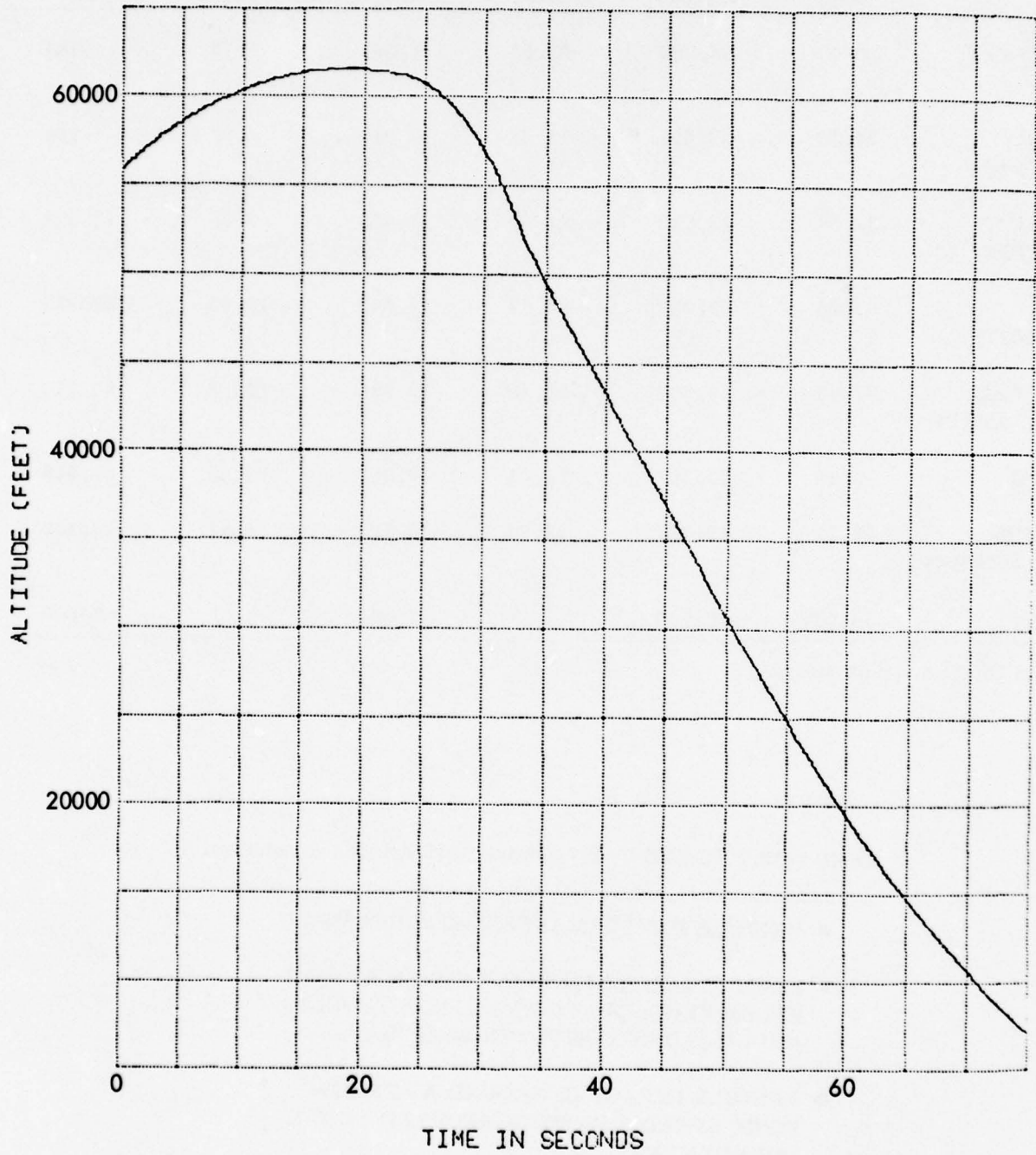


Figure 4-23. FLAME F-006 altitude history.

Table 4-18. FLAME F-007 flight data summary.

	TIME (SEC)	ALTITUDE (FEET)	GAMMA (DEG)	VELOCITY (FT/SEC)	MACH NUMBER	DYNAMIC PRESSURE LB/SQ. FT
AIRCRAFT DROP	0.0	55,869	32.68	1,069	1.14	161
PEDRO IGNITION	24.20	59,518	-15.28	918	.97	100
RECRUIT IGNITION	34.98	43,718	-20.50	7,495	7.75	13,918
MAX VELOCITY	37.05	36,039	-22.03	12,546	12.93	55,929
PAYLOAD SEPARATION	37.48	33,661	-22.16	12,385	12.73	60,619
MAX Q	40.15	22,162	-22.44	10,657	10.38	67,945
FAIRING DEPLOYMENT	40.77	19,746	-22.57	10,198	9.81	67,148
IMPACT	46.91*	~5,600	-----	~1,000	1	~1,000

*From On-Board Telemetry

Table 4-19. FLAME F-007 vehicle performance evaluation.

- VEHICLE PERFORMANCE WAS SUCCESSFUL
- FIRST STAGE IGNITION OCCURRED AT TOO STEEP FLIGHT PATH ANGLE DUE TO ERRONEOUS RADAR/COMPUTER DROP DATA
- VEHICLE IMPACTED GROUND AT TRANSSONIC SPEED BEFORE SCHEDULED CHUTE DEPLOYMENT

TOTAL VELOCITY VS TIME

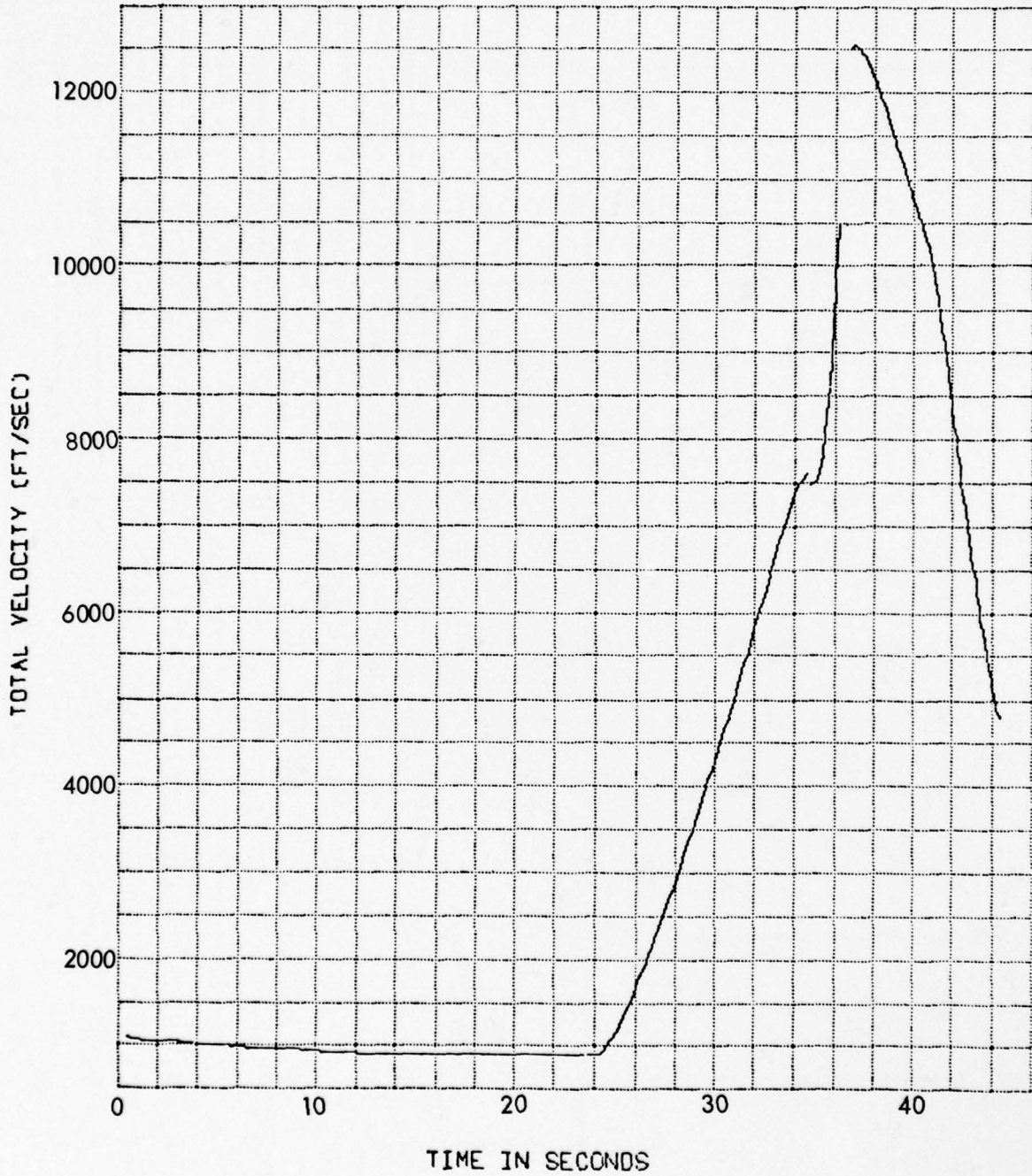


Figure 4-24. FLAME F-007 velocity history.

R422223

OPTICAL

G VS TIME

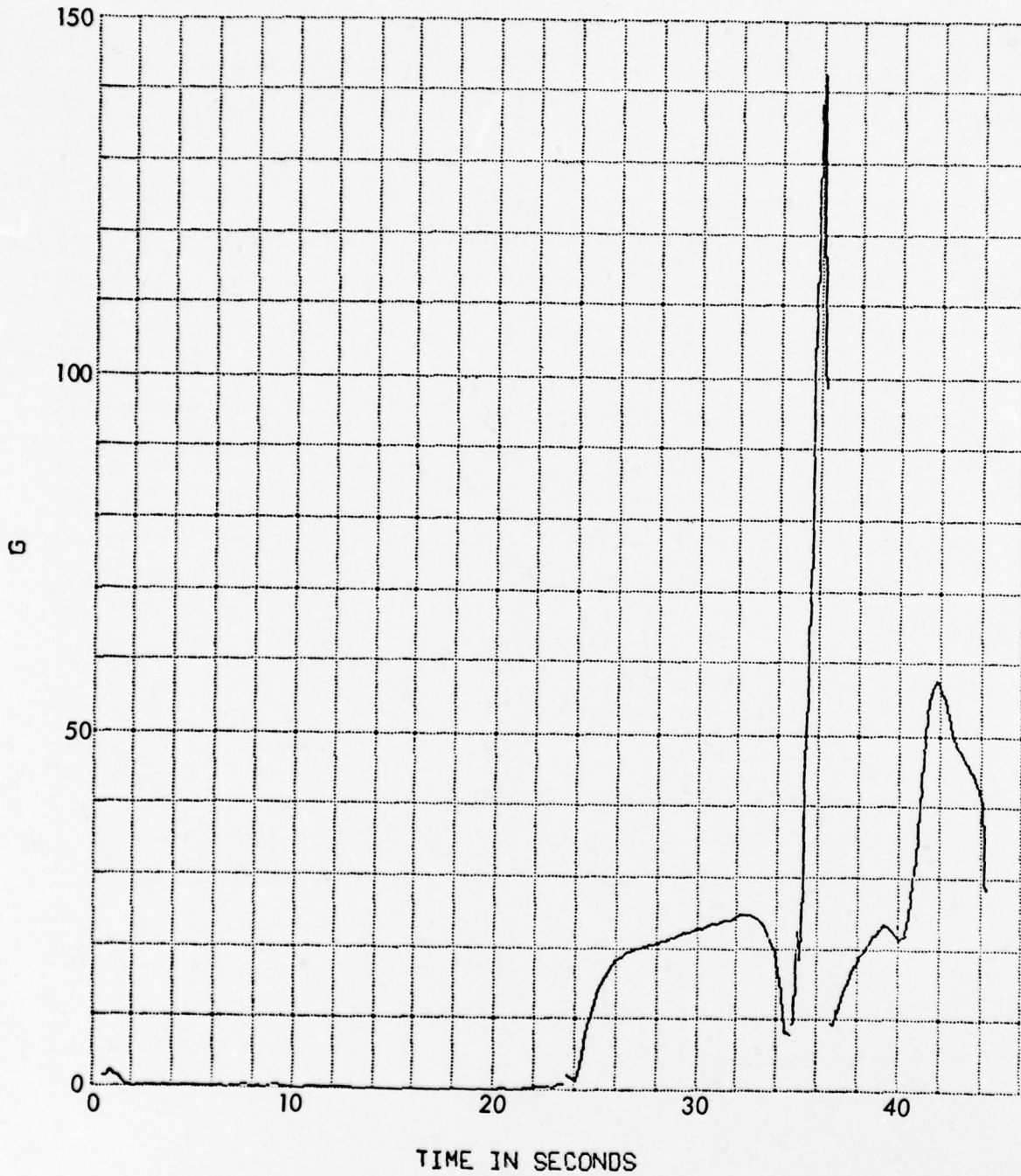


Figure 4-25. FLAME F-007 acceleration history.

ALTITUDE VS TIME

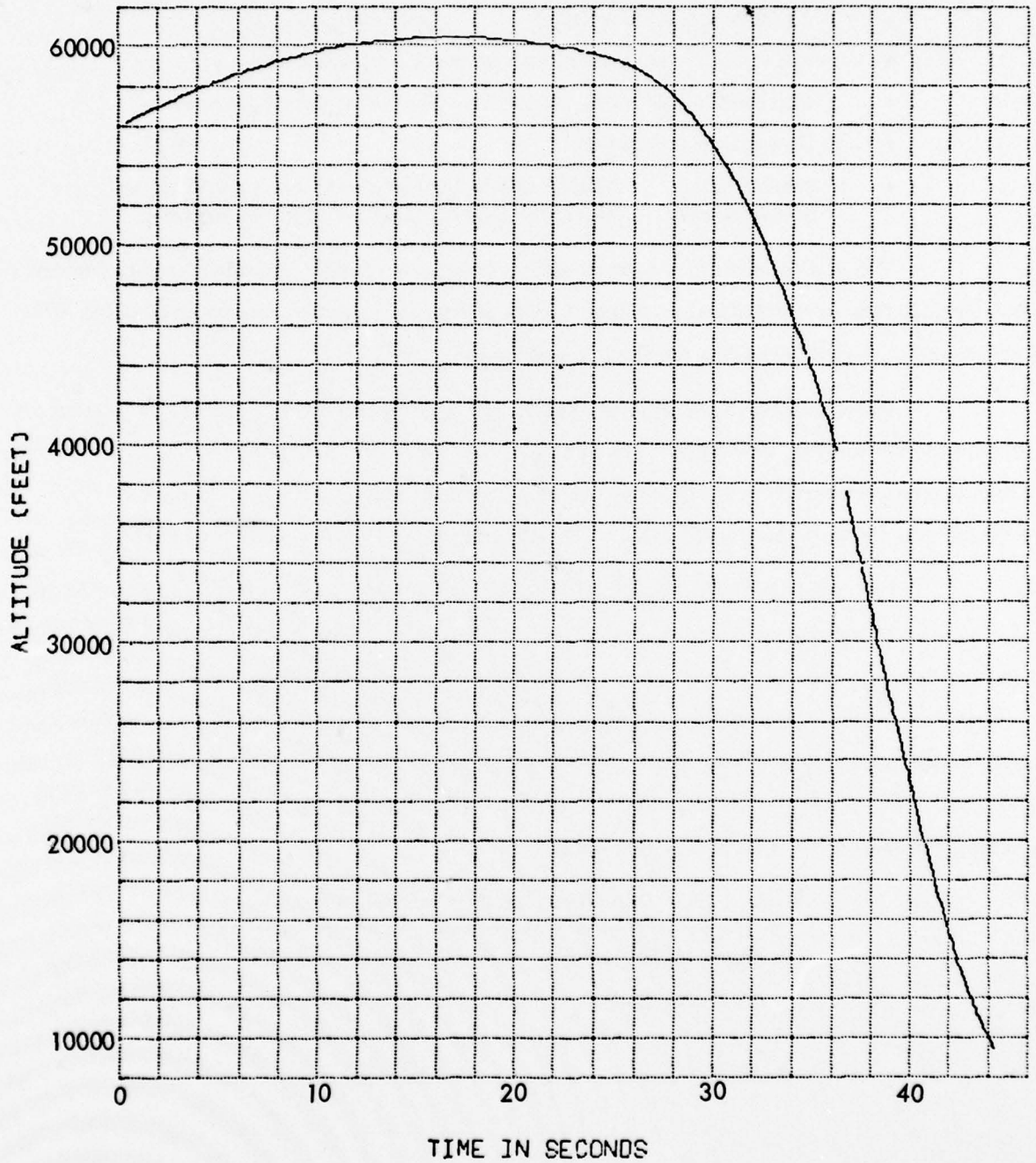


Figure 4-26. FLAME F-007 altitude history.

Flight F-008

The final FLAME flight was conducted at the Tonopah Test Range on 26 January 1976.

The recovery vehicle characteristics were:

- Ta-10W gas jet nosetip.
- 8.4 ft ribbon parachute with no water recovery aids.
- Modified 5-watt Vega Model 228C C-band radar transponder.
- No payload telemetry.
- Weight and Static Margin | 81.125 lb and 14.1 percent before deployment
45.59 lb and 13.8 percent after deployment.

The gas jet nosetip was supplied by Martin Marietta. The nosetip gas generator and vehicle installation were identical to Flight F-006, and again required the removal of the R/V telemetry unit to provide volume for the gas generator.

Performance of the system initially appeared nominal with the exception that the parachute did not deploy, resulting in the vehicle impacting at high subsonic speed. The nosetip and boom were recovered; however, the drogue was not attached to the boom, and no evidence of the drogue was found at the impact site. Table 4-20 summarizes the flight data obtained.

Examination of the optical data and the recovered vehicle indicated that the gas generator for the nosetip exploded during fairing deployment. The optical data showed a large quantity of debris released at that time, and the vehicle emitted a plume of burning material for sometime thereafter. The recovered nosetip is consistent with the hypothesis that the gas generator burst during fairing deployment. Table 4-21 lists the critical mission parameters and Table 4-22 summarizes conclusions reached from the mission. Figures 4-28 through 4-30 present the trajectory obtained from optical tracking data.

Table 4-20. FLAME F-008 data source summary.

● Payload Telemetry	-	None Installed
● Tracking Radar	-	Lost Track During Pedro Burn
● Optics	-	Track to Impact

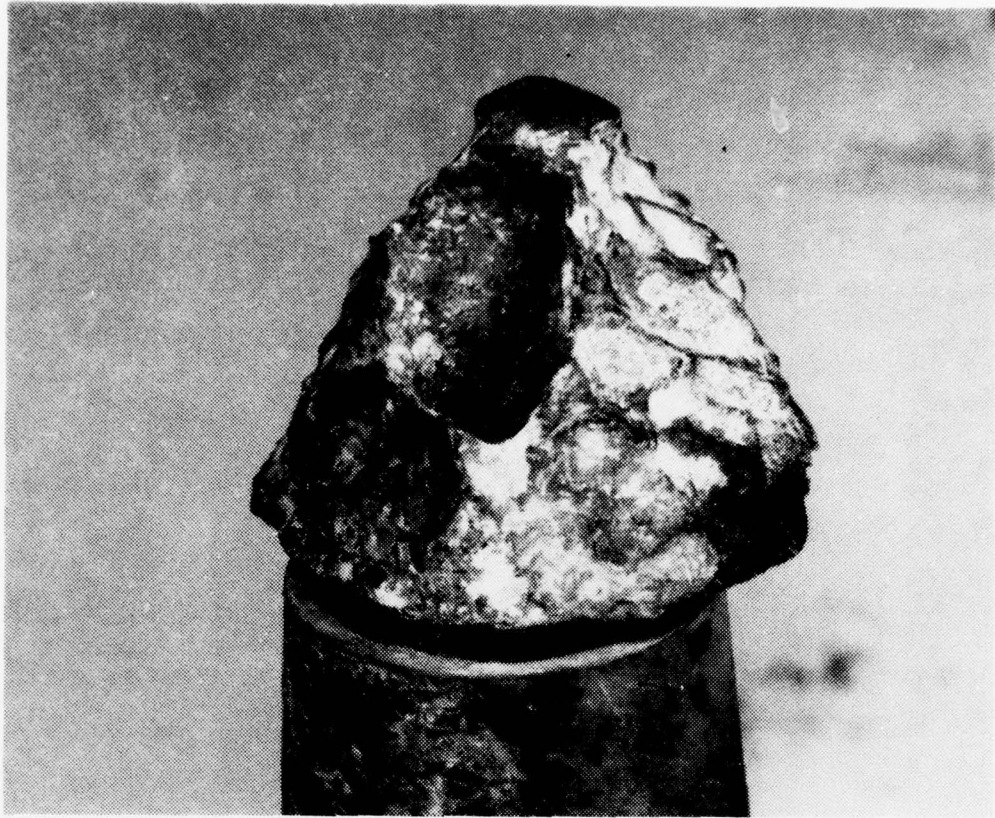


Figure 4-27. Recovered gasjet nosetip from FLAME F-008.

Table 4-21. FLAME F-008 flight data summary.

	Time (Sec)	Altitude (feet)	Gamma (deg)	Velocity (ft/sec)	Mach Number	Dynamic Pressure lb/sq. ft
Aircraft Drop	0.0	55,235	31.96	1243	1.31	226
Pedro Ignition	26.24	60,097	-13.35	1040	1.10	123
Recruit Ignition	37.05	43,954	-19.87	8104	8.47	16,322
Max. Velocity	39.09	36,341	-20.69	12709	13.30	58,940
Payload Separation	39.46	34,524	-20.76	12594	13.06	62,057
Max Q	42.29	22,813	-20.87	10909	10.62	69,702
Fairing Deployment	42.94	20,160	-21.22	10009	9.61	63,885

Table 4-22. FLAME F-008 vehicle performance evaluation.

- Boost system performance was successful.
- Fairing deployment was successful.
- The nosetip gas generator apparently failed at fairing deployment.
- The chute did not deploy and the vehicle impacted supersonically.
- The majority of vehicle was recovered from the impact site. Analysis of the nosetip suggests that gas flow ceased at side panel deployment.

TOTAL VELOCITY VS TIME

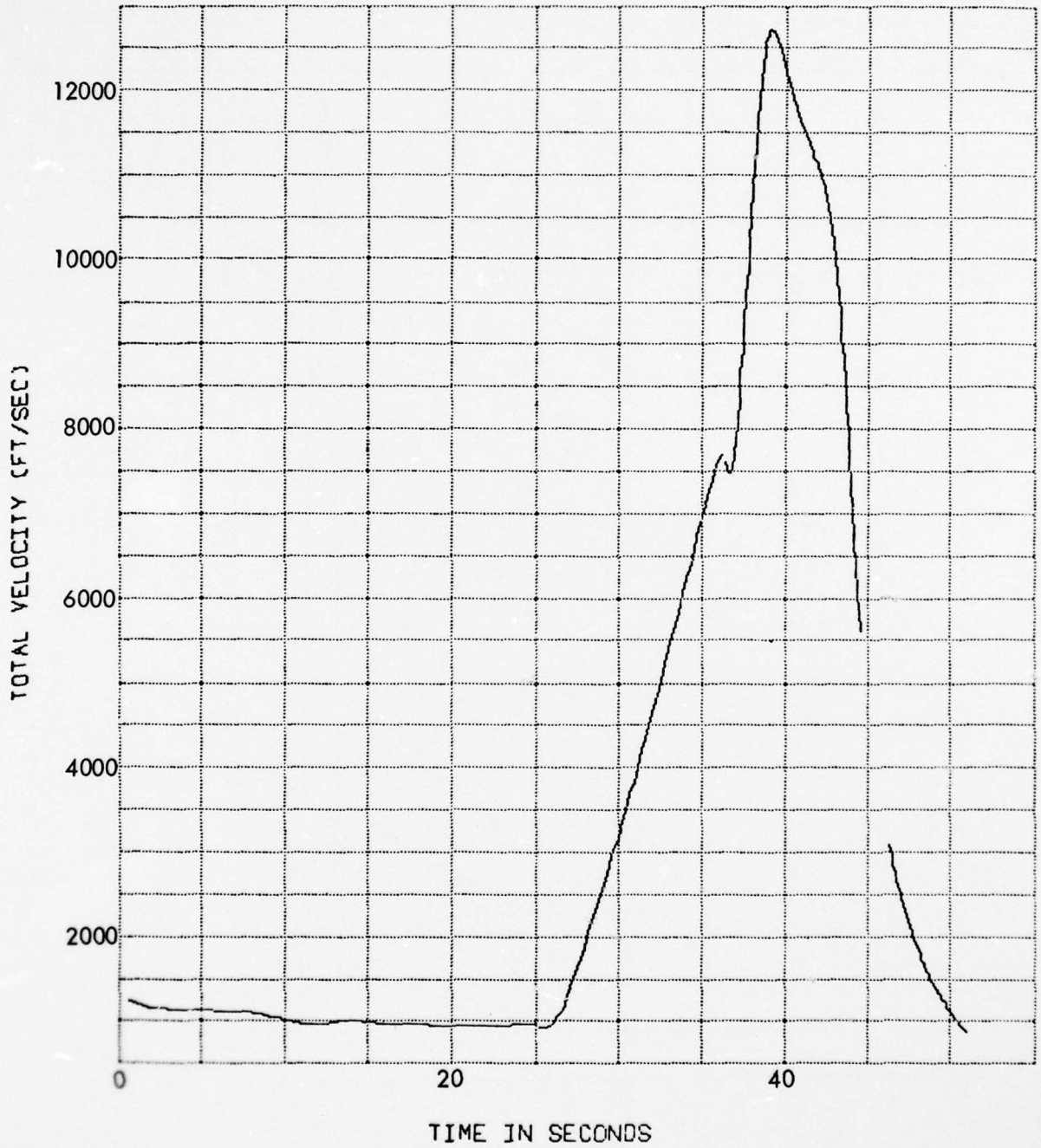


Figure 4-28. FLAME F-008 velocity history.

G VS TIME

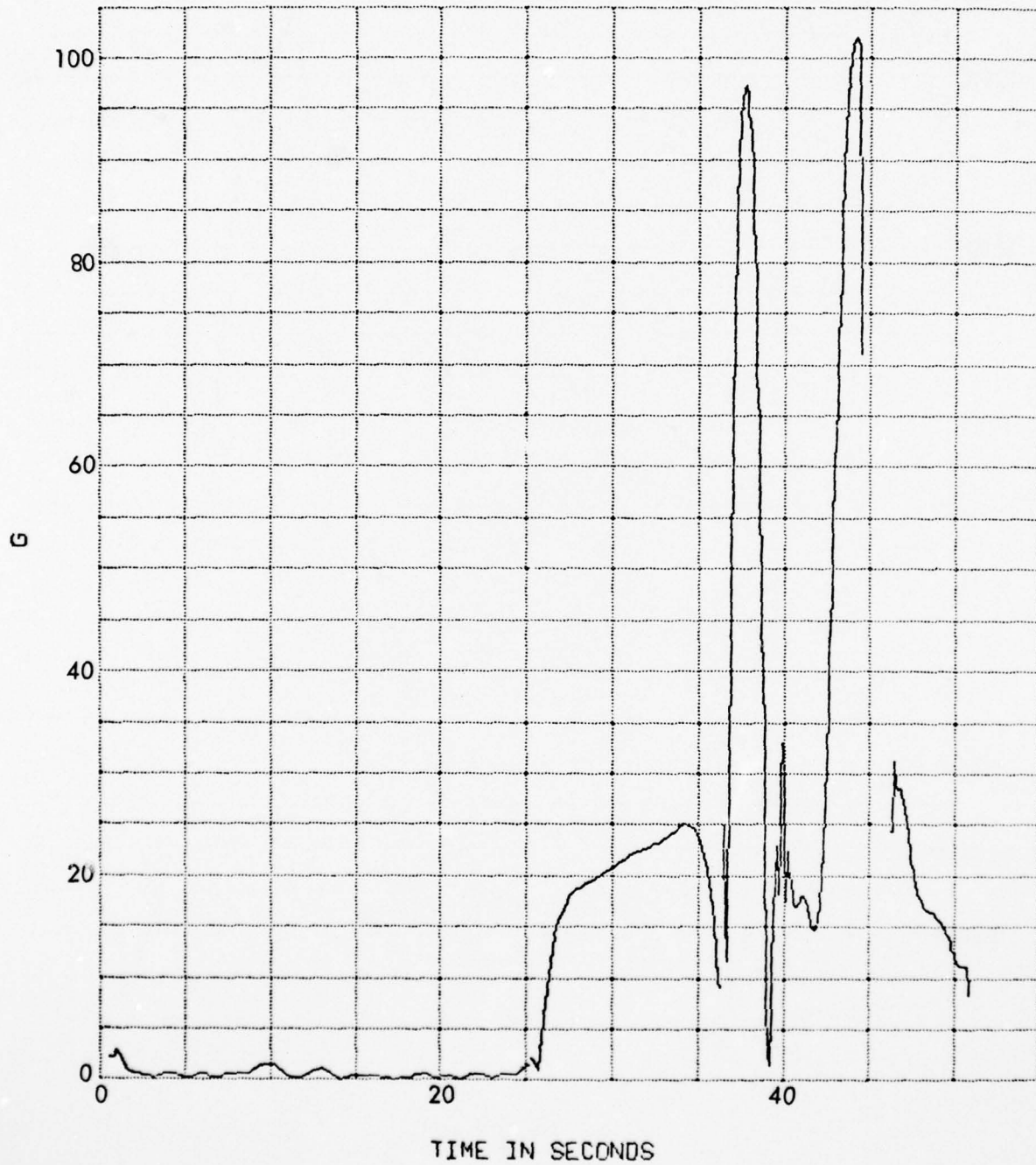


Figure 4-29. FLAME F-008 acceleration history.

ALTITUDE VS TIME

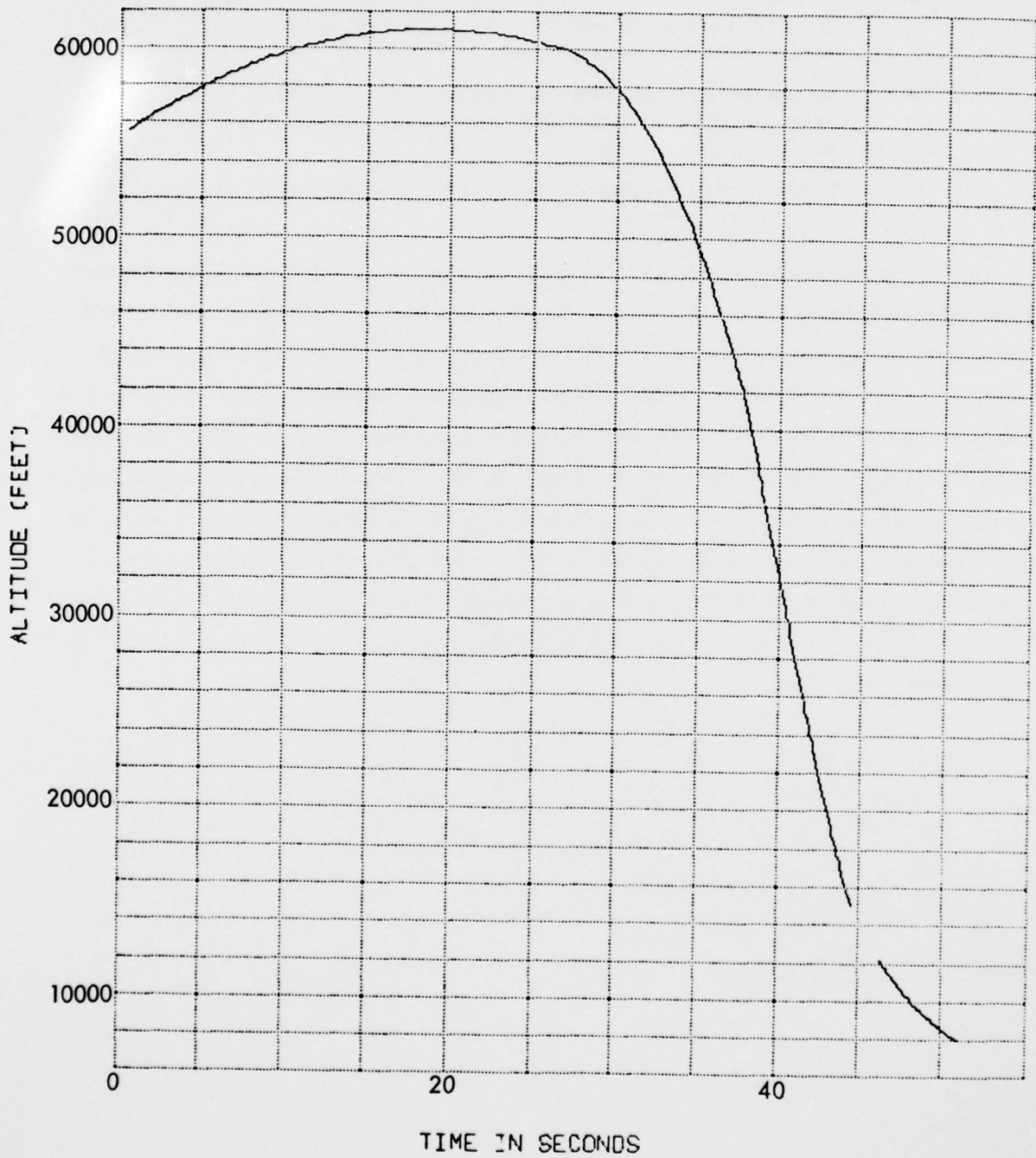


Figure 4-30. FLAME F-008 altitude history.

CONCLUSIONS

Three principal conclusions were reached during the FLAME Program:

- The mass-jettison drogue (MJD) concept provides a practical means of recovering nosetips from high ballistic coefficient reentry vehicles at low altitude.
- All necessary equipment for operation and recovery on either water or land can be packaged in the drogue volume, even for sub-ICBM size vehicles.
- Refinement of the external geometry can substantially increase vehicle performance.

The successful recovery of the tungsten nosetip on Flight F-005 demonstrated the effectiveness of the mass-jettison drogue concept. However, evaluation of aerodynamic data from various flights indicates that the external geometry is not optimum. Figure 5-1 compares data from two flights to the maximum and minimum possible curves. It can be seen that the two data curves differ greatly above Mach 3.2. Apparently the flow around the drogue on the FLAME vehicle is marginally stable. Small changes in nosetip shape or perhaps angle-of-attack can cause separated flow that sharply reduces vehicle drag. Before the next series of MJD vehicles is designed, a reassessment of the external geometry should be conducted, perhaps including wind tunnel testing, to identify configurations that combine maximum internal volume and ballistic coefficient change at fairing deployment, with insensitivity to nosetip shape and vehicle angle-of-attack.

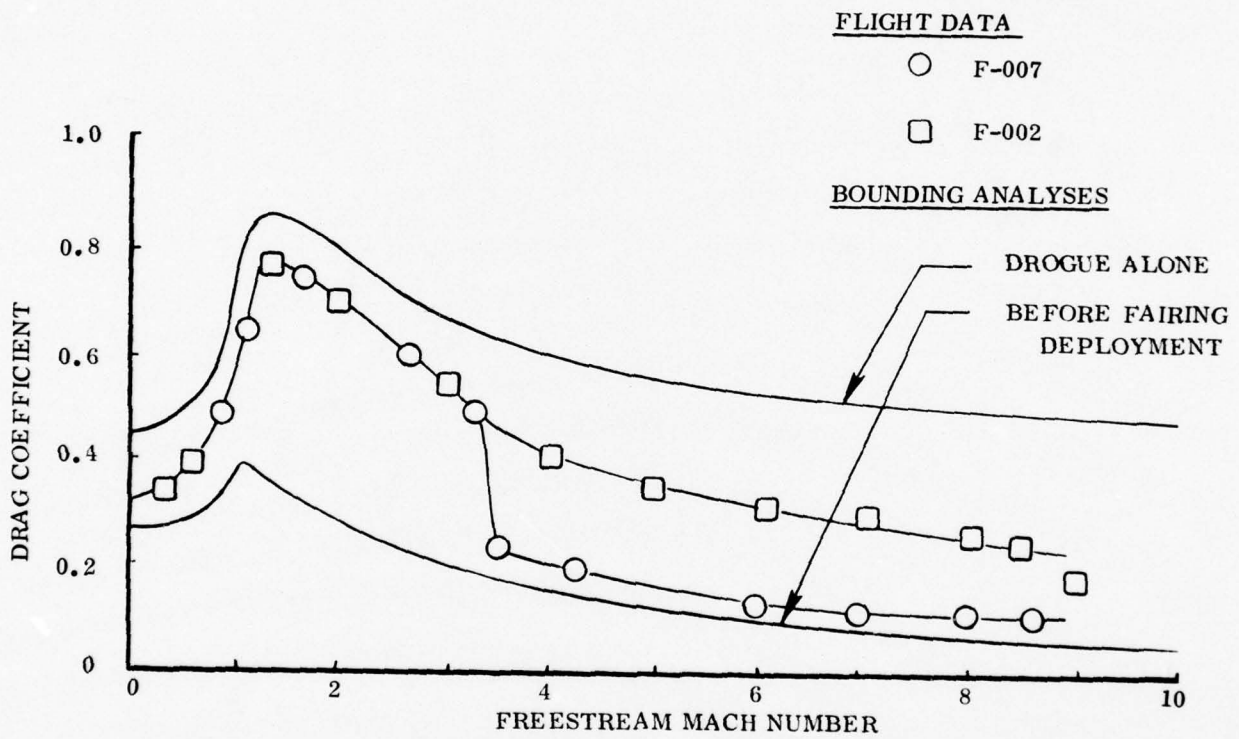


Figure 5-1. FLAME drag data comparison.

DISTRIBUTION LIST

DEPARTMENT OF DEFENSE

Assistant to the Secretary of Defense
Atomic Energy

ATTN: Executive Assistant

Defense Advanced Rsch. Proj. Agency

ATTN: TIO

Defense Communications Agency

ATTN: CCTC

Defense Documentation Center

12 cy ATTN: DD

Defense Intelligence Agency

ATTN: DB-4D

ATTN: DT-2

ATTN: DT-1C

Defense Nuclear Agency

ATTN: STSP

ATTN: SPAS

ATTN: SPTD

ATTN: SPSS

ATTN: DDST

4 cy ATTN: TITL

Field Command

Defense Nuclear Agency

ATTN: FCTMOT

ATTN: FCTMOF

ATTN: FCTMD

ATTN: FCPR

Livermore Division, Field Command, DNA

ATTN: FCPRL

Under Secretary of Defense for Rsch. & Engrg.

ATTN: Engineering Technology, J. Persh

ATTN: Strategic & Space Systems (OS)

DEPARTMENT OF THE ARMY

BMD Advanced Technology Center

Huntsville Office

Department of the Army

ATTN: ATC-T, M. Capps

BMD Systems Command

Department of the Army

ATTN: BMDSC-H, N. Hurst

Deputy Chief of Staff for Ops. & Plans

Department of the Army

ATTN: Dep. Dir. for Nuc. Plans & Policy

Deputy Chief of Staff for Rsch. Dev. & Acq.

Department of the Army

ATTN: Nuclear Team

Harry Diamond Laboratories

Department of the Army

ATTN: DELHD-N-TF, R. Oswald, Jr.

ATTN: DELHD-N-P, J. Gwaltney

DEPARTMENT OF THE ARMY (Continued)

U.S. Army Ballistic Research Labs

ATTN: DRDAR-BLV, W. Schuman, Jr.

ATTN: DRDAR-BLE, J. Keefer

ATTN: DRDAR-BL, R. Eichelberger

ATTN: DRDAR-BLV, J. Meszaros

ATTN: DRDAR-BLT, R. Vitali

ATTN: DRXBR-BLT, J. Frasier

U.S. Army Material & Mechanics Rsch. Ctr.

ATTN: DRXMR-HH, J. Dignam

U.S. Army Materiel Dev. & Readiness Cmd

ATTN: DRCDE-D, L. Flynn

U.S. Army Missile R&D Command

ATTN: DRDMI-XS

ATTN: DRDMI-TKP, W. Thomas

ATTN: DRDMI-TRR, B. Gibson

U.S. Army Nuclear & Chemical Agency

ATTN: Library

U.S. Army TRADOC Systems Analysis Activity

ATTN: ATAA-TDC, R. Benson

DEPARTMENT OF THE NAVY

Naval Research Laboratory

ATTN: Code 6770, G. Cooperstein

ATTN: Code 2627

ATTN: Code 7908, A. Williams

Naval Sea Systems Command

ATTN: SEA-0352, M. Kinna

Naval Weapons Evaluation Facility

ATTN: P. Hughes

ATTN: L. Oliver

Office of Naval Research

ATTN: Code 465

Office of the Chief of Naval Operations

ATTN: R. Blaise

ATTN: OP 604

ATTN: Code 604C3, R. Piacesi

Strategic Systems Project Office

Department of the Navy

ATTN: NSP-272

Naval Surface Weapons Center

White Oak Laboratory

ATTN: Code F31

ATTN: Code R15, J. Petes

ATTN: Code K06, C. Lyons

DEPARTMENT OF THE AIR FORCE

Aeronautical Systems Division, AFSC

2 cy ATTN: ENFTV, D. Ward

Air Force Flight Dynamics Laboratory

2 cy ATTN: FXG

DEPARTMENT OF THE AIR FORCE (Continued)

Air Force Geophysics Laboratory
ATTN: C. Touart

Air Force Materials Laboratory
ATTN: MBC, D. Schmidt
ATTN: MBE, G. Schmitt
ATTN: T. Nicholas

Air Force Rocket Propulsion Laboratory
ATTN: LKCP, G. Beale

Air Force Systems Command
ATTN: SOSS
ATTN: XRTO

Air Force Weapons Laboratory
ATTN: DYV, A. Sharp
ATTN: DYT
ATTN: DYV
ATTN: SUL
ATTN: DYS
ATTN: Technical Review
ATTN: Dr. Minge
2 cy ATTN: NTO

Arnold Engineering Development Center
Department of the Air Force
ATTN: XRRP

Deputy Chief of Staff
Research, Development, & Acq.
Department of the Air Force
ATTN: AFRDQSM
ATTN: AFRD
ATTN: AFRDPX
ATTN: AFRDQ

Foreign Technology Division, AFSC
ATTN: SDBG
ATTN: TQTD
ATTN: SDBS, J. Pumphrey

Space & Missile Systems Organization/DY
Air Force Systems Command
ATTN: DYS

Space & Missile Systems Organization/MN
Air Force Systems Command
ATTN: MNNH
ATTN: MNNR

Space & Missile Systems Organization/RS
Air Force Systems Command
ATTN: RSSE
ATTN: RSS
ATTN: RST
ATTN: RSSP
ATTN: RSP
ATTN: RSSR

Strategic Air Command/XPFS
Department of the Air Force
ATTN: DOXT
ATTN: XPQM
ATTN: XOBM
ATTN: XPFS

Deputy Chief of Staff
Operations, Plans and Readiness
ATTN: XOSS

DEPARTMENT OF DEFENSE CONTRACTORS

Acurex Corporation
ATTN: C. Nardo
ATTN: J. Huntington
ATTN: R. Rindal
ATTN: J. Cortney

Aerospace Corporation
ATTN: R. Strickler
ATTN: R. Mortensen
ATTN: W. Barry
ATTN: W. Grabowsky
ATTN: J. Kyser

Analytic Services, Inc.
ATTN: J. Selig

Avco Research & Systems Group
ATTN: J. Stevens
ATTN: Document Control
ATTN: W. Broding
ATTN: G. Weber
ATTN: J. Gilmore

Battelle Memorial Institute
ATTN: M. Vanderlind
ATTN: E. Unger

The Boeing Company
ATTN: R. Dyrdaahl
ATTN: E. York
ATTN: B. Lempriere
ATTN: R. Homes

Boeing Wichita Company
ATTN: T. Swaney

California Research & Technology, Inc.
ATTN: K. Kreyenhagen

Calspan Corporation
ATTN: M. Holden

University of Dayton
Industrial Security Super., KL-505
ATTN: D. Gerdiman
ATTN: H. Swift

Effects Technology, Inc.
ATTN: R. Parisse
ATTN: R. Wengler

Ford Aerospace & Communications Corporation
ATTN: P. Spangler

General Electric Co.
Space Division
ATTN: D. Edelman
ATTN: C. Anderson
ATTN: G. Harrison

General Electric Co.
Re-Entry & Environmental Systems Div.
ATTN: P. Cline

General Electric Co.-TEMPO
Center for Advanced Studies
ATTN: DASIAC

DEPARTMENT OF DEFENSE CONTRACTORS (Continued)

General Research Corporation
Santa Barbara Division
ATTN: T. Stathacopoulos

General Research Corporation
ATTN: R. Patrick

Institute for Defense Analyses
ATTN: Classified Library
ATTN: J. Bengston

Kaman Avidyne
Division of Kaman Sciences Corporation
ATTN: R. Ruetenik
ATTN: E. Criscione
ATTN: N. Hobbs

Kaman Sciences Corporation
ATTN: D. Sachs
ATTN: J. Hoffman
ATTN: T. Meagher
ATTN: J. Keith
ATTN: F. Shelton

Lawrence Livermore Laboratory
University of California
ATTN: Doc. Con. for L-92, C. Taylor
ATTN: Doc. Con. for G. Staihle
ATTN: Doc. Con. for L-125, J. Keller
ATTN: Doc. Con. for L-216, J. Knox

Lockheed Missiles & Space Co., Inc.
ATTN: R. Walz

Lockheed Missiles and Space Co., Inc.
ATTN: F. Borgardt

Lockheed Missiles and Space Co., Inc.
ATTN: T. Fortune

Los Alamos Scientific Laboratory
ATTN: Doc. Con. for R. Thurston
ATTN: Doc. Con. for R. Dingus
ATTN: Doc. Con. for J. Taylor
ATTN: Doc. Con. for J. McQueen
ATTN: Doc. Con. for R. Skaggs

Martin Marietta Corporation
Orlando Division
ATTN: G. Aiello
ATTN: J. Potts
ATTN: L. Kinnaid

McDonnell Douglas Corporation
ATTN: E. Fitzgerald
ATTN: H. Hurwicz
ATTN: J. Garibotti
ATTN: R. Reck
ATTN: H. Berkowitz
ATTN: D. Dean
ATTN: L. Cohen
ATTN: P. Lewis, Jr.

Northrop Corporation
ATTN: D. Hicks

Pacific-Sierra Research Corporation
ATTN: G. Lang

DEPARTMENT OF DEFENSE CONTRACTORS (Continued)

Physics International Company
ATTN: J. Shea

Prototype Development Associates, Inc.
ATTN: J. McDonald
ATTN: J. Slaughter
ATTN: D. Smith
ATTN: J. Dunn

R & D Associates
ATTN: P. Rausch
ATTN: J. Carpenter
ATTN: C. MacDonald
ATTN: W. Graham, Jr.
ATTN: H. Brode
ATTN: F. Field

Rand Corporation
ATTN: J. Mate

Sandia Laboratories
Livermore Laboratory
ATTN: Doc. Con. for Library & Security
Classification Div.
ATTN: Doc. Con. for H. Norris, Jr.

Sandia Laboratories
ATTN: Doc. Con. for A. Chabai
ATTN: Doc. Con. for R. Boade
ATTN: Doc. Con. for M. Cowan
ATTN: Doc. Con. for T. Cook

Science Applications, Inc.
ATTN: D. Hove
ATTN: O. Nance
ATTN: J. Warner
ATTN: W. Yengst
ATTN: G. Ray

Science Applications, Inc.
ATTN: G. Burghart
ATTN: C. Swain

Science Applications, Inc.
ATTN: W. Seebaugh
ATTN: W. Layson

Science Applications, Inc.
ATTN: A. Martellucci

Southern Research Institute
ATTN: C. Pears

SRI International
ATTN: D. Curran
ATTN: P. Dolan
ATTN: G. Abrahamson
ATTN: H. Lindberg

System Planning Corporation
ATTN: F. Adelman

Systems, Science & Software, Inc.
ATTN: G. Gurtman
ATTN: R. Duff

Terra Tek, Inc.
ATTN: S. Green

DEPARTMENT OF DEFENSE CONTRACTORS (Continued)

TRW Defense & Space Sys. Group

ATTN: P. Dai
ATTN: R. Plebuch
ATTN: G. Arenguren
ATTN: W. Wood
ATTN: P. Brandt
ATTN: D. Baer
ATTN: T. Williams
ATTN: I. Alber

DEPARTMENT OF DEFENSE CONTRACTORS (Continued)

TRW Defense & Space Sys. Group

San Bernardino Operations
ATTN: W. Polich
ATTN: L. Berger
ATTN: E. Allen
ATTN: V. Blankenship
ATTN: E. Wong